Mesures cinématiques et dynamiques en production de la parole

Takayuki Ito
GIPSA-lab
takayuki.ito@grenoble-inp.fr

Plan

- Présentation des enjeux
- Mesure des mouvements des articulateurs non visibles
  - Électromagnétométrie -EMA
  - Echographie - Ultrasound
  - Endoscopie & Transillumination
  - Electroglottographie -EGG
  - Electropalatographie -EPG
- Mesures dynamiques
  - Capteurs de force
  - Electromyographie
- Exemples de paradigmes expérimentaux.

Présentation des enjeux
Speech motor control

Purpose:
To know how ariticulatory organs are moved (descriptive) and how those articulatory organs are controlled (functional).

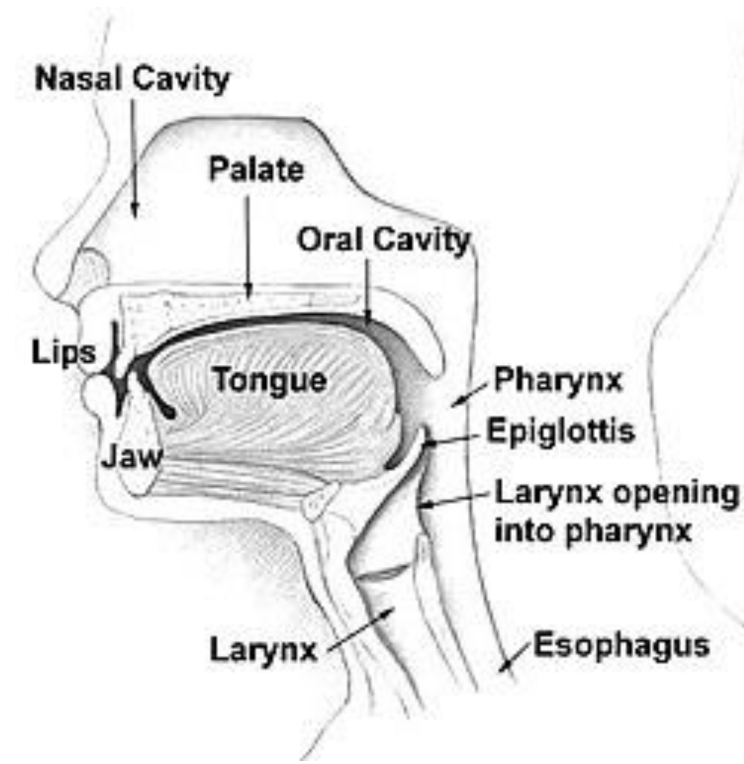

Présentation des enjeux
Speech motor control

Challenges:
Multiple-articulators are involved.

- **Required specific measurement device for each articulator**

Some of articulatory organs are difficult to observe from the outside.

- **Measurement device specific for interior organe**

Each organ and movement are relatively fast and small.

- **Not distrub speech movement**

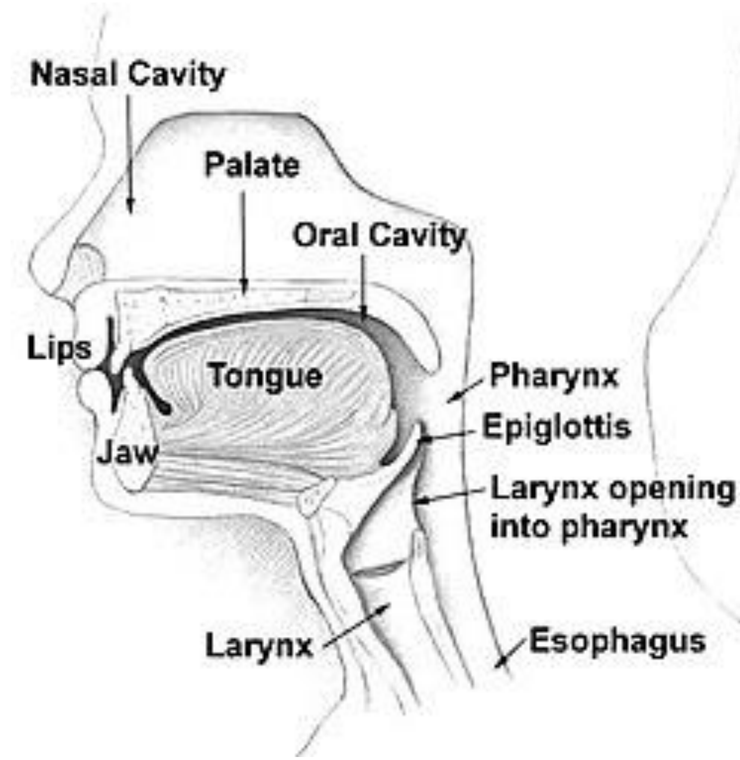

Présentation des enjeux
Le signal acoustique de la parole

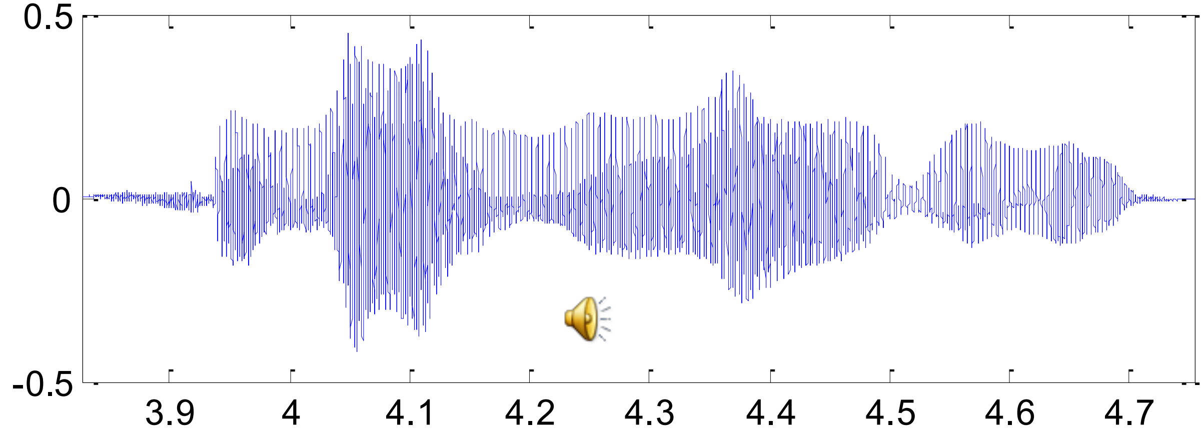

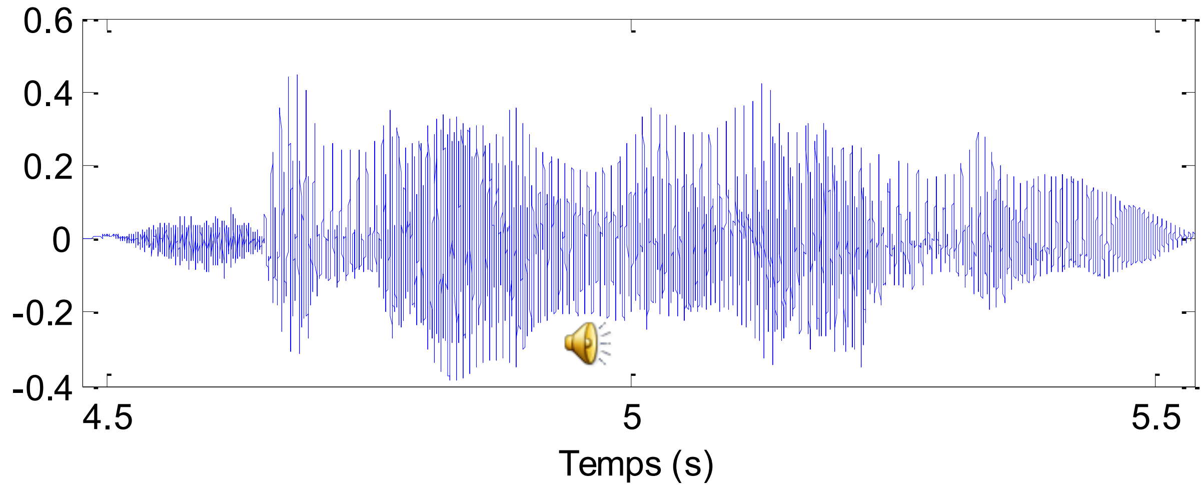

Présentation des enjeux
Le signal acoustique de la parole

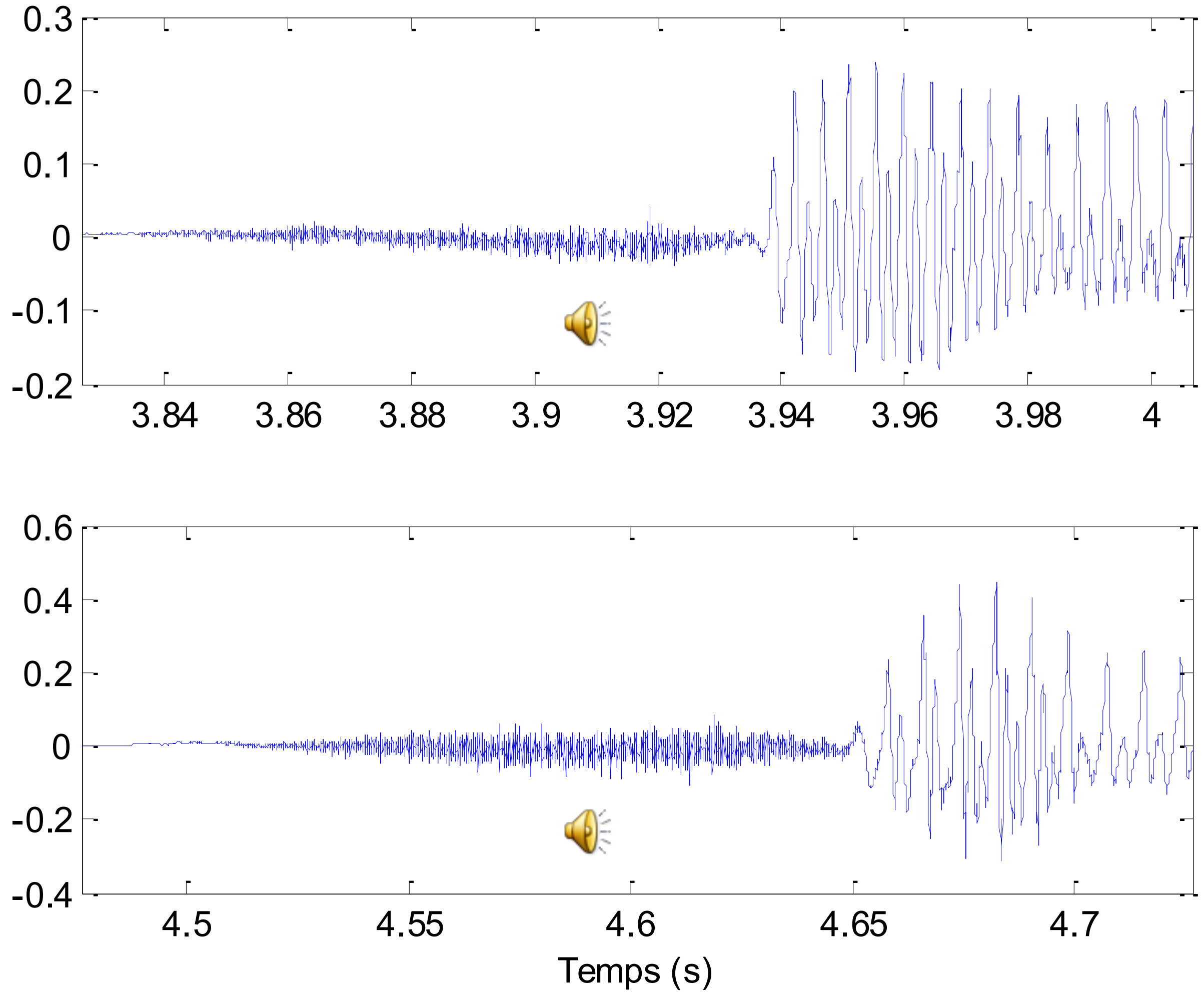

Analyse à court terme

Principes

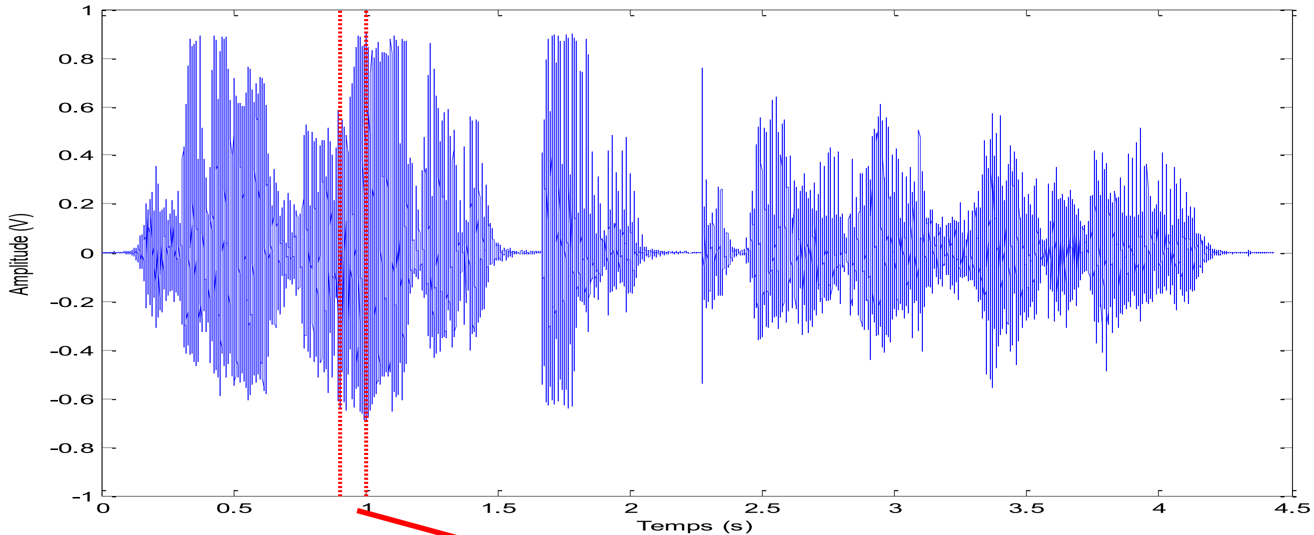

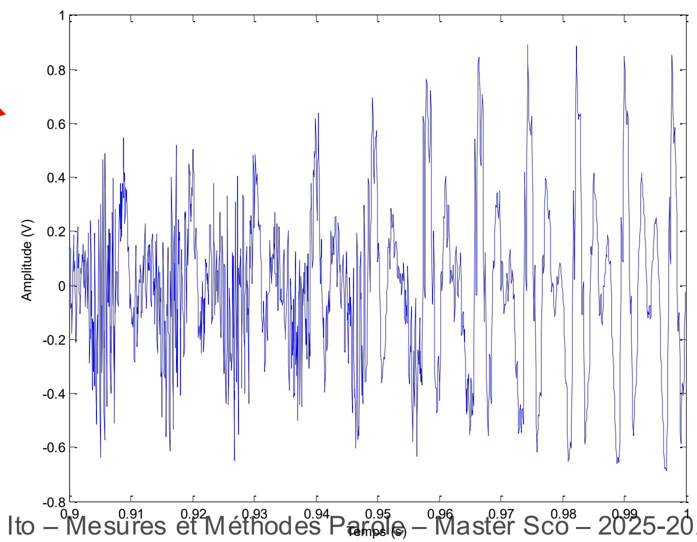

$$s_m(n) = s\big((m-1).N + n\big), \qquad n \in [0, (N-1)]$$

$$s_m(n) = 0, \qquad n \notin [0, (N-1)]$$

$$|S_m(f)| = |S(f) * W_N(f)|$$

Signal de Parole

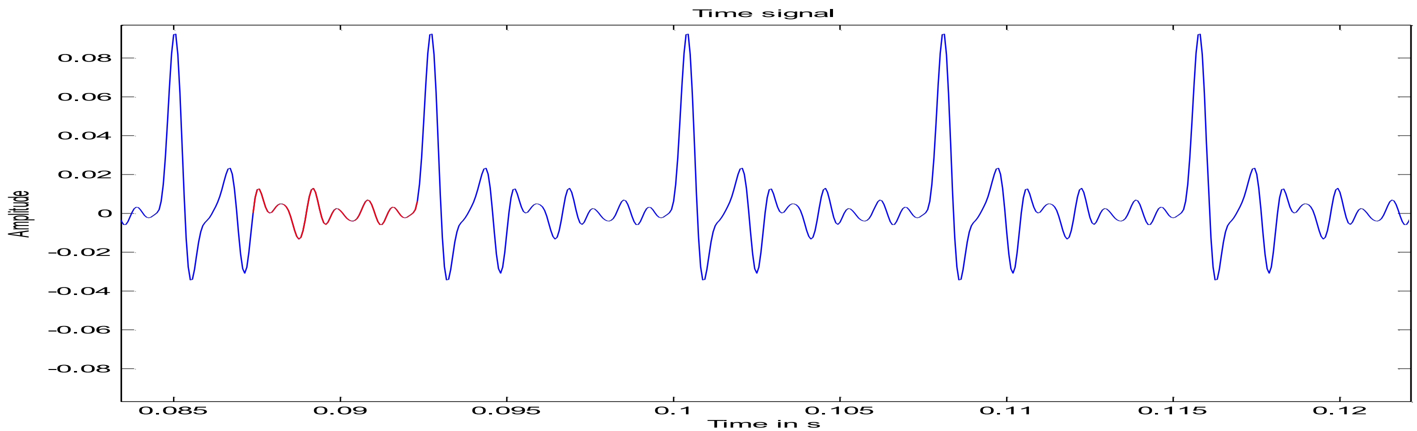

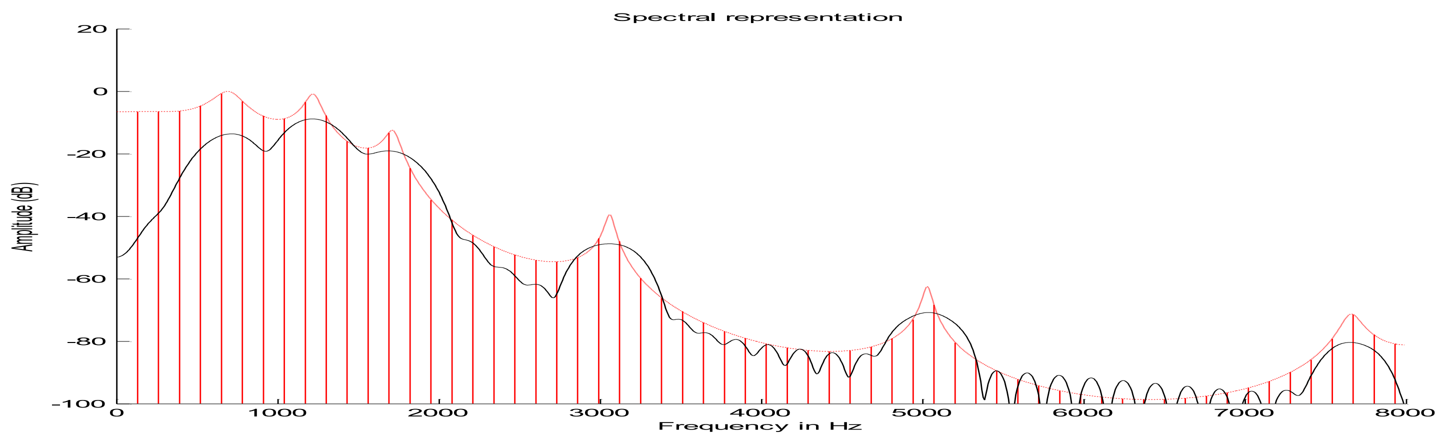

Présentation des enjeux
Le signal acoustique de la parole

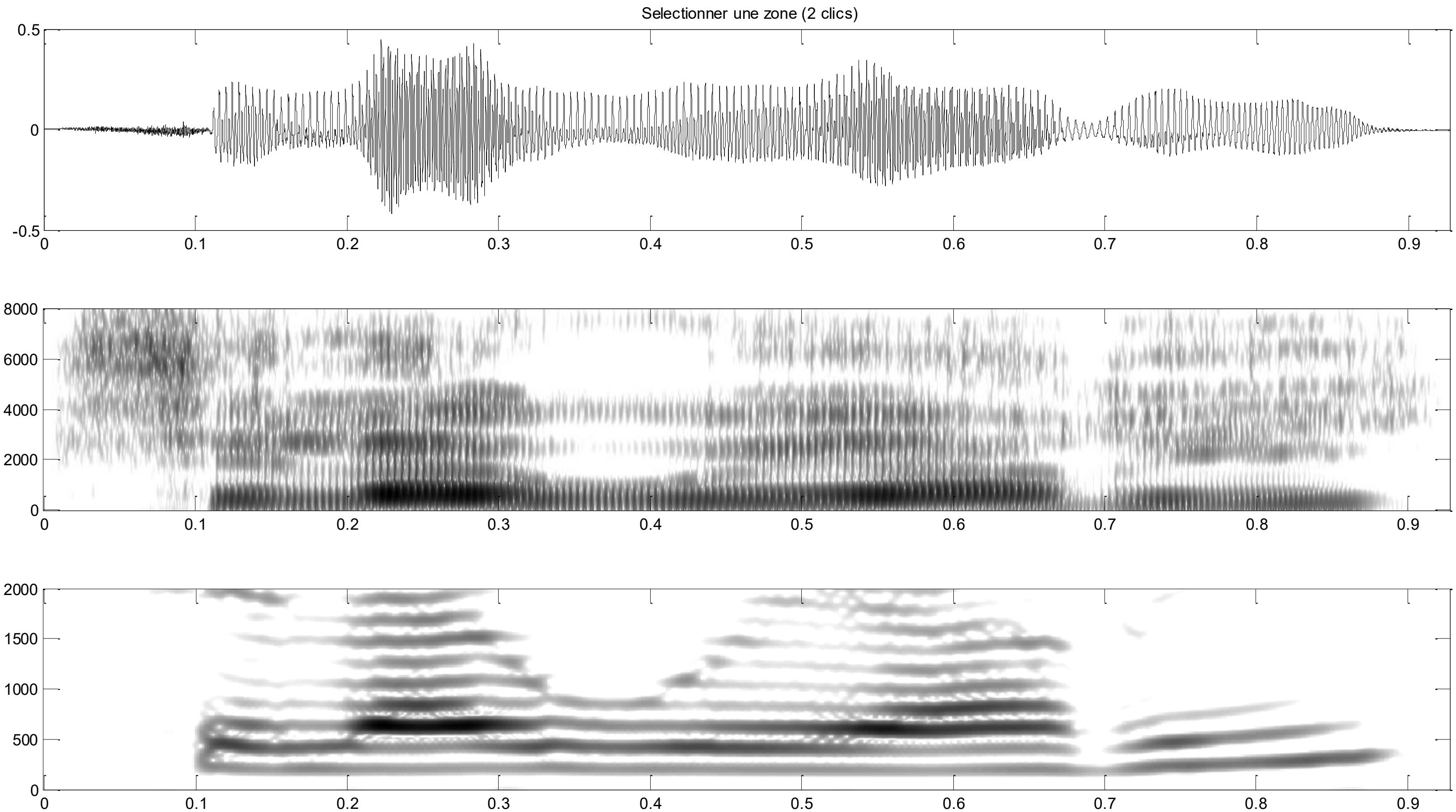

Présentation des enjeux
Le signal acoustique de la parole

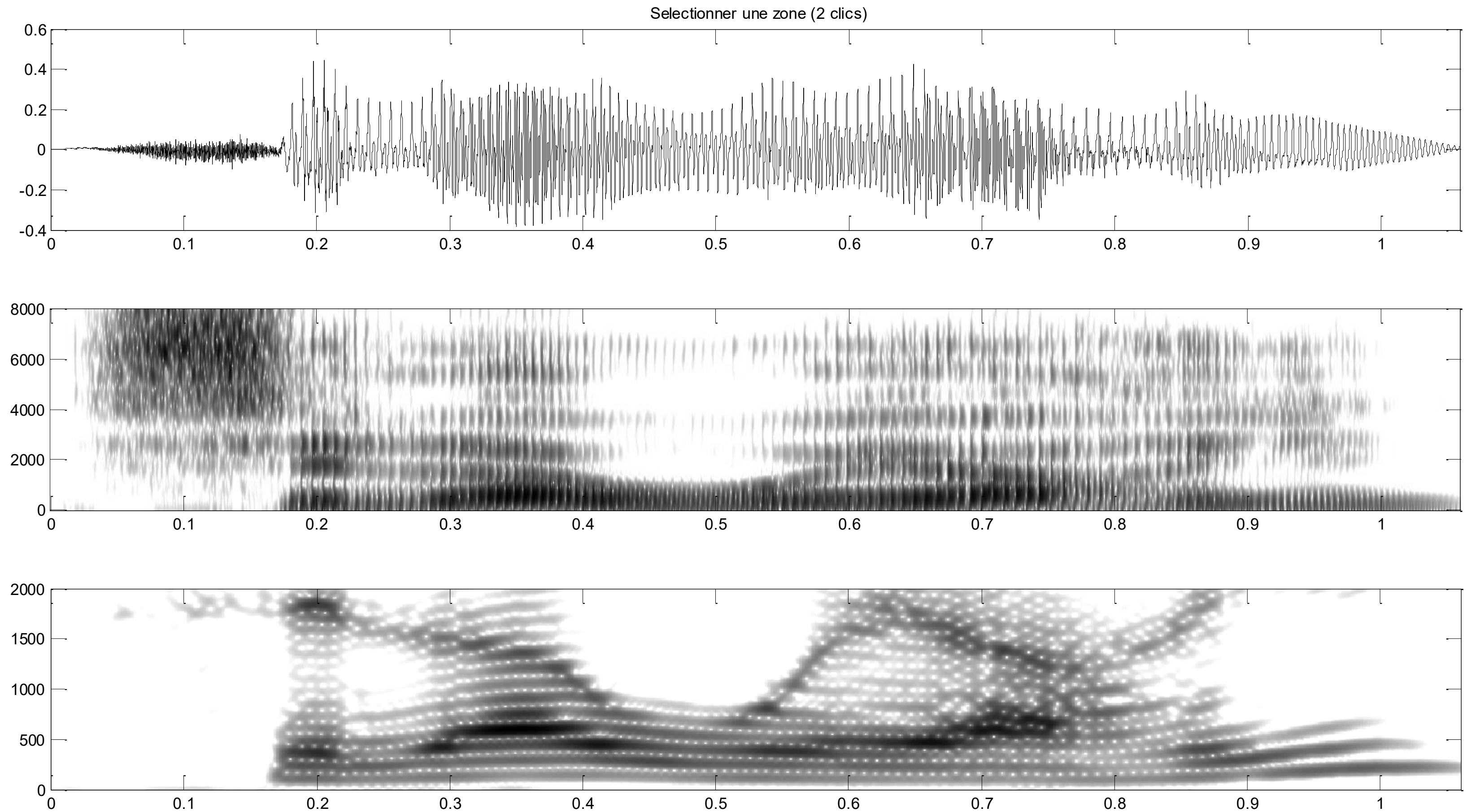

Présentation des enjeux
Produce speech sounds

Consonant

- Place of articulation
  - Labial, alveolar, etc.
- Manner of articulation
  - Stop, Fricative, etc.
  - Voiced and unvoiced

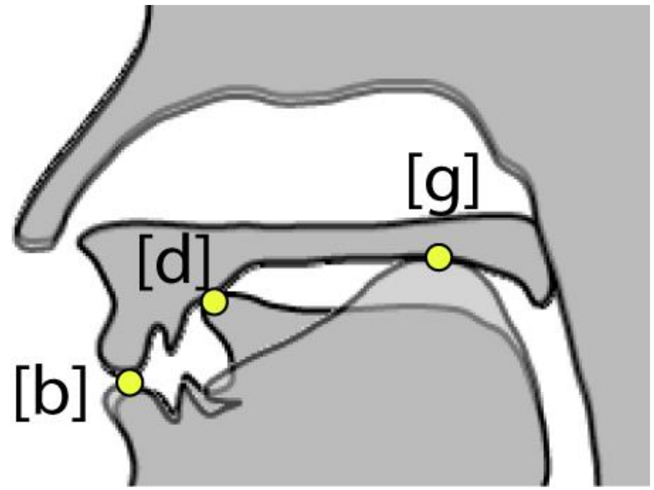

Signal de Parole
Formant

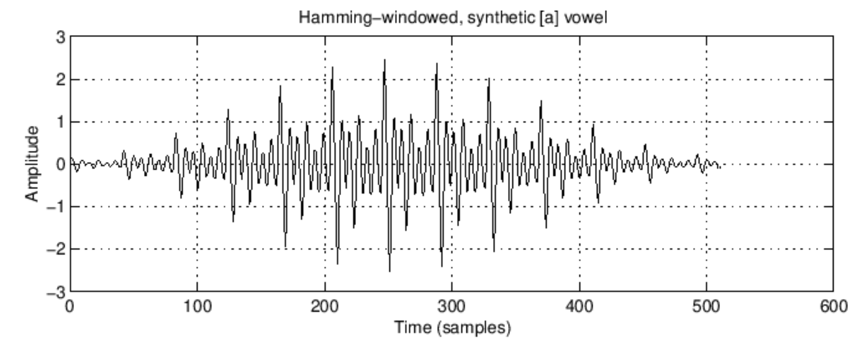

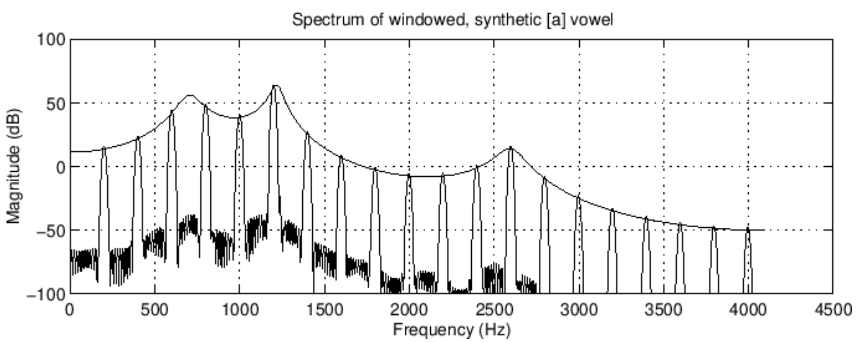

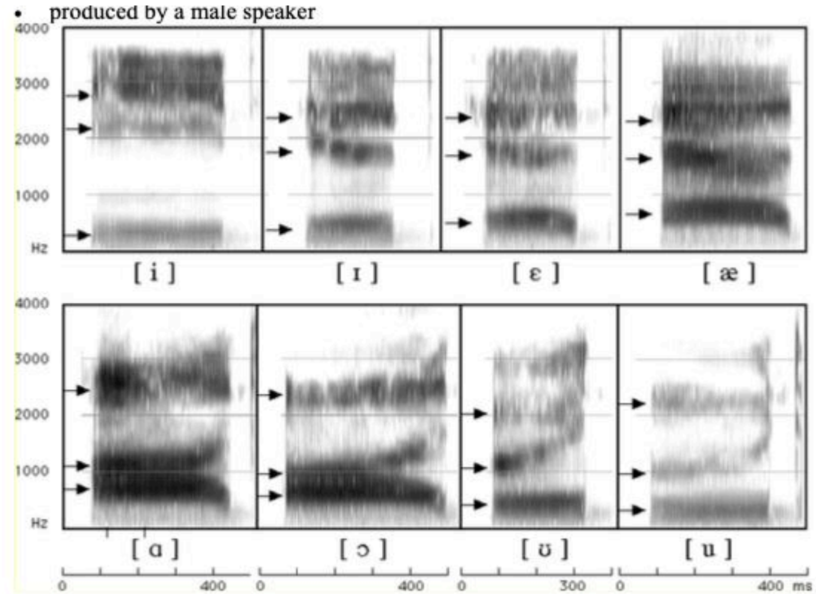

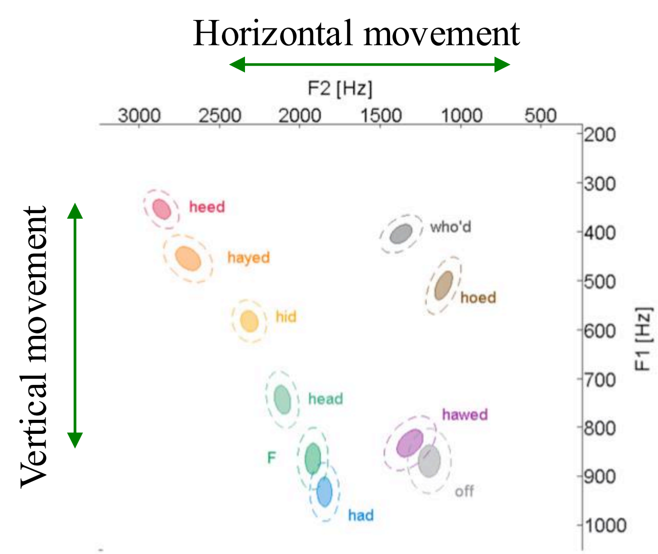

Présentation des enjeux
Produce speech sounds

Vowel
- Source-flilter theory
  - Vocal tract shape

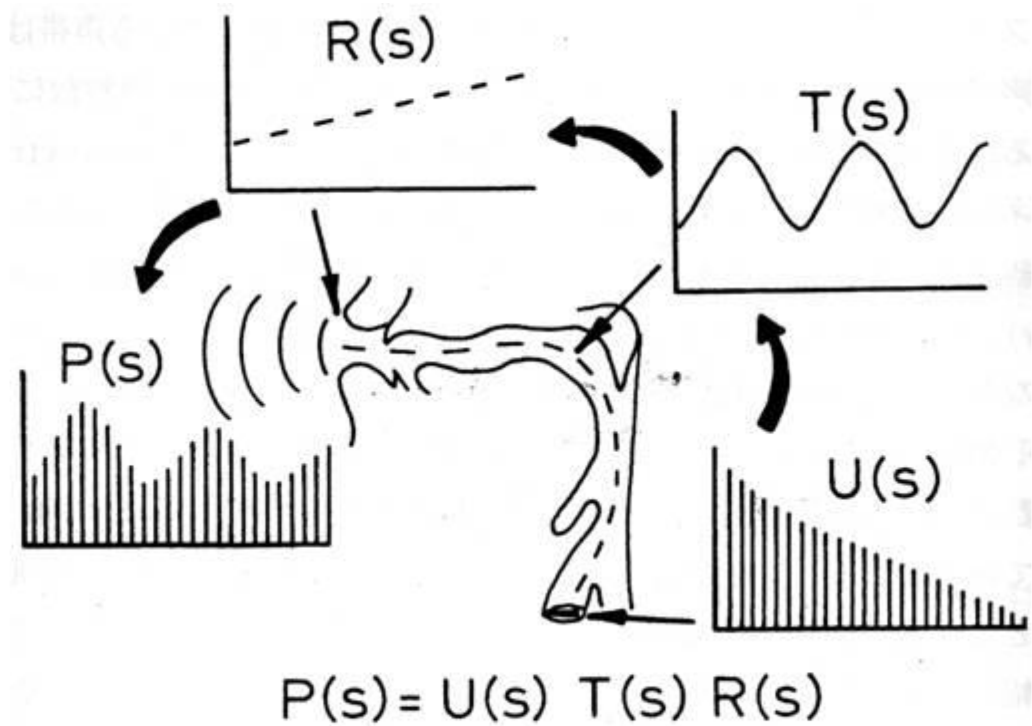

Stevens KN, 1998

Présentation des enjeux
Speech motor control

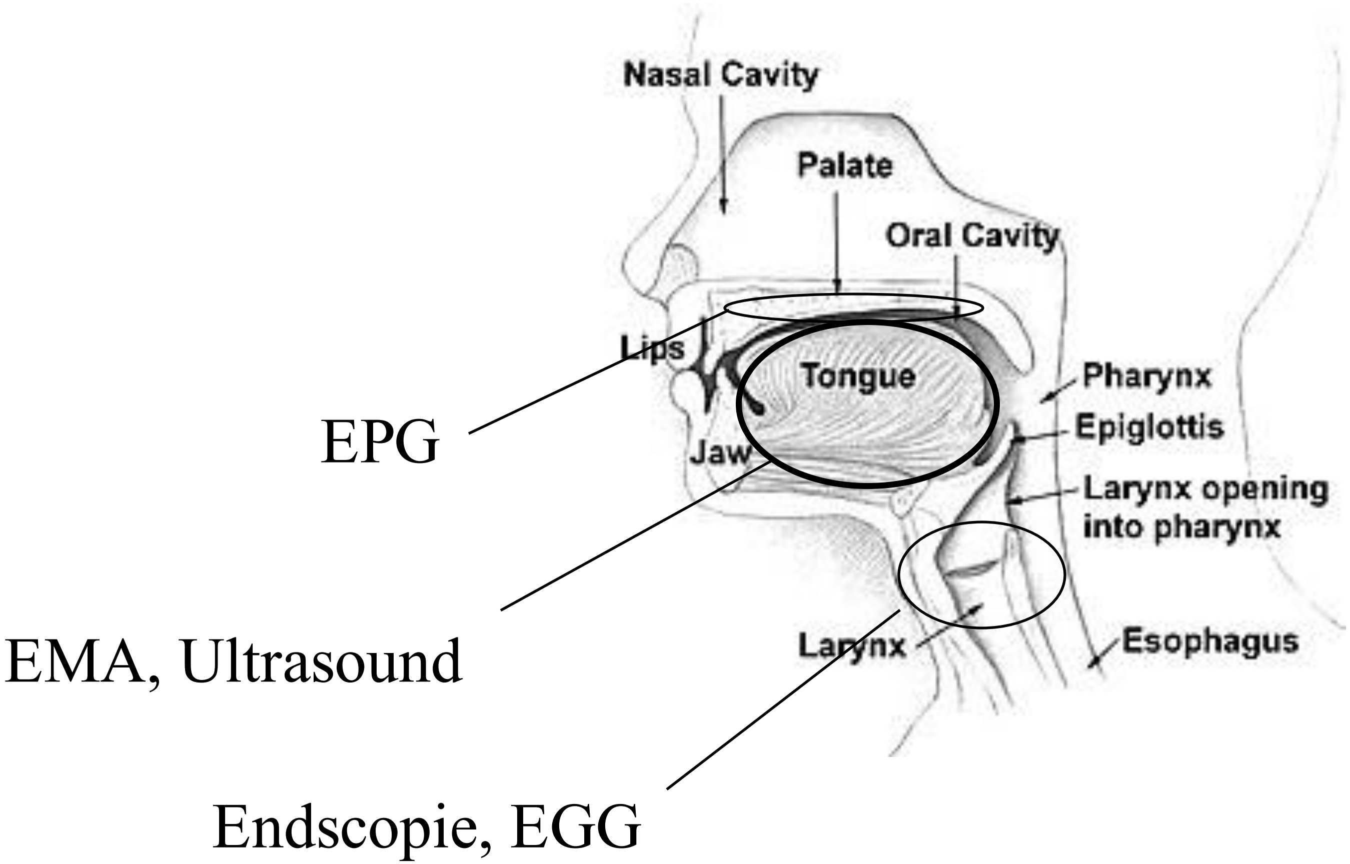

Mesures cinématiques
Anatomical basis for vocal tract

Anatomical basis

Coupe sagittale du conduit vocal

Netter (1984)
Atlas of Human Anatomy.

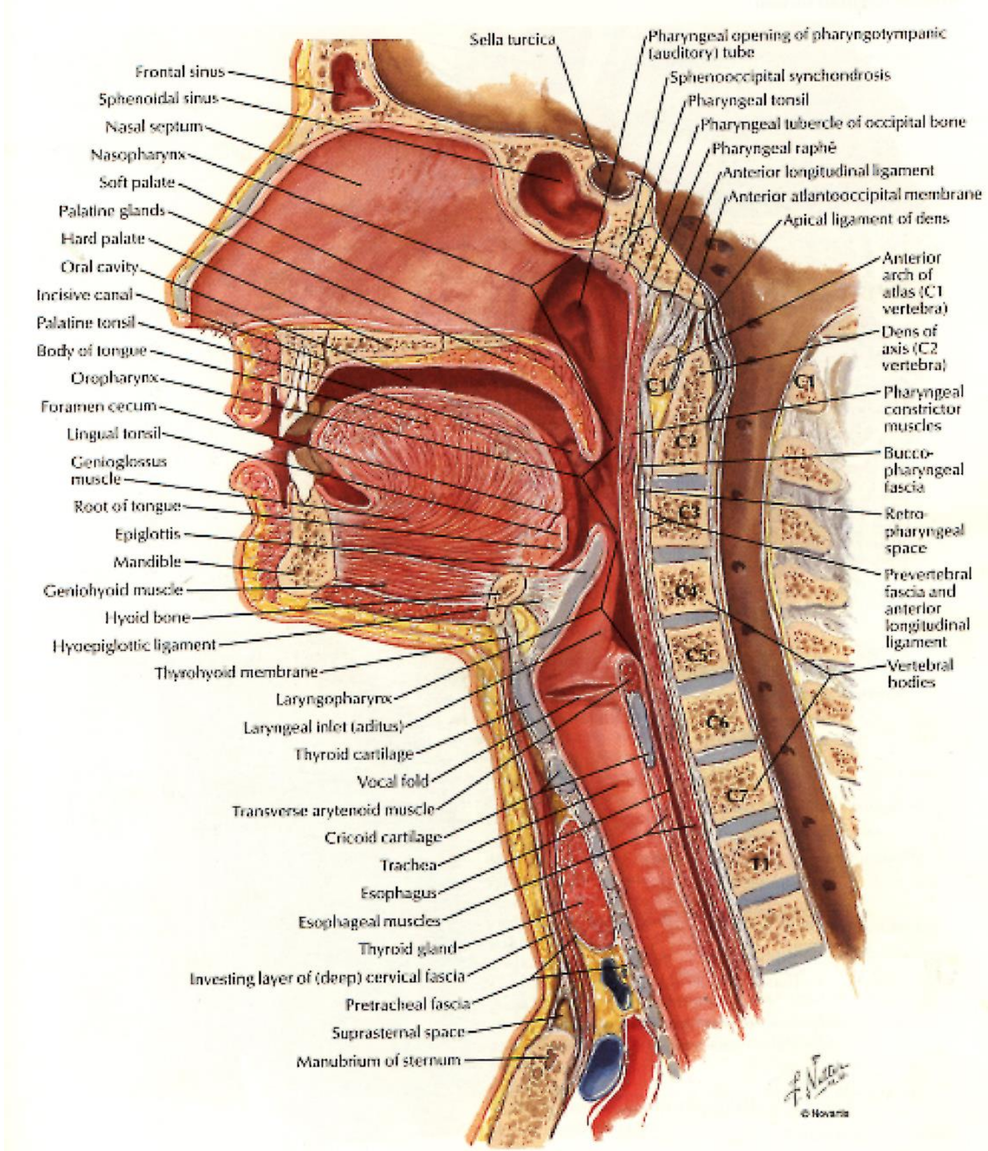

Anatomical basis

Vue de dessus

Netter (1984)
Atlas of Human Anatomy.

Tongue and Mouth
Horizontal Section - Superior View

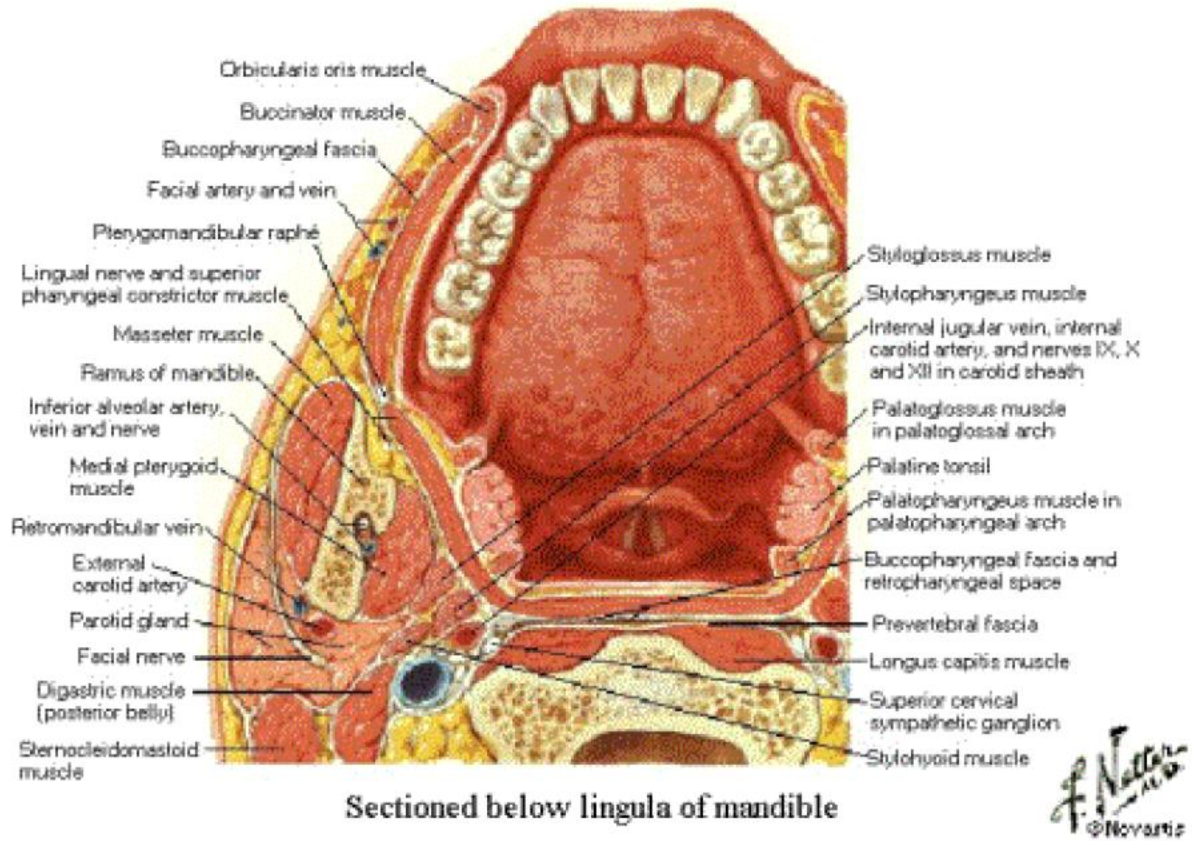

Sectioned below lingula of mandible

Anatomical basis

Vue de profil

Netter (1984)
Atlas of Human Anatomy.

Muscular hydrostat

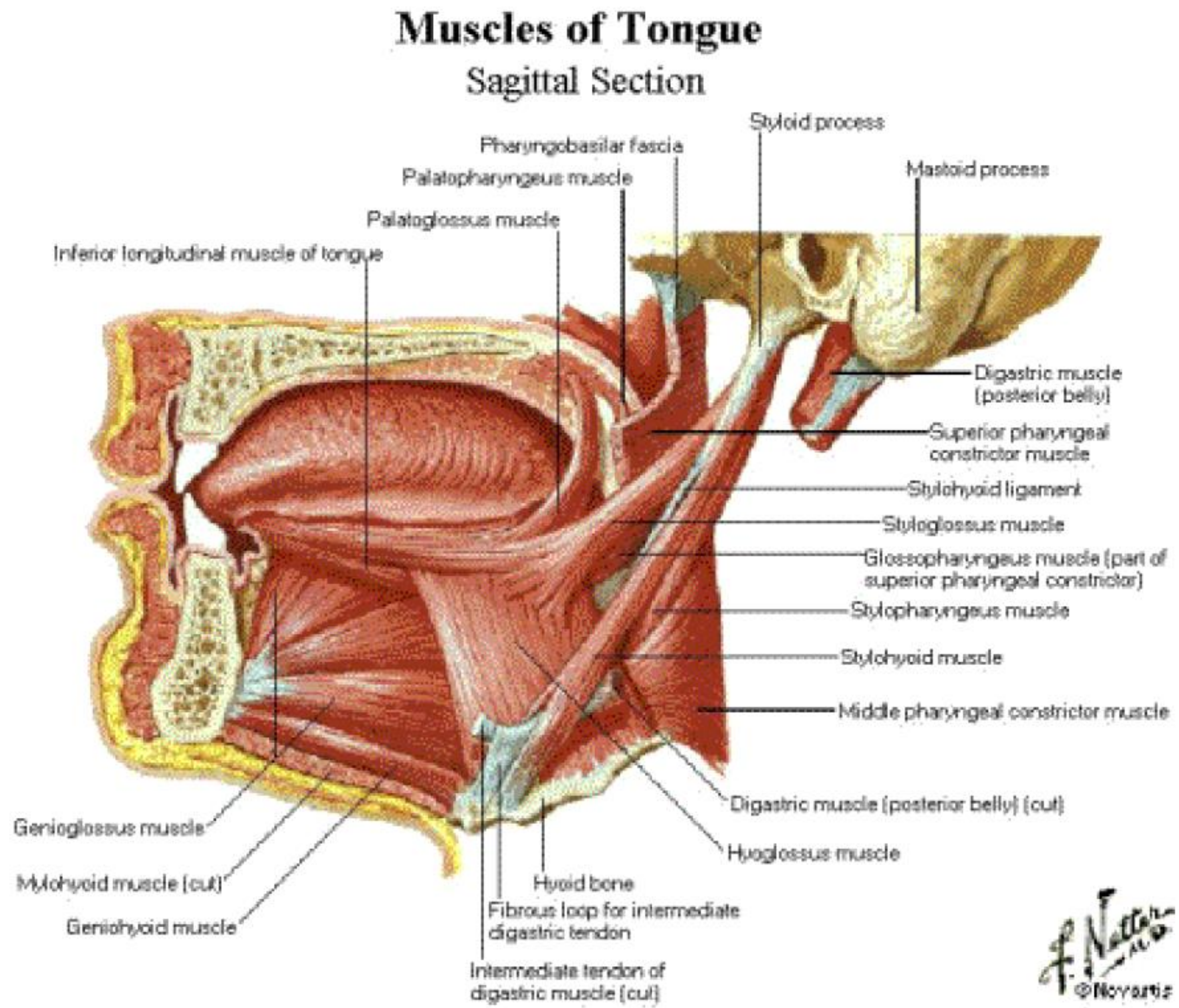

Anatomical basis

Coupe transversale

Netter (1984)
Atlas of Human Anatomy.

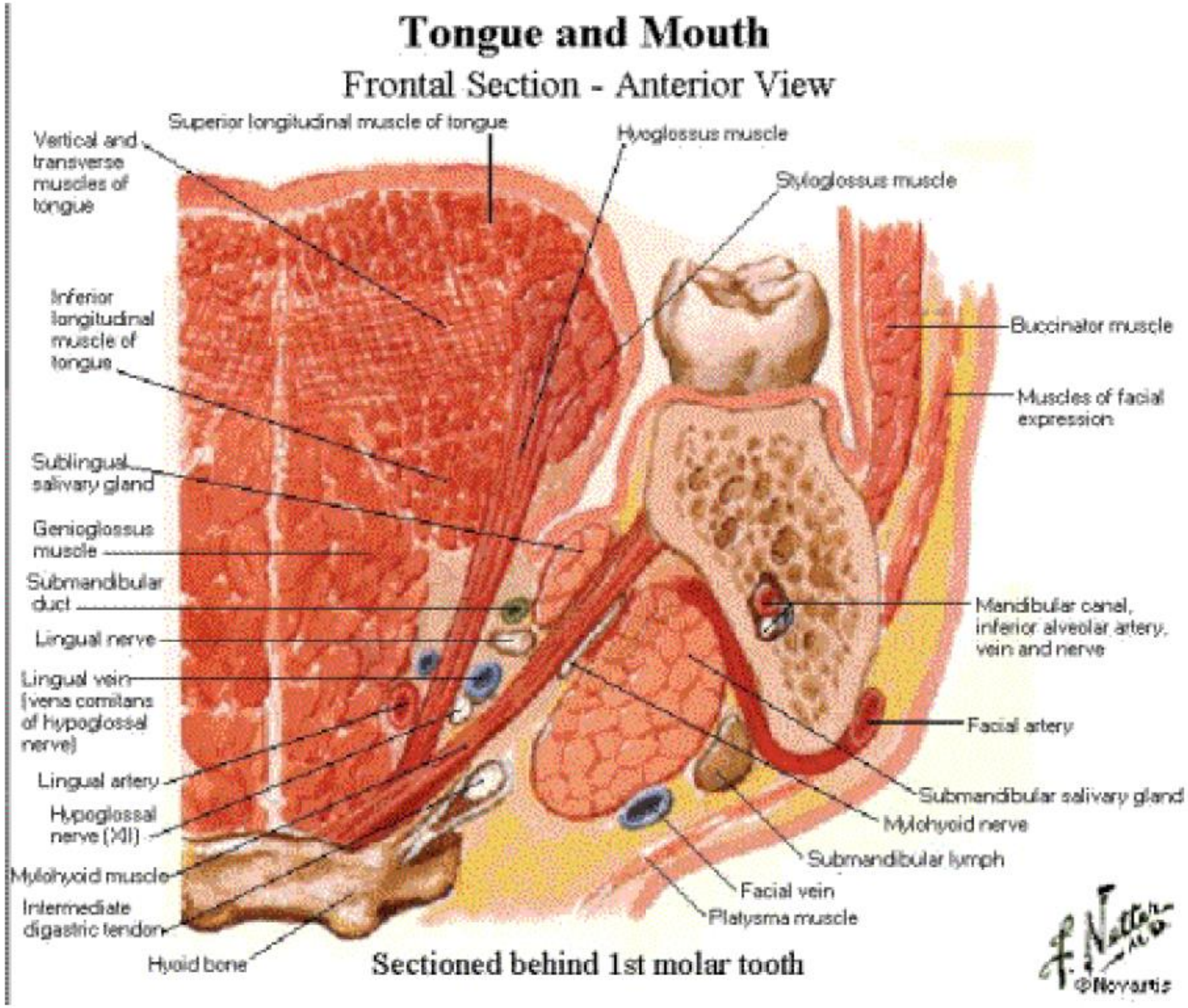

Anatomical basis

Berkovitz et al. (2003), 3D Head and Neck Anatomy with Special Senses and Basic Neuroanatomy (www.anatomy.tv)

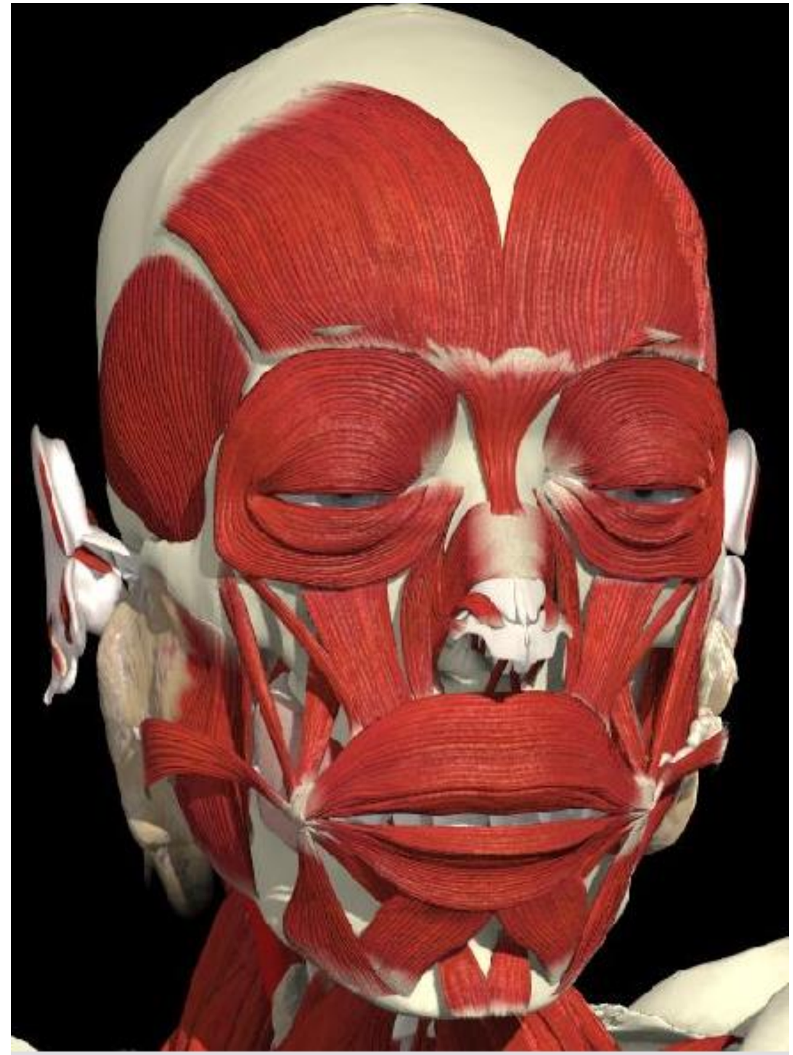

Anatomical basis

O'Dwyer NJ et al. JSHR, 1981

Mesures cinématiques Electromagnétométrie

ElectroMagnetic Midsagittal Articulometer (EMMA)

Perkell J.S et al.(1992). The Journal of the Acoustical Society of America, 92(6), 3078-3096.

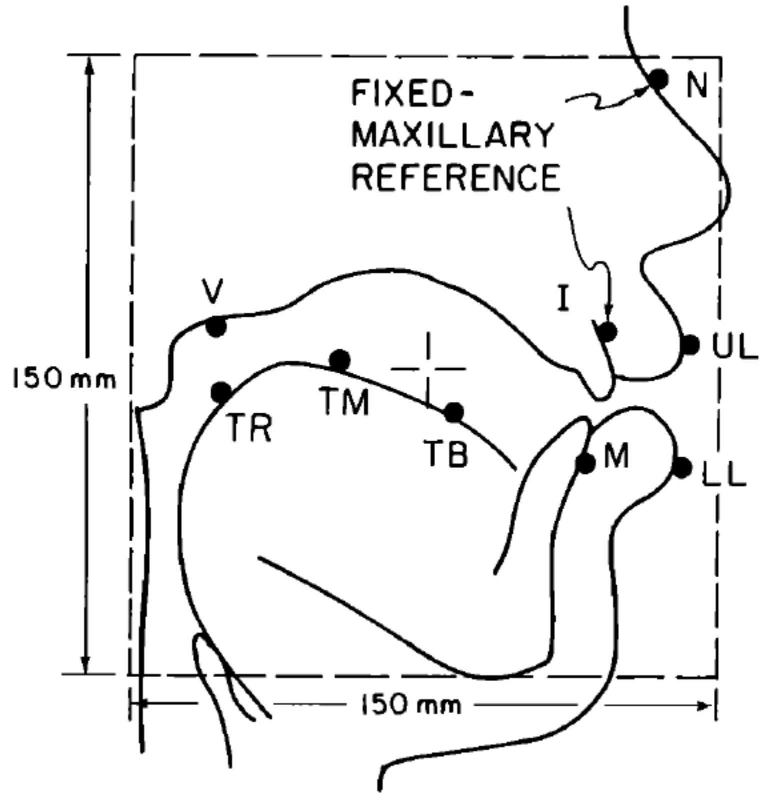

FIG. 1. A schematic midsagittal view of a subject with nine possible measurement points (indicated by filled circles) corresponding to fixed points on the bridge of the nose (N) and the upper central incisors (I) for a maxillary frame of reference, and movable points on the mandible (M), lips (UL,LL), tongue (TB, TM, TR) and velum (V).

Perkell J.S et al.(1992). The Journal of the Acoustical Society of America, 92(6), 3078-3096.

F1, F2, F3
autour de 60 kHz

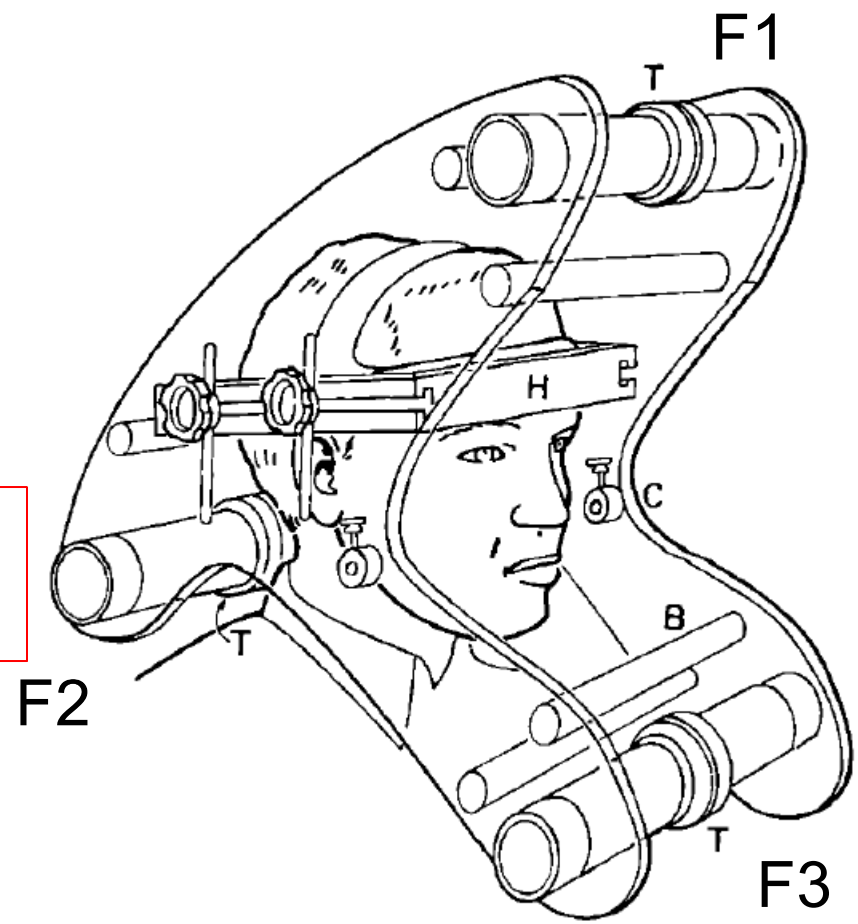

ElectroMagnetic Midsagittal Articulometer (EMMA)

$$i(t) = \frac{k.\varphi(t)}{d^3}$$

$$i(t) = \frac{k.\varphi(t)}{d^3} * \cos\theta$$

Perkell J.S et al.(1992). The Journal of the Acoustical Society of America, 92(6), 3078-3096.

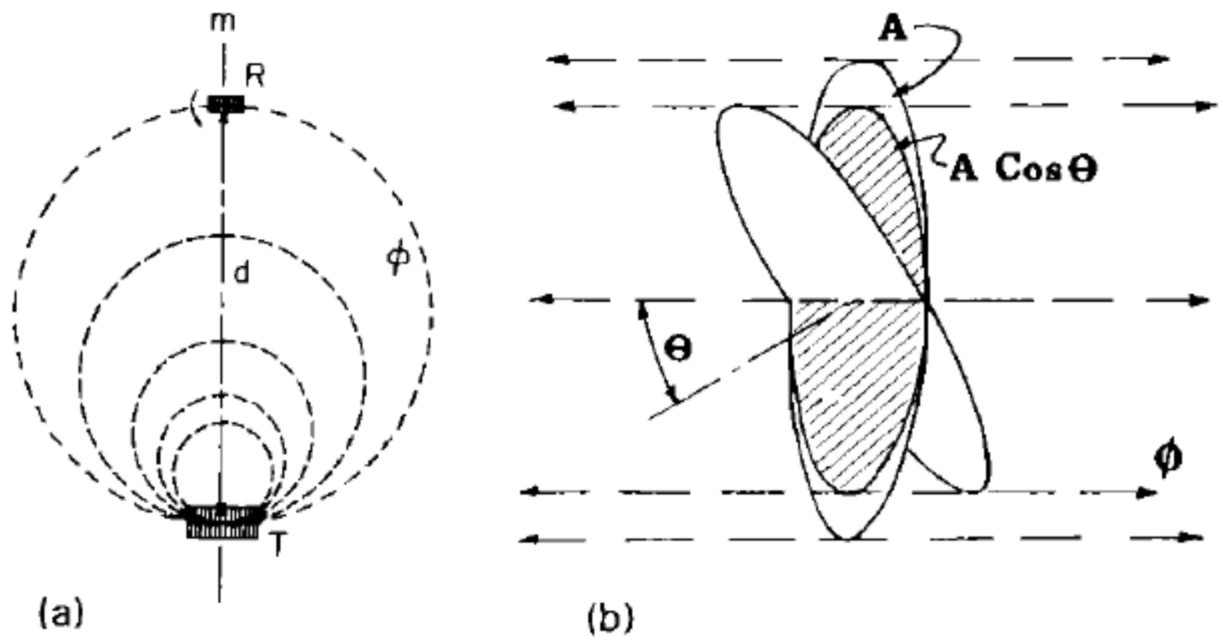

R: Tannsducer coil
T: Transmitter coil

ElectroMagnetic Midsagittal Articulometer
(EMMA)

Perkell J.S et al.(1992). The Journal of the Acoustical Society of America, 92(6), 3078-3096.

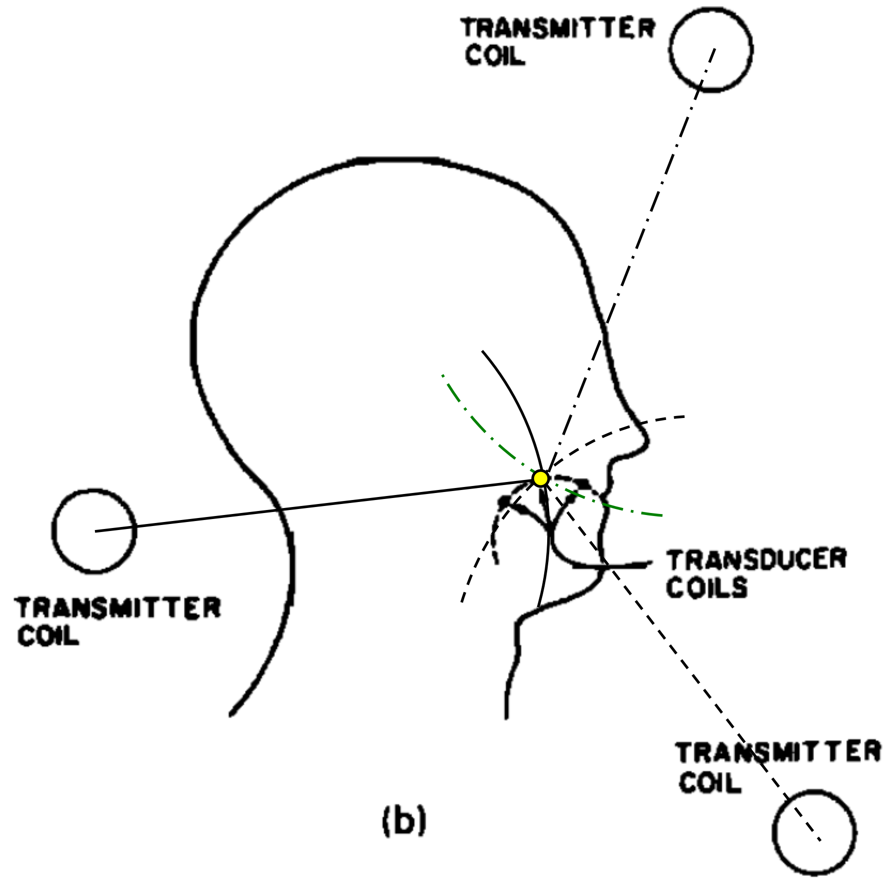

Electromagnétomètres

2D
AG200 – Carstens

5D
AG500 – Carstens

5D
AG501 – Carstens

5D
Wave – NDI

Electromagnétométrie: 5D Articulographes

Les capteurs ne doivent plus être
dans le plan sagittal !

5 variables:

•3 coordonnées cartésiennes : x, y, z

•2 angles : inclinaison (tilt)
rotation horizontale (twist)

6 bobines émettrices

→ Pas de solution analytique – Problème optimal

Electromagnétométrie: 5D Articulographes

Correction efficace des mouvements de la tête

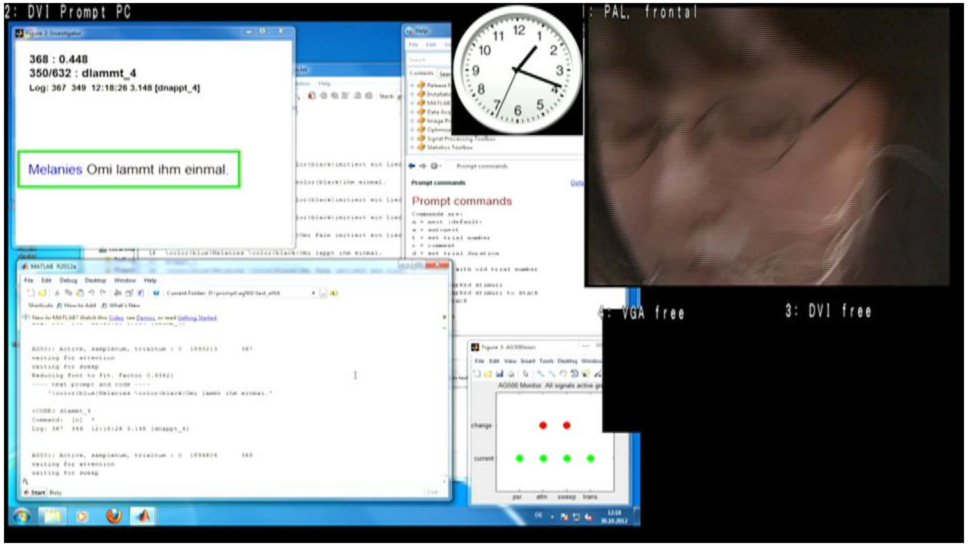

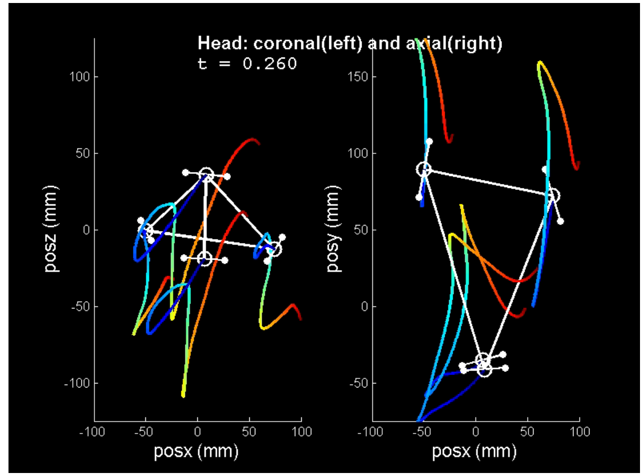

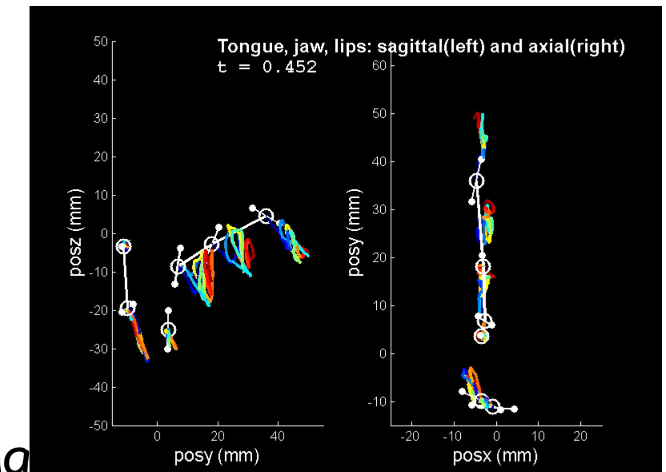

Phil Hoole
Institut für Phonetik und Sprachverarbeitung
Munich

Limits

- Number of recorded points
- Relatively expensive

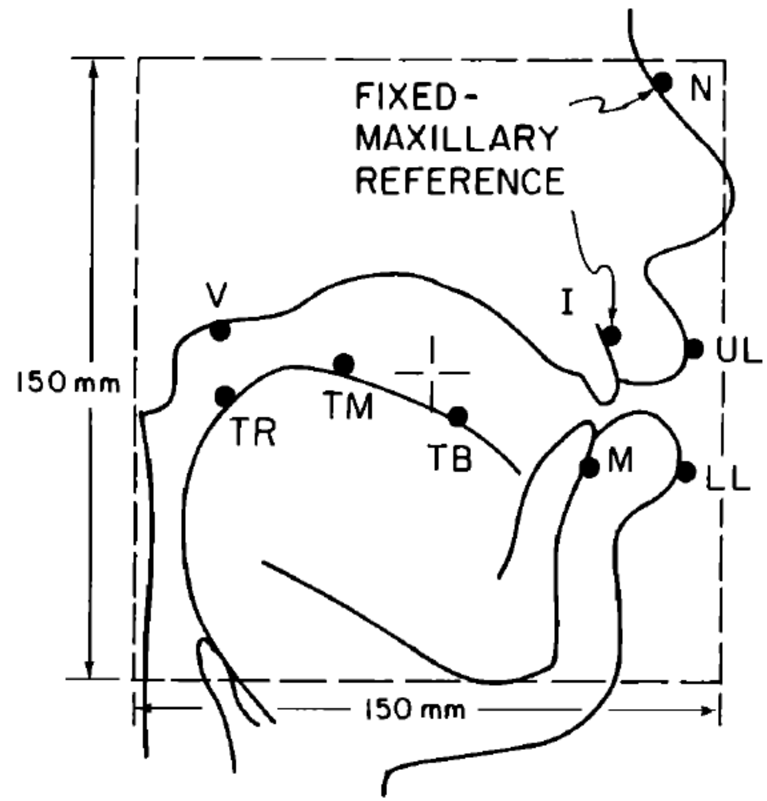

FIG. 1. A schematic midsagittal view of a subject with nine possible measurement points (indicated by filled circles) corresponding to fixed points on the bridge of the nose (N) and the upper central incisors (I) for a maxillary frame of reference, and movable points on the mandible (M), lips (UL,LL), tongue (TB, TM, TR) and velum (V).

Perkell J.S et al.(1992). The Journal of the Acoustical Society of America, 92(6), 3078-3096.

Electromagnétomètres : Mesures

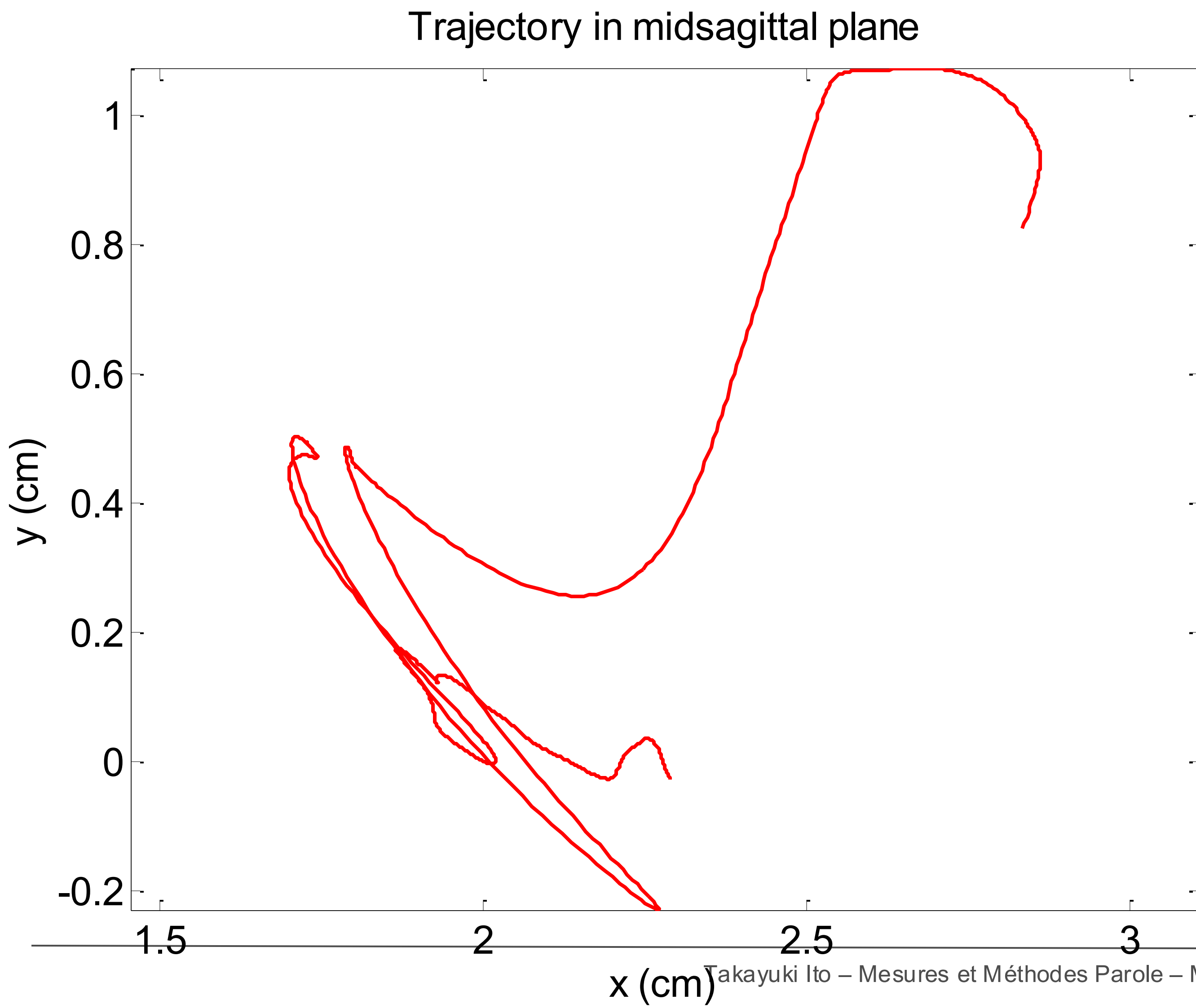

Electromagnétomètres : Mesures

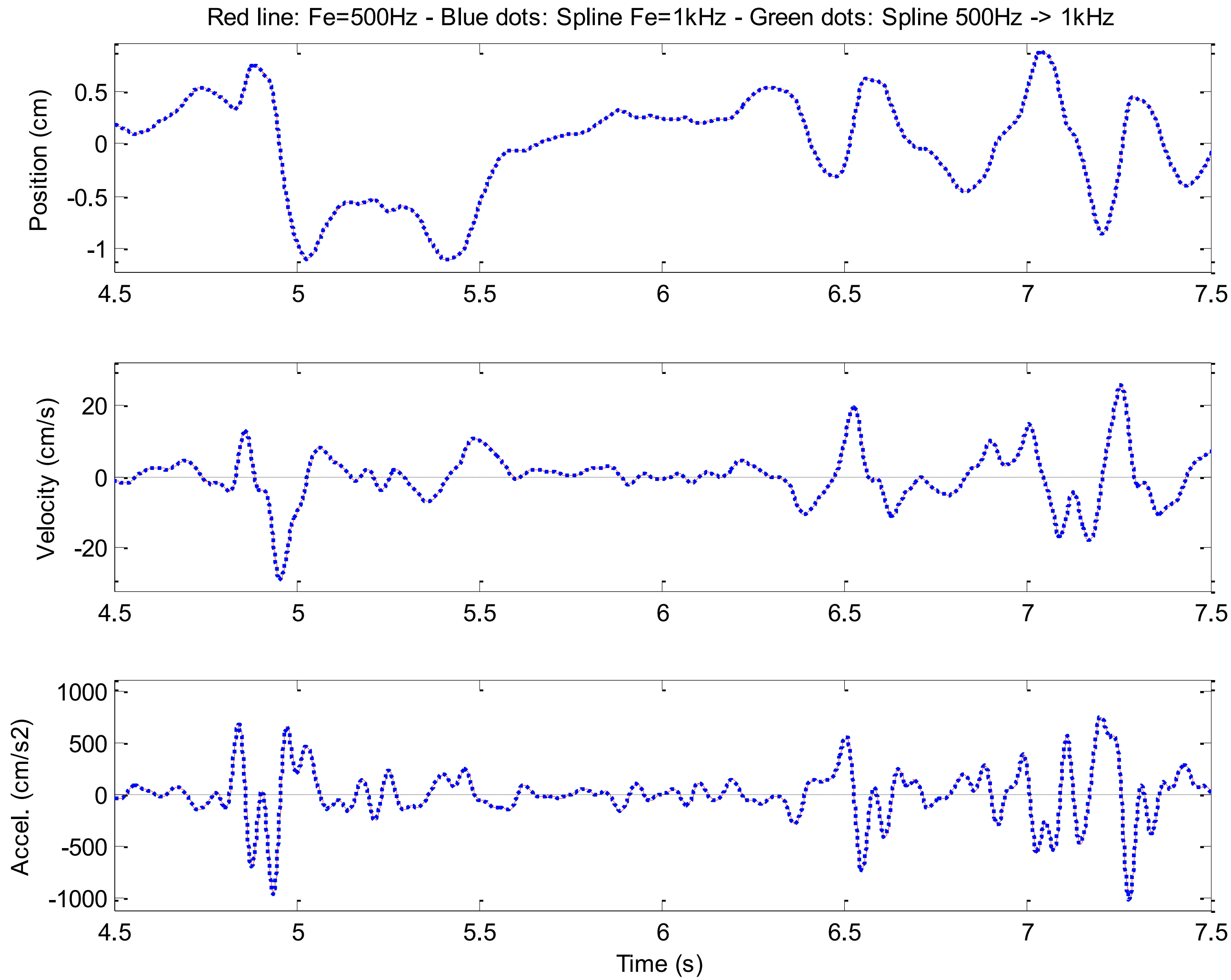

Electromagnétomètres : Segmentation

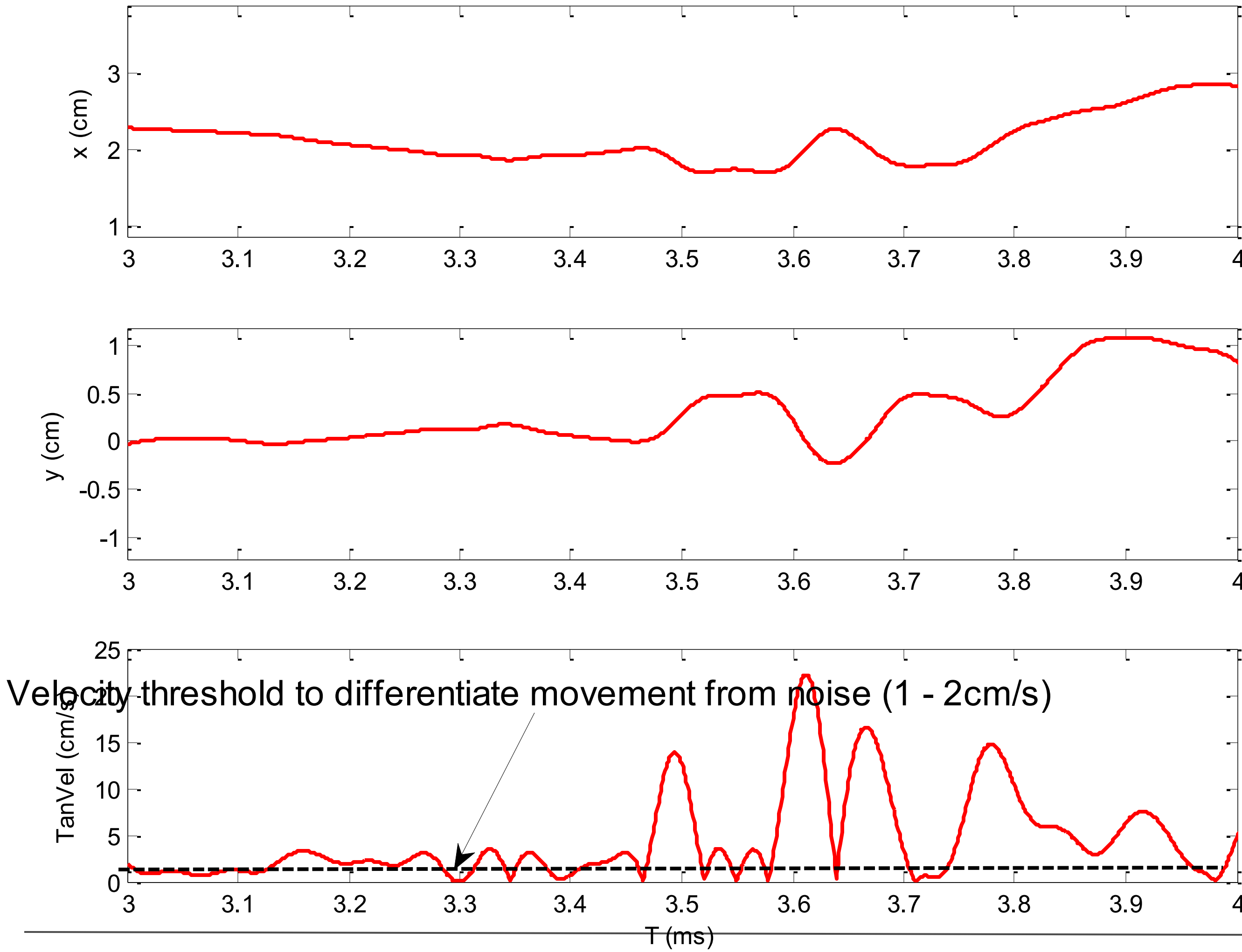

Articulographie : Mesures cinématiques

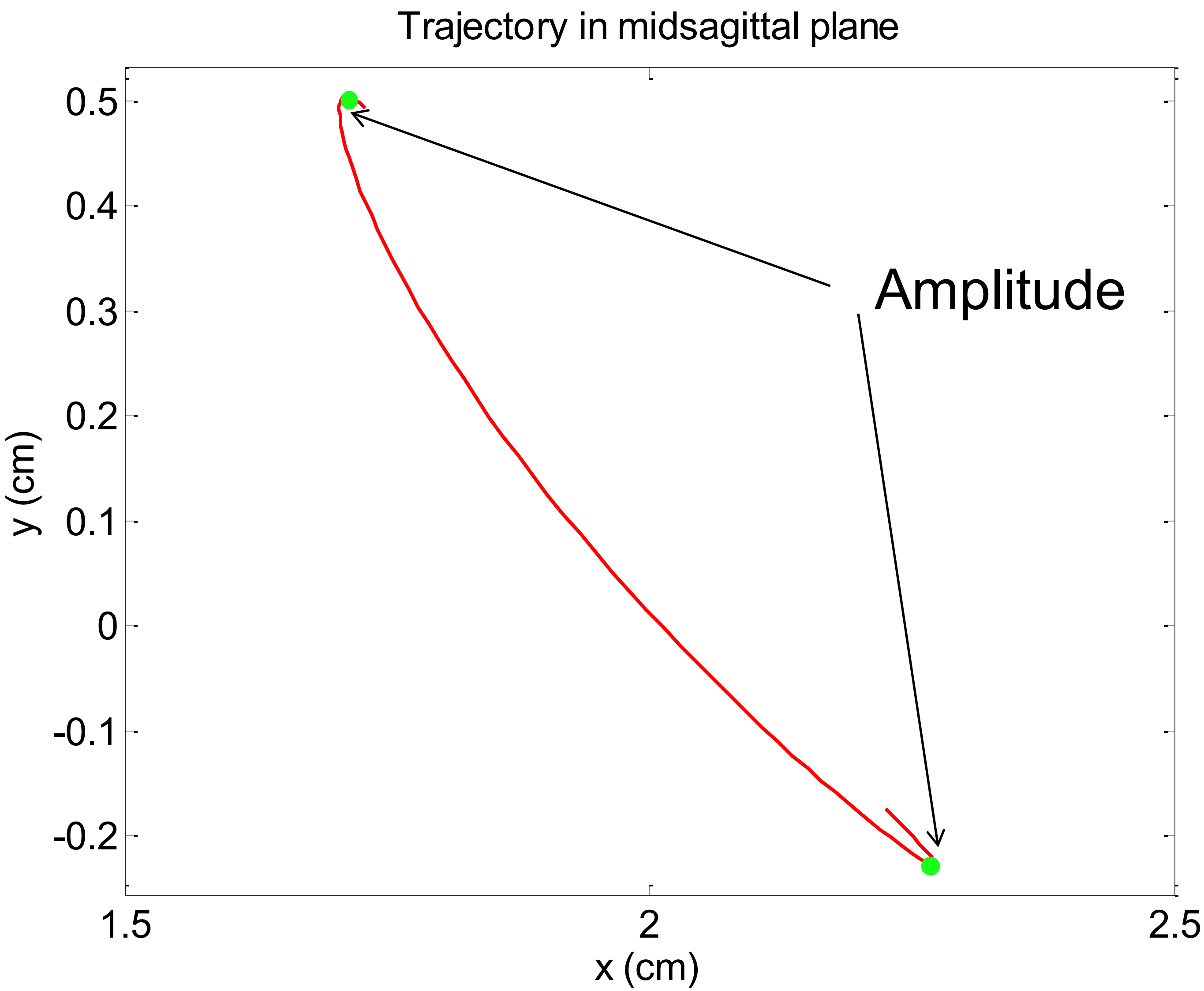

Electromagnétomètres : Mesures

Profil de vitesse

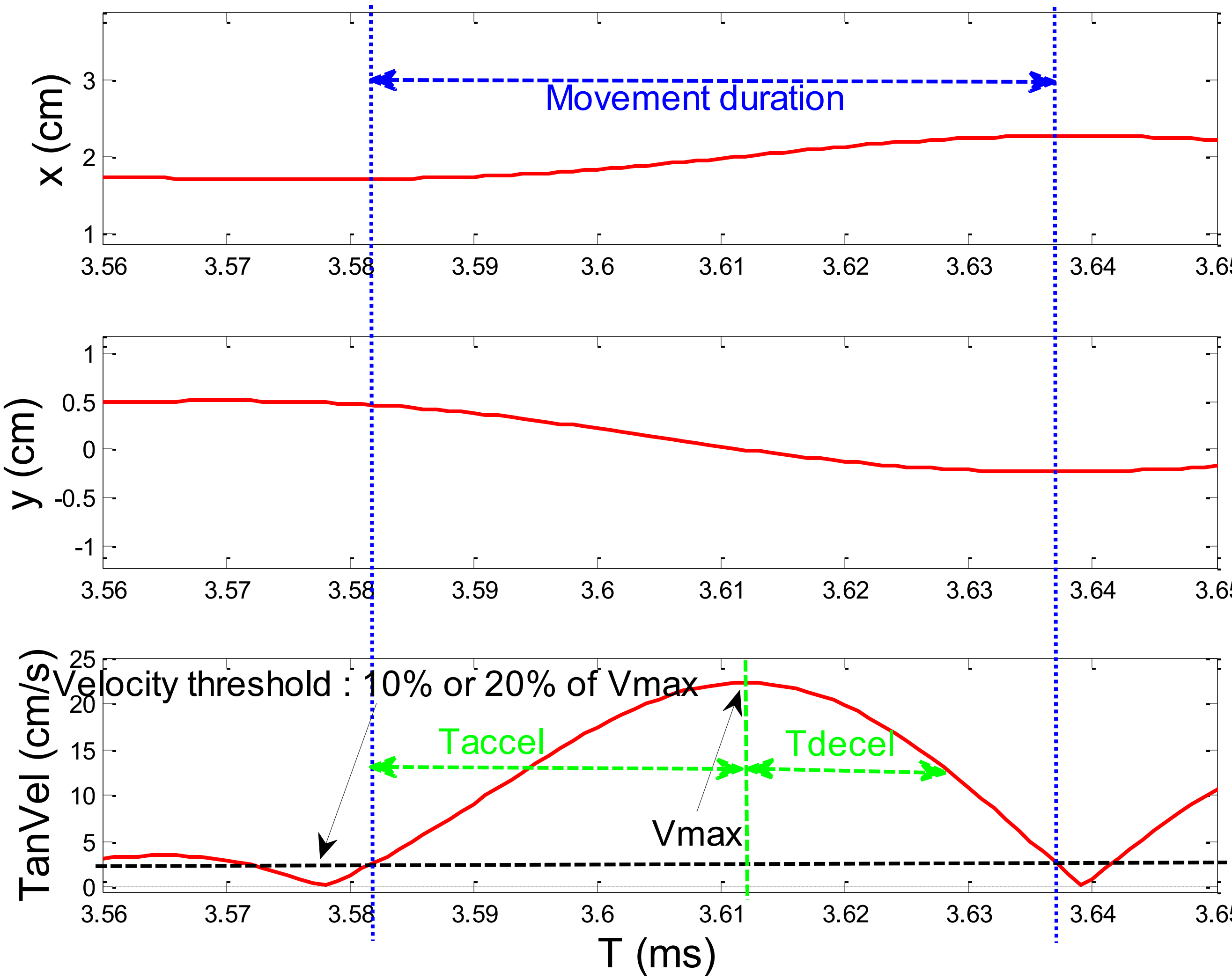

Electromagnétomètres : Evaluer l'optimisation des gestes

Nelson, 1983

time cost: $T =$ movement time

force cost: $A = \max_{t \in (0, T)} |u(t)|,$

impulse cost: $I = \frac{1}{2} \int_0^T |u(t)| dt,$

energy cost: $E = \frac{1}{2U} \int_0^T u^2(t) dt,$

jerk cost: $J = \frac{1}{2} \int_0^T \dot{a}^2(t) dt,$

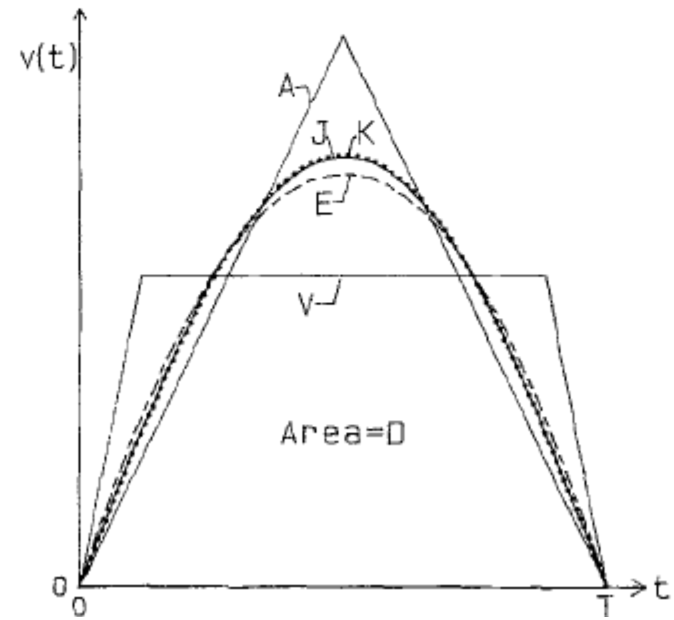

Fig. 3. Comparison of velocity patterns for the same movement time and distance which are optimum with respect to five different objectives: *A*-minimum peak acceleration (solid line), *E*-minimum energy (dashed line), *J*-minimum jerk (solid), *K*-constant stiffness (dotted), and *V*-minimum peak velocity, or impulse (solid line)

Electromagnétomètres : Extract movement characteristics

Ito et al., 2020

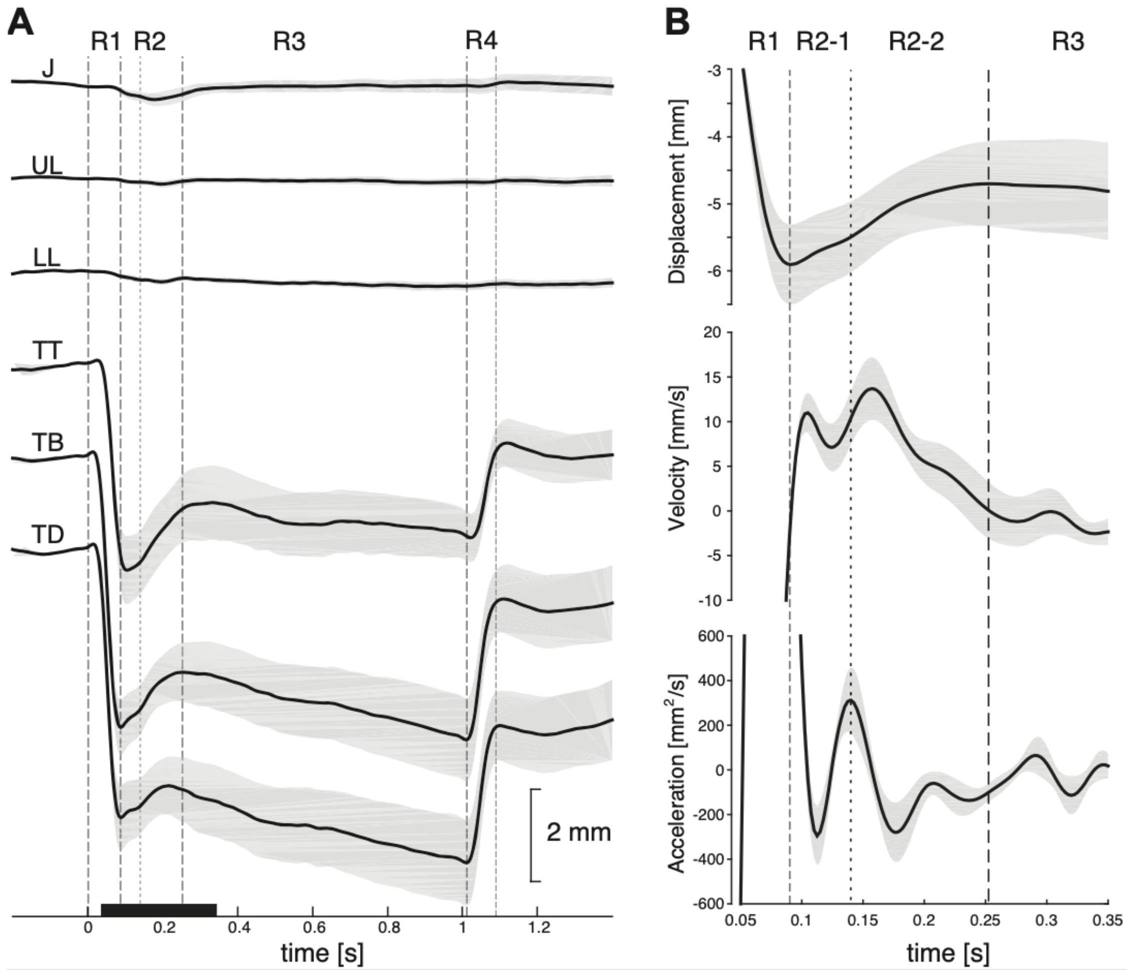

Mesures cinématiques
Echographie – ultrasound system

Echographie - Principes

- Premiers travaux en parole
  - Keller & Ostry (JASA,1983)
  - Ostry & Munhall (JASA,1985)

D=1/2(T* Vsound)
Vsound=1540m/s

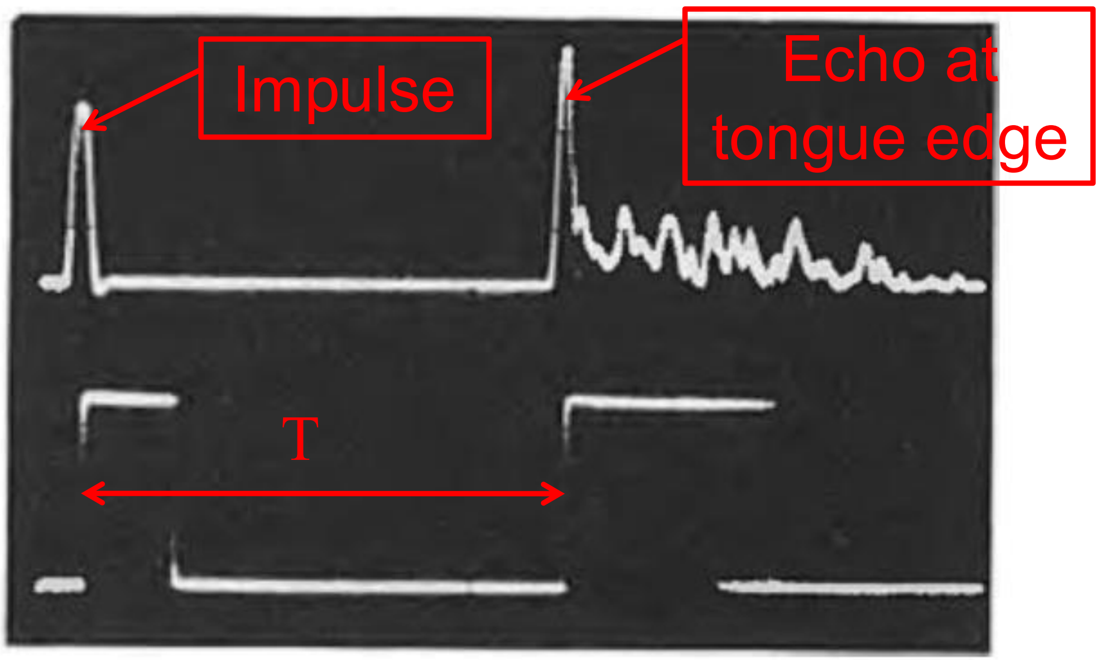

Picker 104 – 3.5 MHz –Single transducer

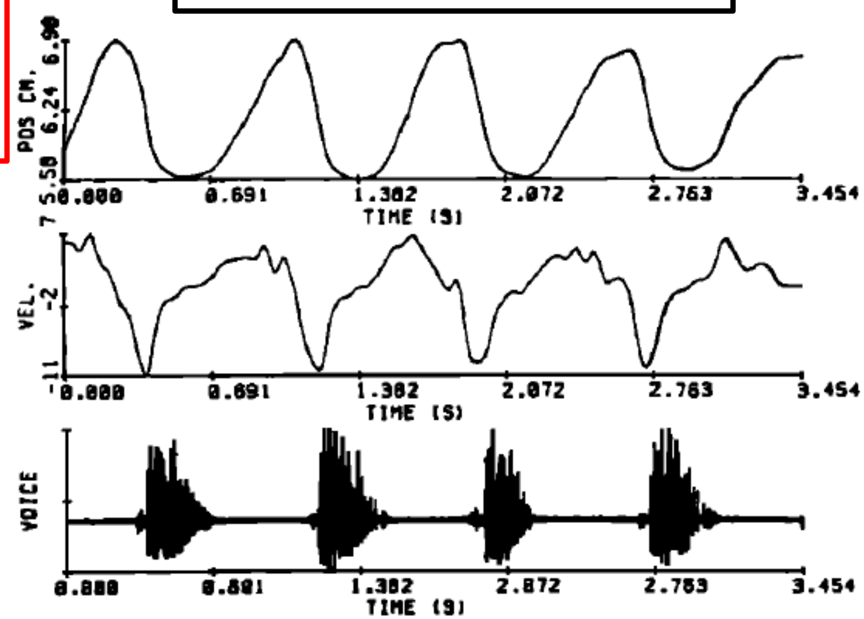

Tongue dorsum – Fs= 1kHz

Echographie

Unser, M., & Stone, M. (1992). *The Journal of The Acoustical Society of America, 91*(5), 3001-3007.

Echographie

- Acoustic Imaging, Model AI5200S
- 2-4 MHz multifrequency array transducer
- Fs=28 Hz
- 90 degree sector
- Contour detection
- Edgetrack - © Video/Image Modeling and Synthesis Lab

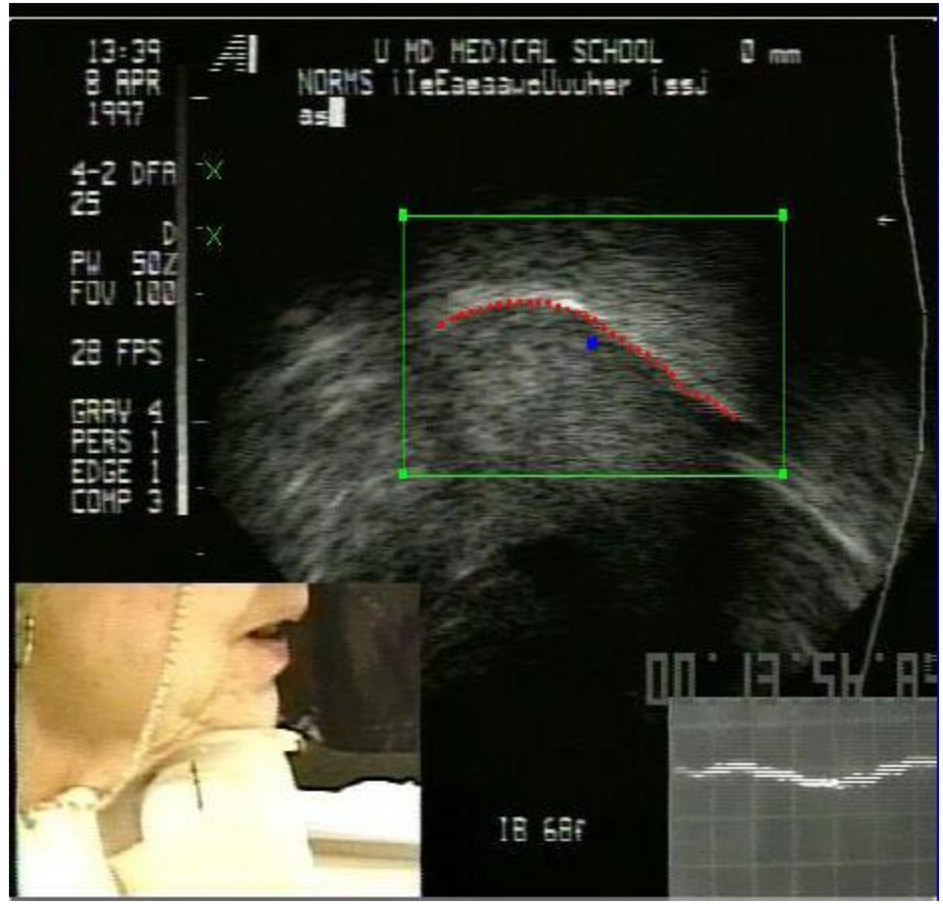

Stone et al., 2010 – Ultrafest V
http://www.haskins.yale.edu/conferences/UltrafestV/present.html

Echographie : Limites

Aubin, 2006

Echographie : Limites

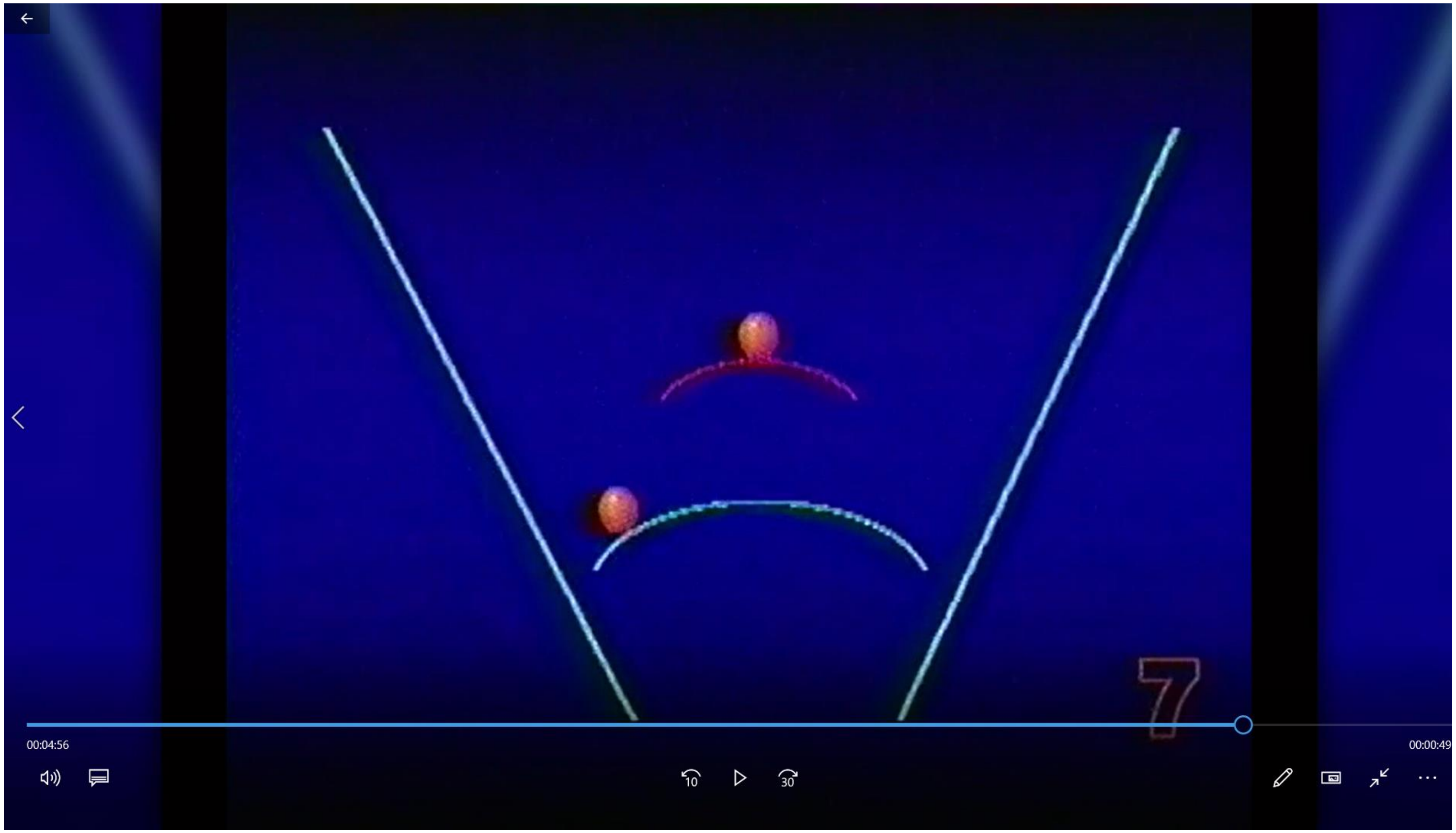

Pas de point de chair

Echographie – Limiter les mouvements de la tête

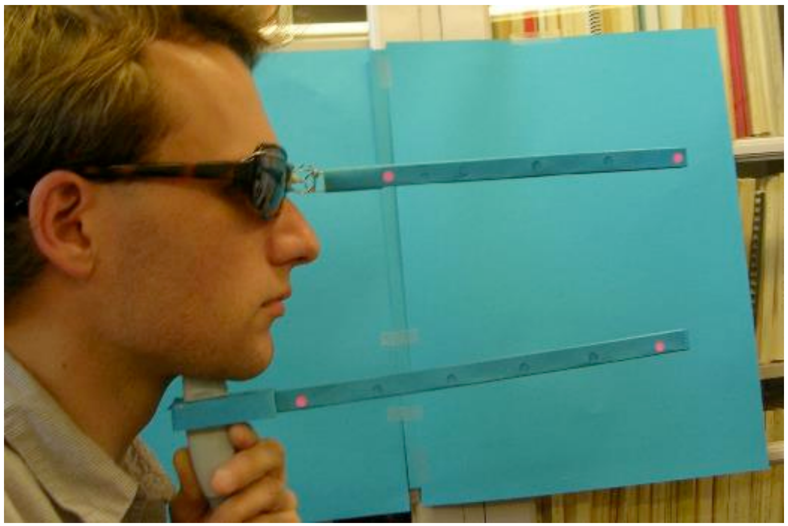

Mielke et al., 2005,University of Arizona

HATS
Stone & Davis, JASA 1995
Image from Hueber, PhD Thesis 2006

Echographie – Compenser les mouvements de la tête

Hocus (Haskins Lab)
Whalen et al., JSLHR 2005

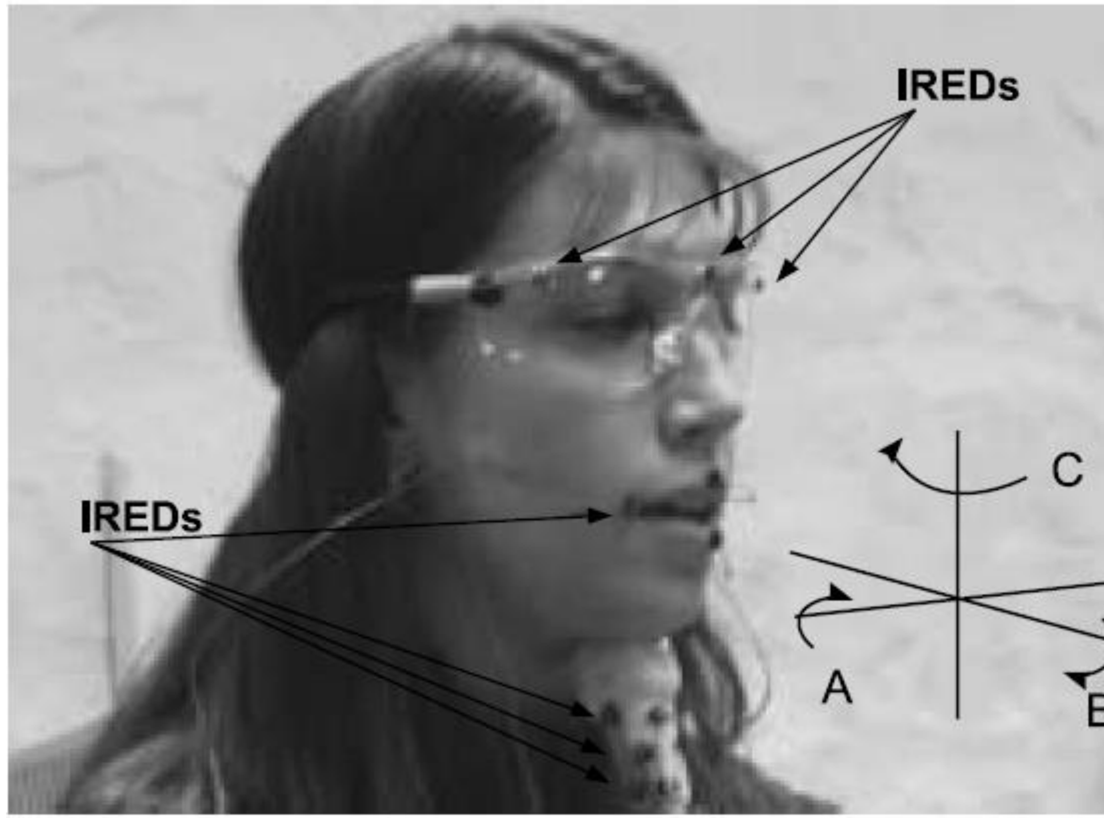

Echographie

Stone et al., 2010, Ultrafest.

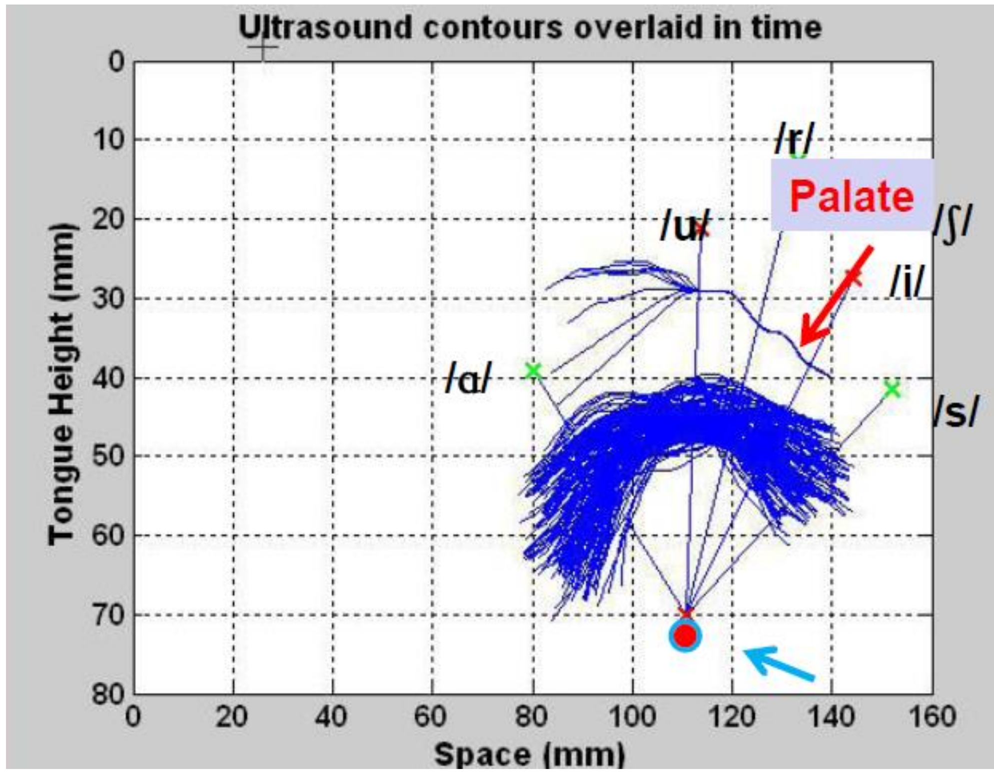

CAVITE (Contour Analysis and Visualization Technique)

Echographie : « Speckle tracking »

Jacob et al., ISSP08

Calcule les variations entre deux images successives

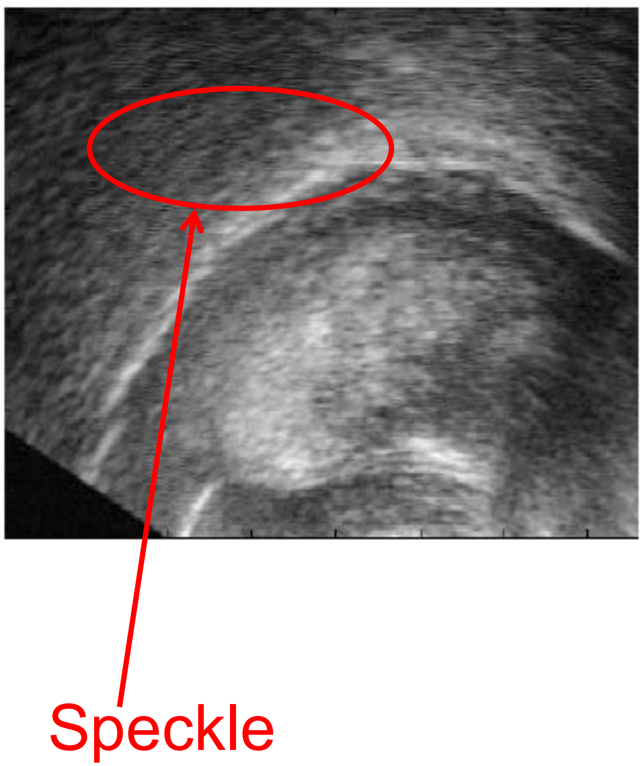

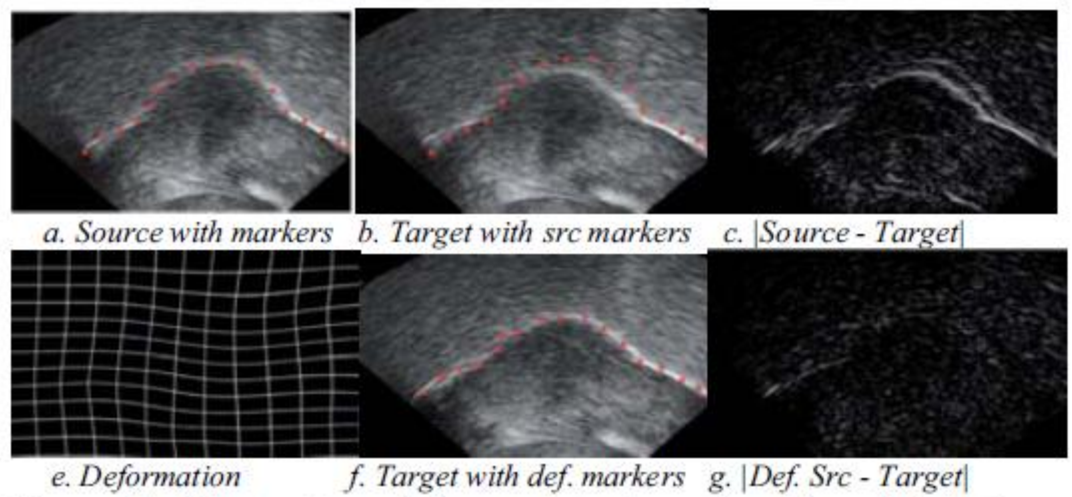

Figure 1: *Illustration of the registration algorithm. (a) is the source image with virtual tongue markers (b) is the target image (next frame) with the markers at the same location as the source. (c) is the absolute difference between the source and the target images. (e) is the estimated deformation and (f) is the target image with the deformed markers. (g) is the difference between the deformed source and the target images.*

Articulographie : Speckle tracking

Jacob et al., ISSP08

Variation des formes de la langue dans une séquence CV

Déplacements de la Consonne (Ref) à la Voyelle

Début de groupe accentuel

Début de mot

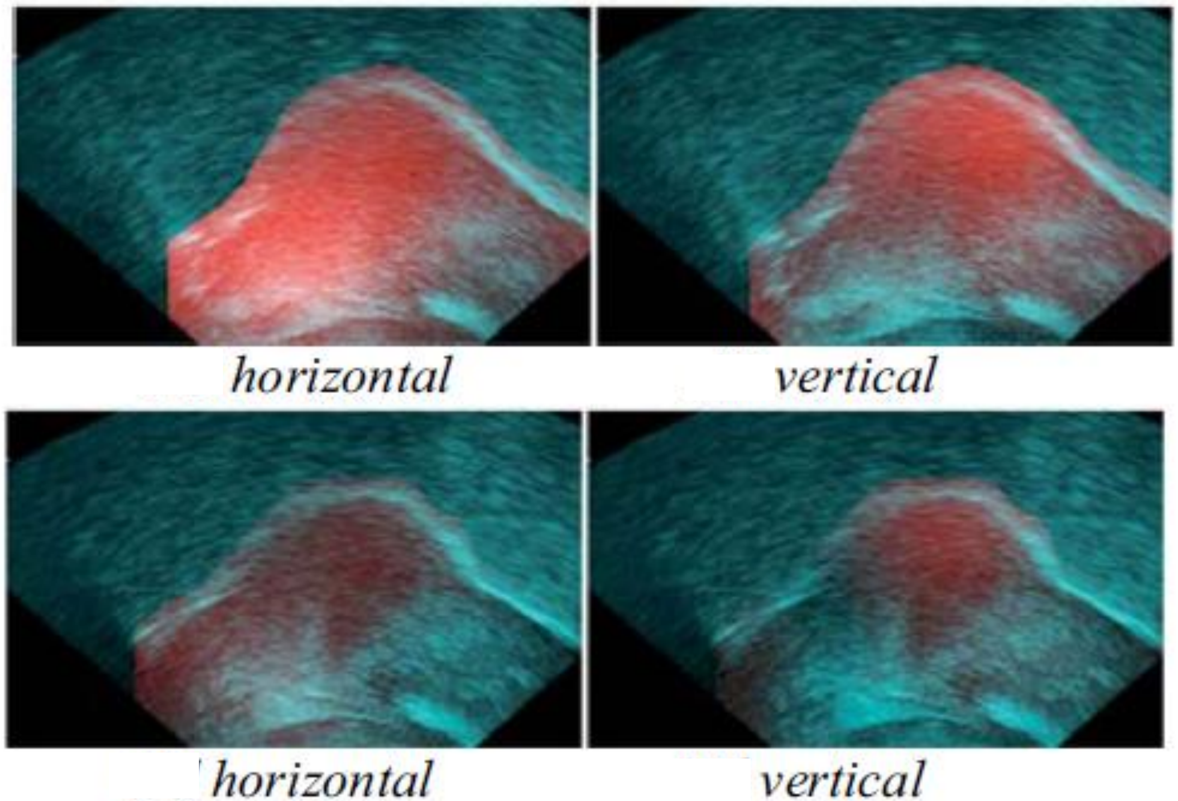

Articulographie : Speckle tracking

Jacob et al., ISSP08

Variation des formes de la langue dans une séquence CV

Vitesse

Début de groupe accentuel

Début de mot

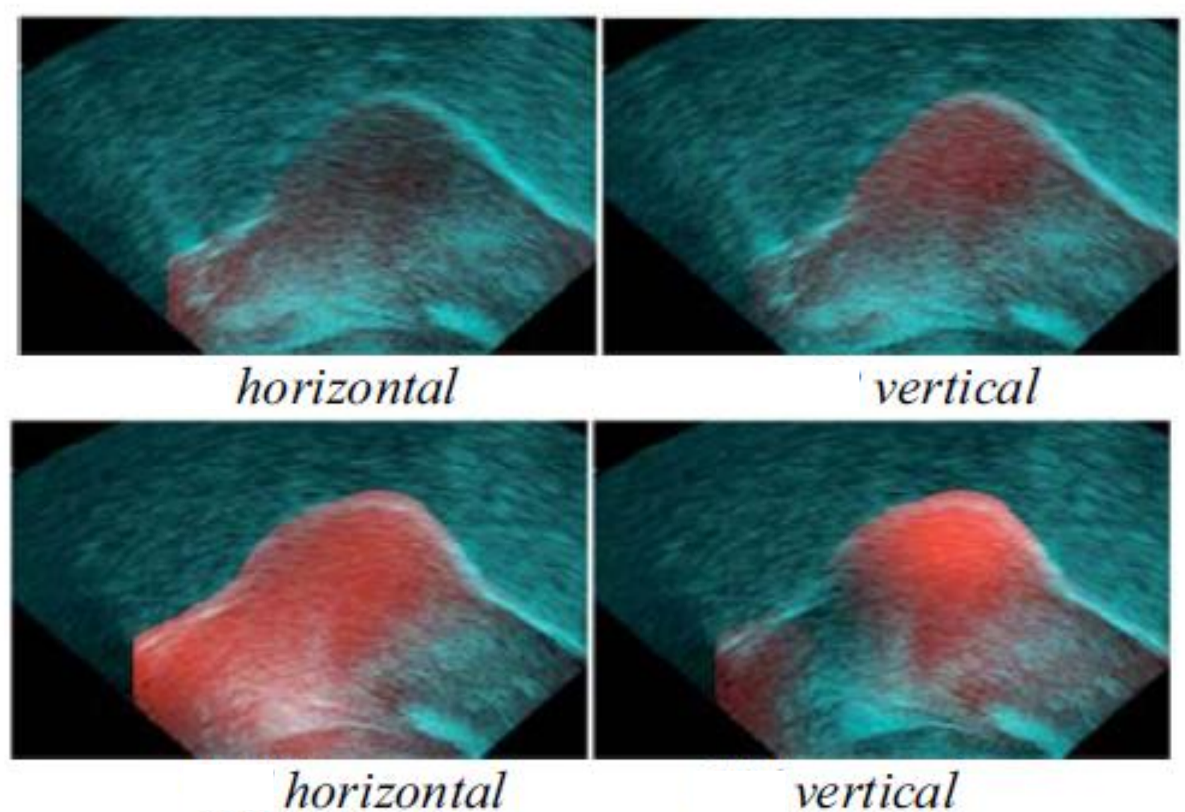

Echographie : Formes 3D de la langue

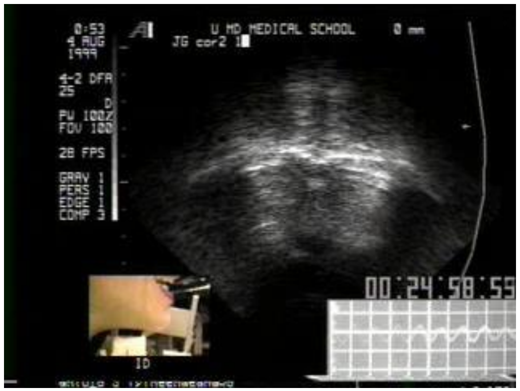

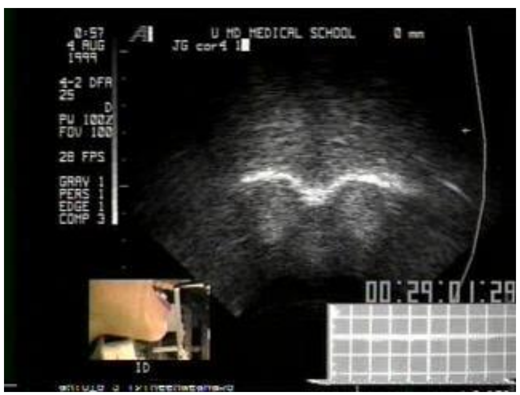

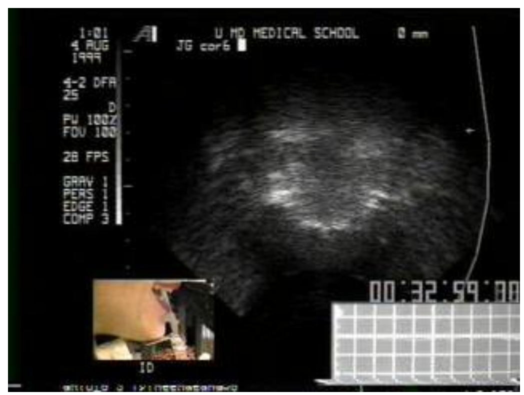

Echographie : Formes 3D de la langue

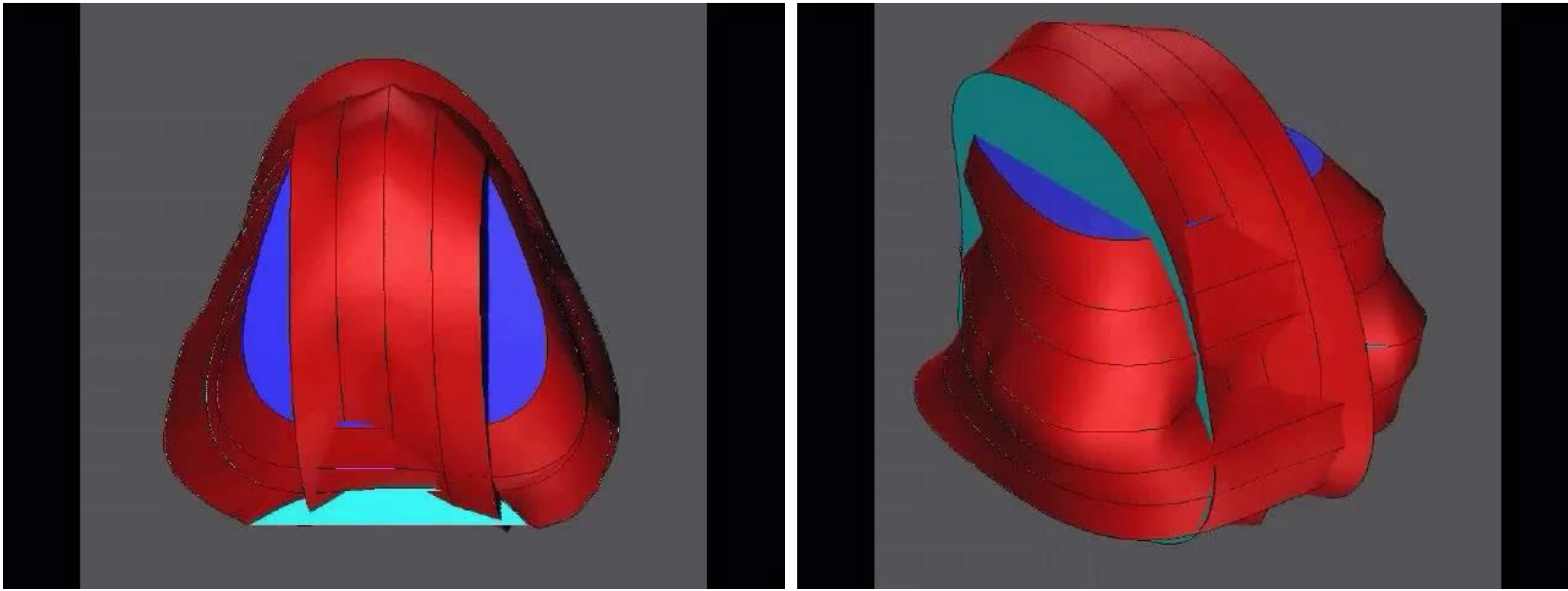

Syllabe ‘scha’ en anglais

Mesures cinématiques sur les cordes vocales
Endoscopie & Electroglottographie

Endoscopie : Le larynx
Laryngeal endoscopy

Cartilages et muscles

Netter (1984) Atlas of Human Anatomy.

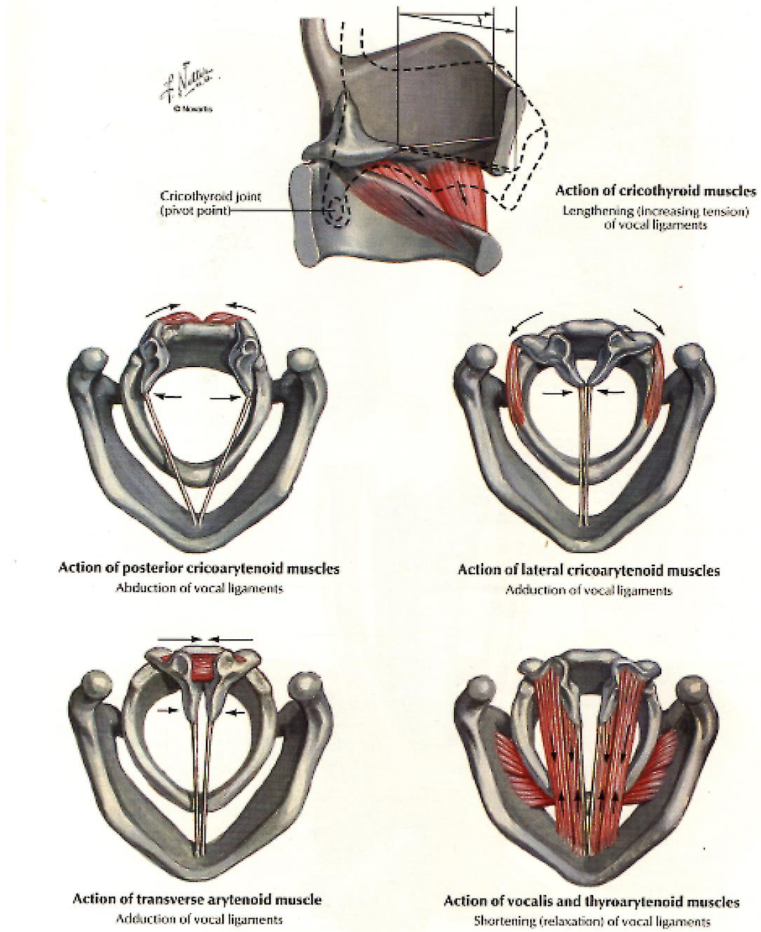

Endoscopie : les cordes vocales

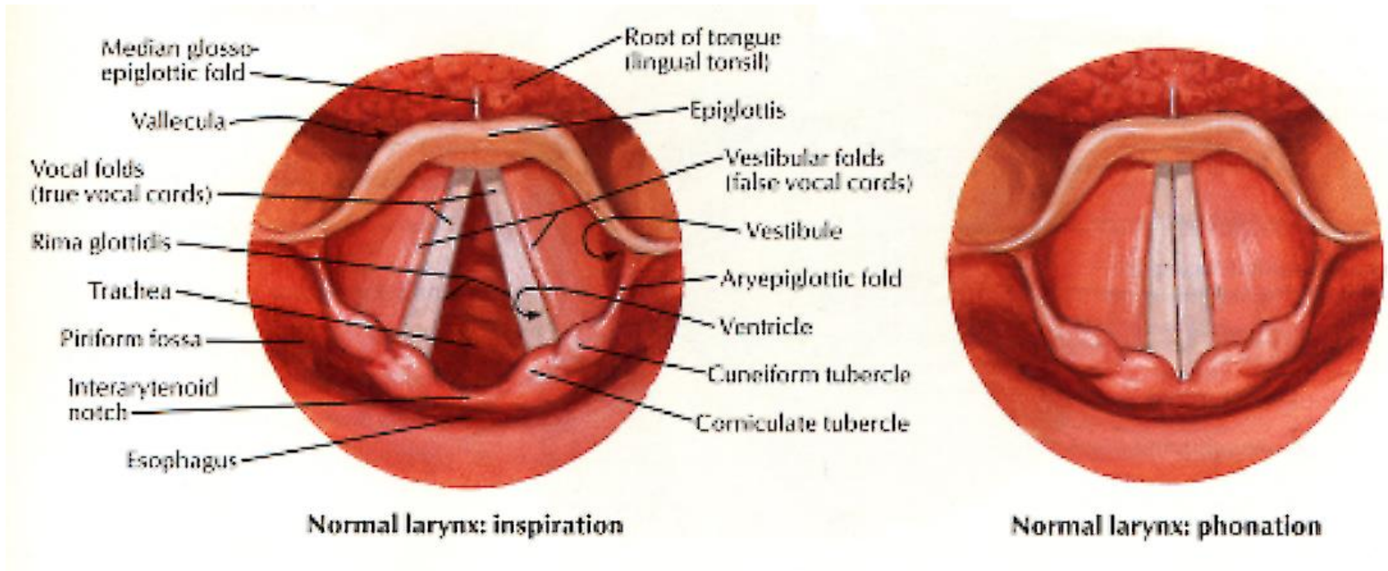

Les plis vocaux

Netter (1984) Atlas of Human Anatomy.

Vibration des cordes vocales: Voisement

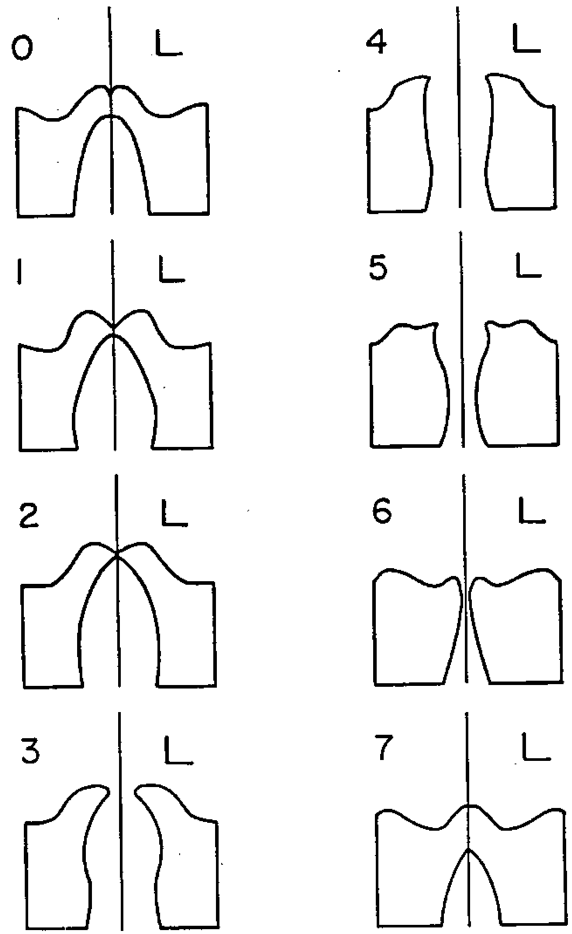

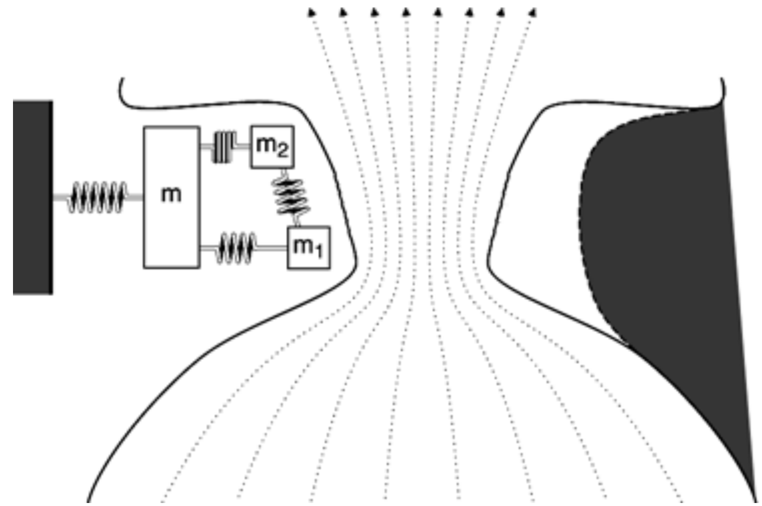

Interaction fluide-parois : vibrations

Vibration des cordes vocales : Voisement

Stevens (1998)

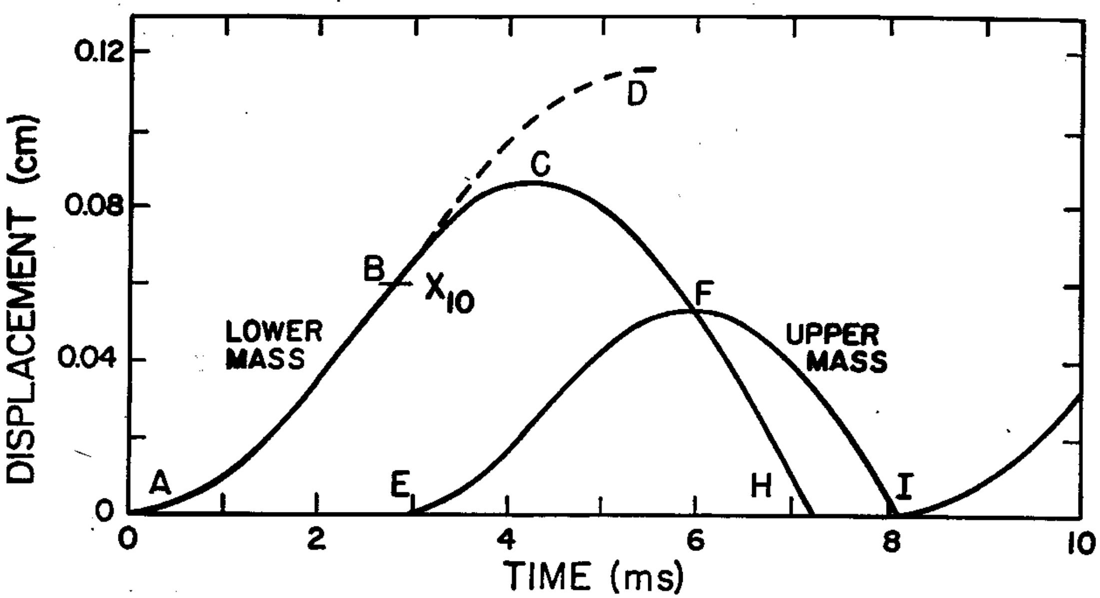

Mouvement des parties inférieures et supérieures

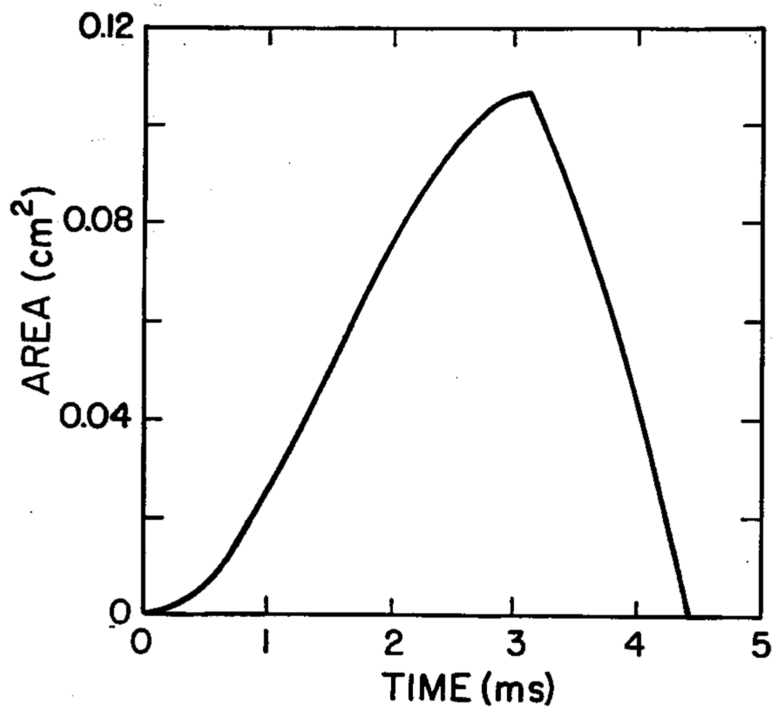

Aire à la glotte

Endoscopie : Méthode

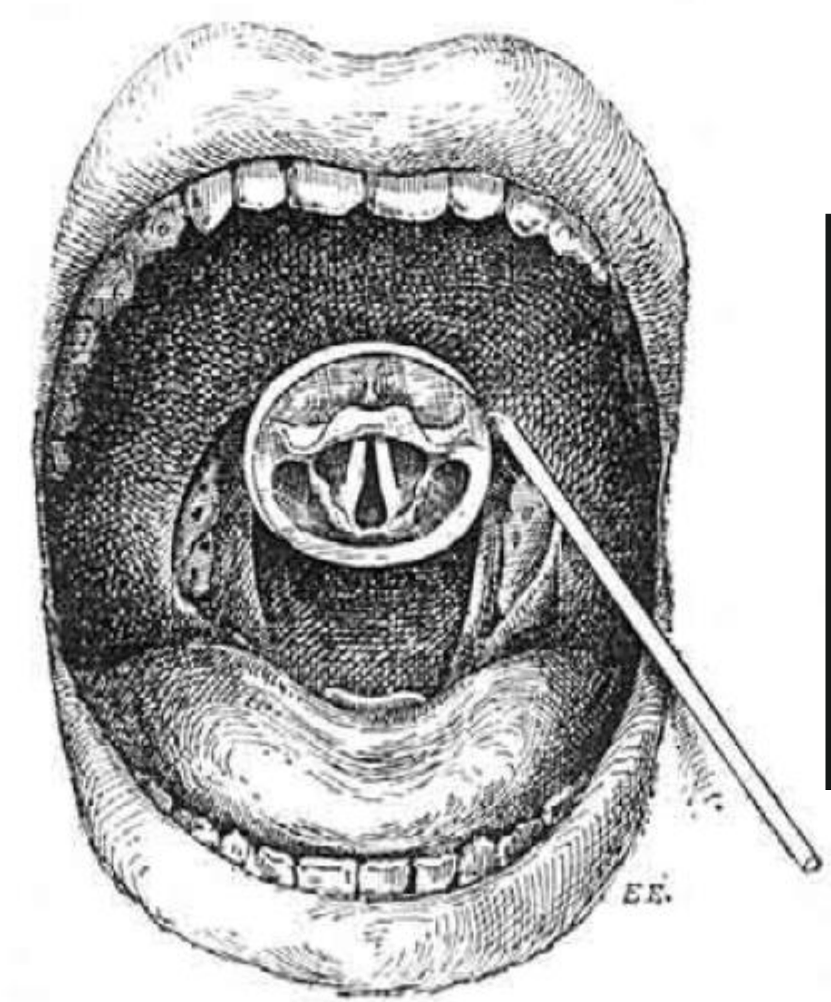

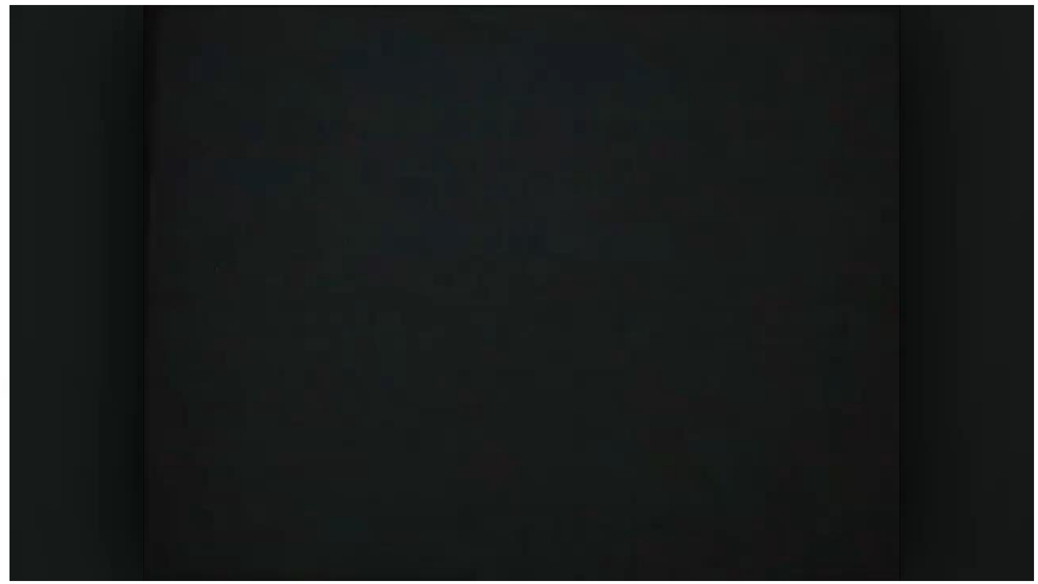

Transillumination

Electroglottographie (EGG) – Impédance du larynx

North Carolina State University Phonetics Lab
https://phon.wordpress.ncsu.edu/

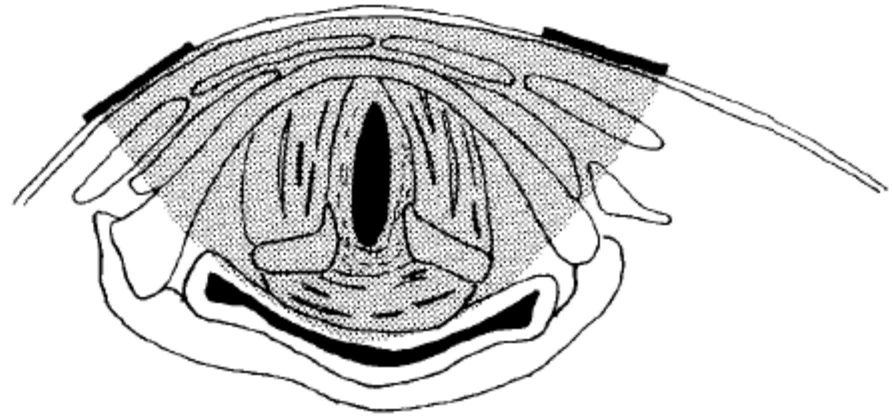

FIG. 1. The larynx in its anatomic environment. Superficial black rectangles represent electrodes on the skin. Gray shading suggests the cross-sectional region through which electric current flows.

Baken, R.J., Journal of Voice, 1992

Electroglottographie – Impédance du larynx

Variation de l'impédance

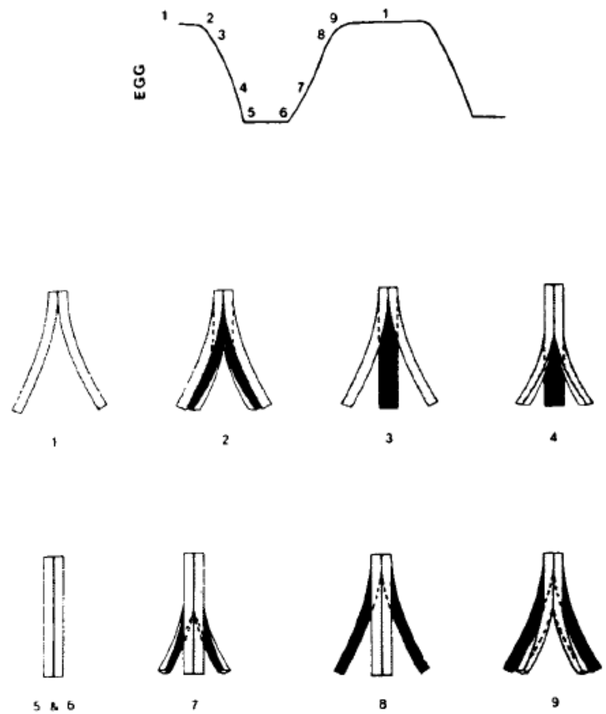

FIG. 8. Geometric two-mass model of the vocal fold activity underlying features in the Lx wave. Note that the Lx wave at the top of the figure is oriented with increasing vocal fold contact (decreasing trans-neck impedance) *downward*. White areas represent the upper mass of the vocal fold, black areas the lower mass. 1: both masses open; 2: upper open, lower ½ closed; 3: upper open, lower closed; 4: upper ½ closed, lower closed; 5 and 6: both closed; 7: upper closed, lower ½ open; 8: upper closed, lower open; 9: upper ½ open, lower open. Reprinted with permission (38).

Baken, R.J., Journal of Voice, 1992

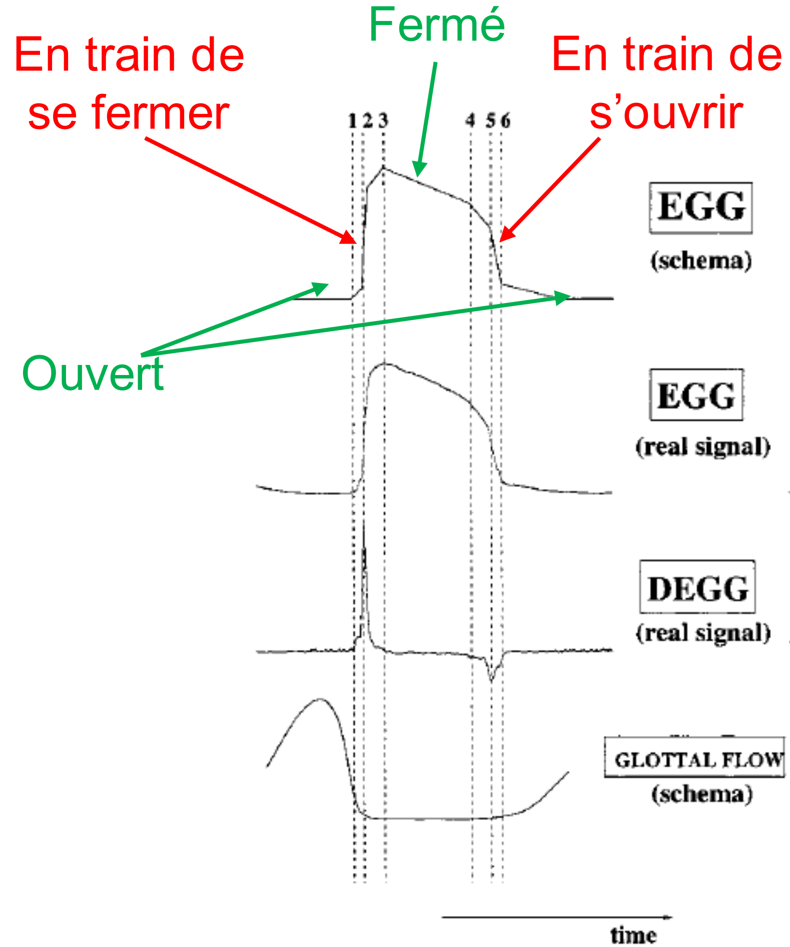

Henrich, N. et al. JASA, 2004

Electroglottographie - Mesures

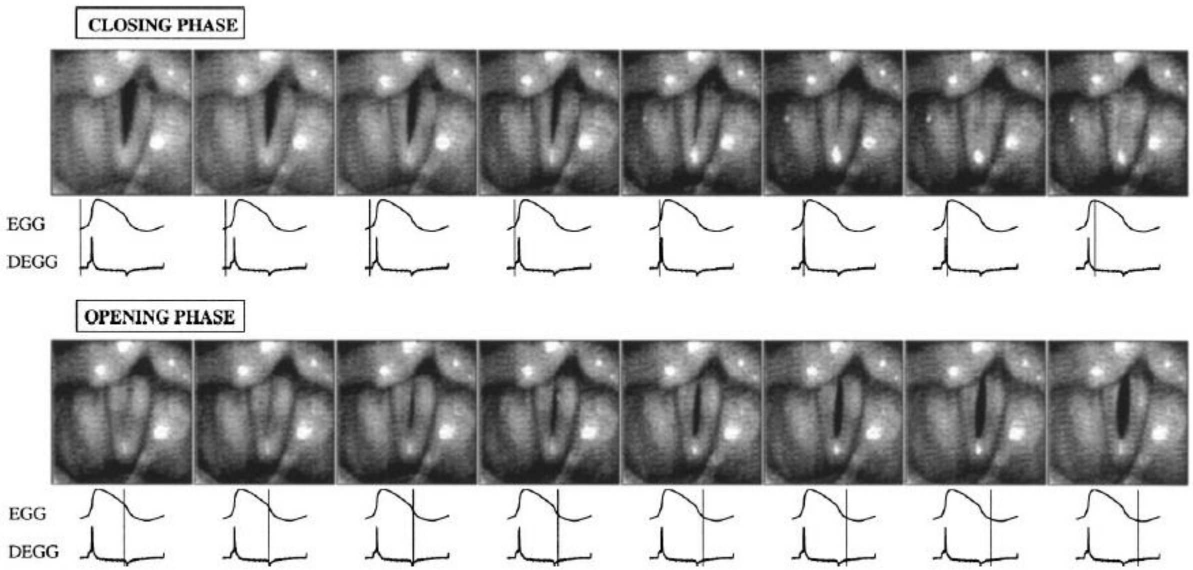

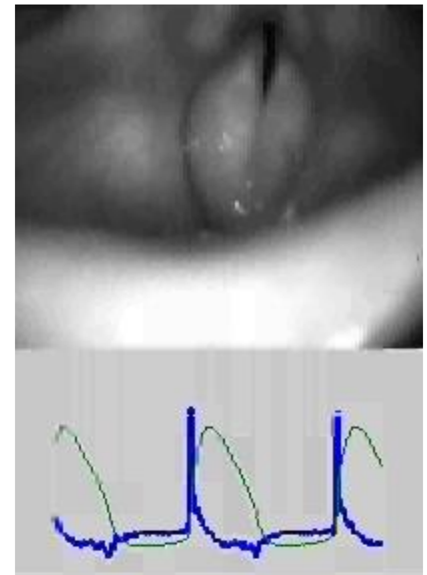

Henrich, N. et al. JASA, 2004

Mesures des contacts

Electropalatographie-Electropalatography

Electropalatographie

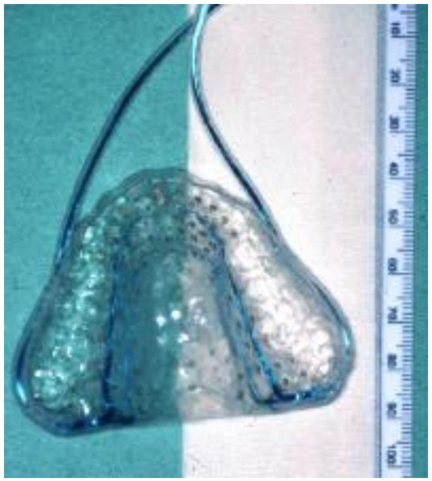

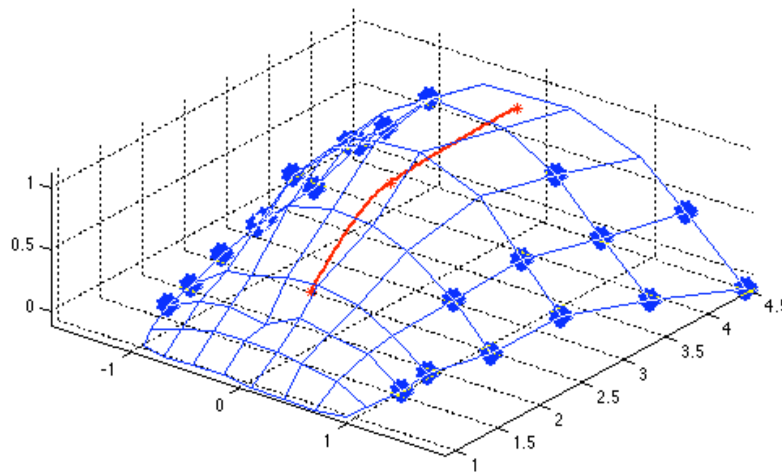

Electropalatographie

Mesures dynamiques
Capteurs de forces

Capteurs de force

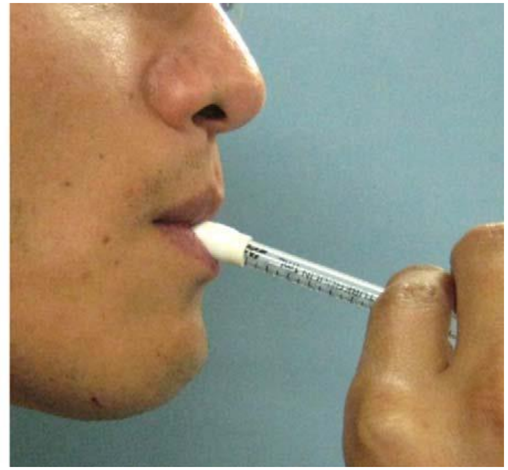

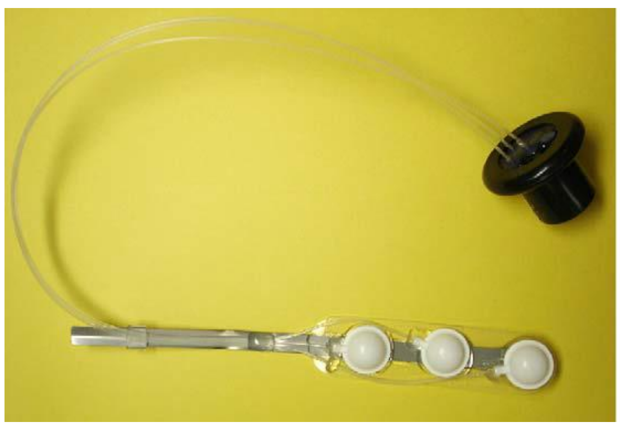

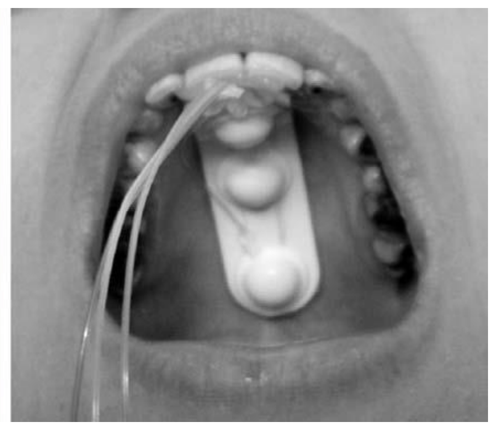

Capteurs de force : jauge de contrainte

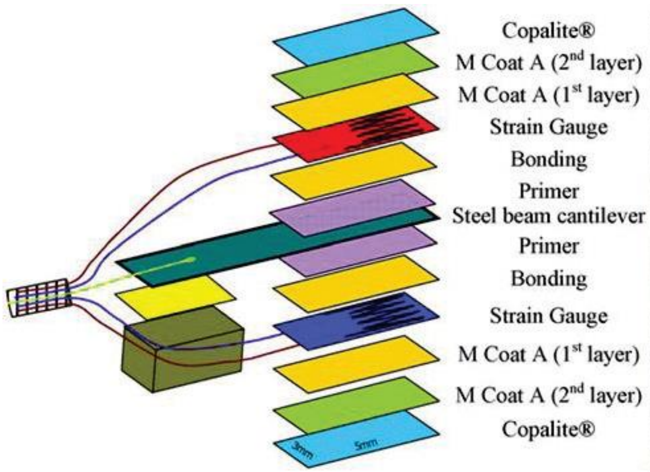

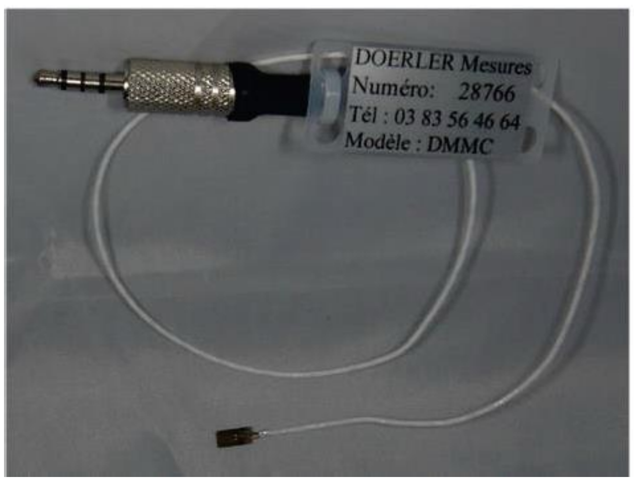

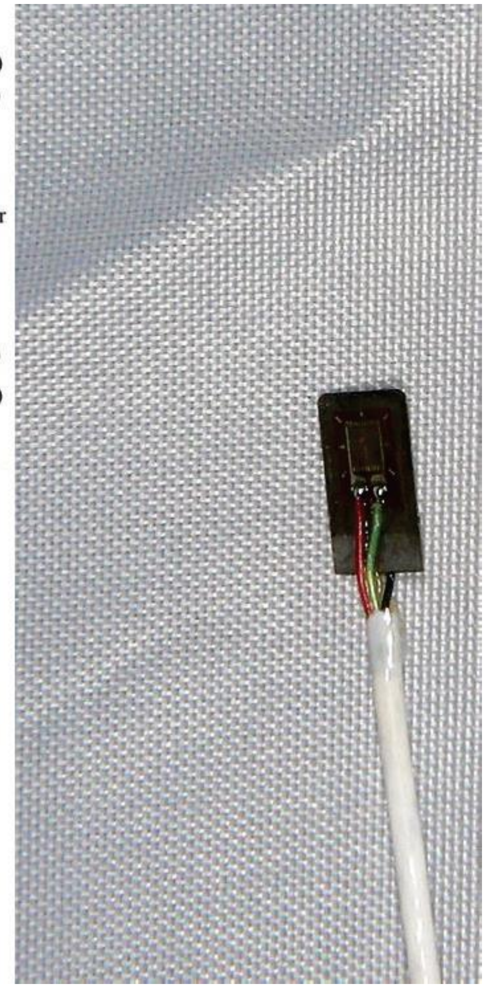

Capteurs de force : calibration

Jeannin & Perrier, 2023

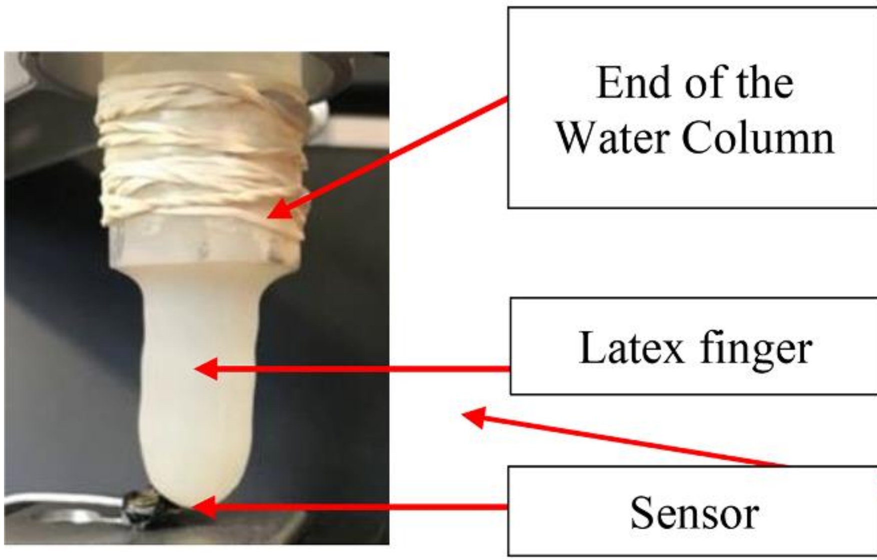

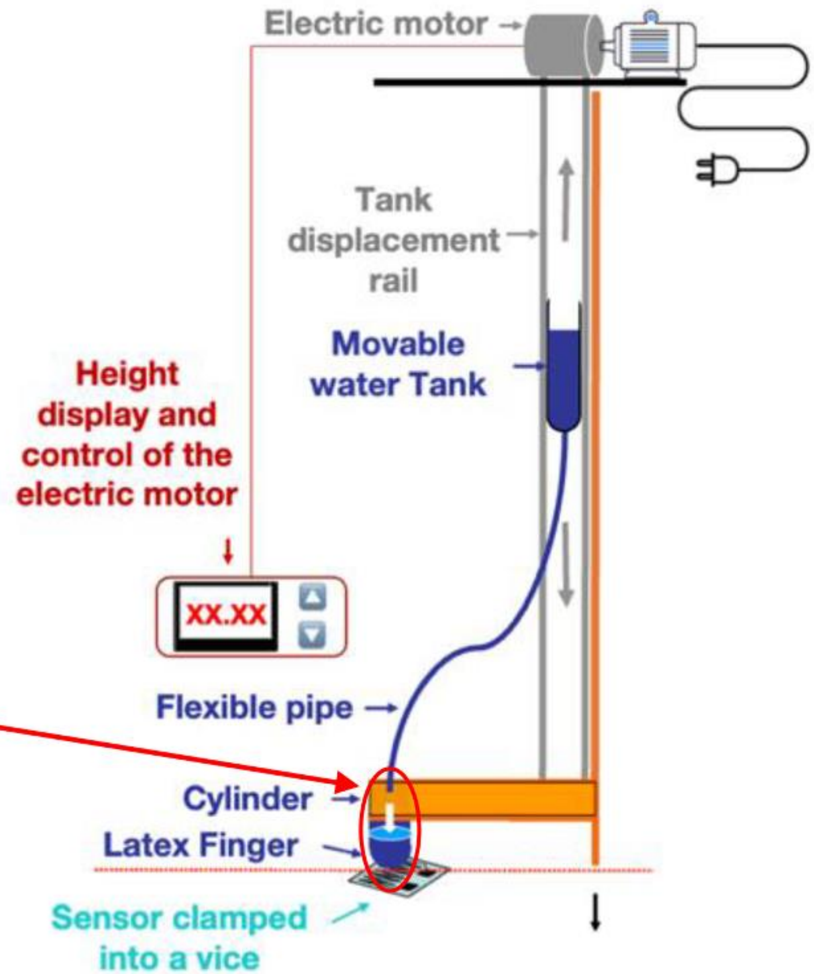

Capteurs de force : mesures

Mirchandani et al., 2020

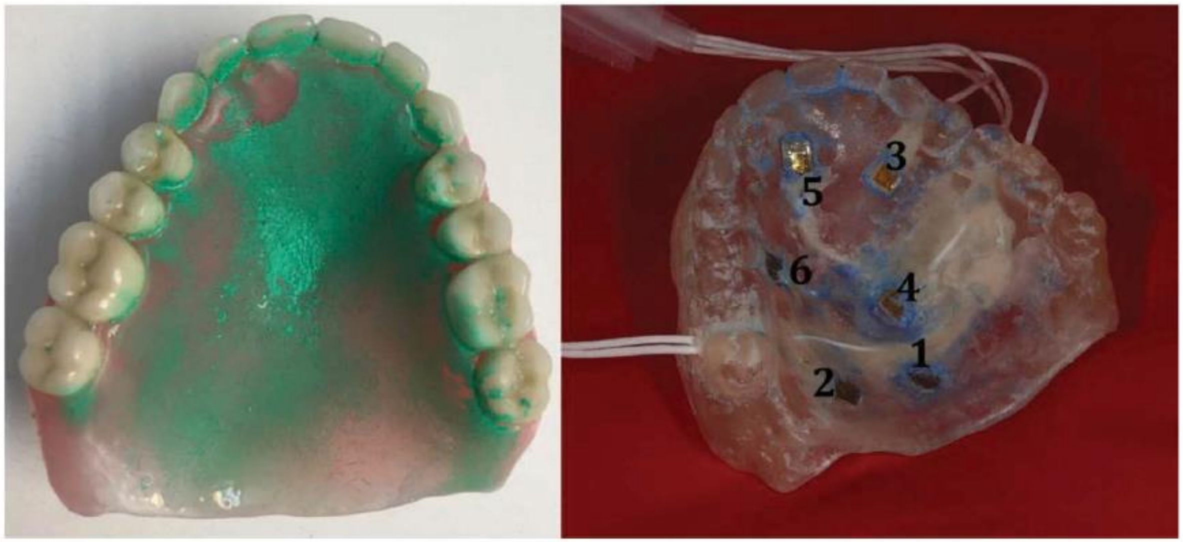

Figure 2. Left panel: palatogram for /ita/ on a of the complete denture; the replica was initially covered with green powder; as the tongue touched it, the powder was removed in the region where contact occurred; thus, the palatogram informs about the location where strain gauge sensors have to be inserted, in order to measure the tongue-to-palate pressure. Right panel: Location of the six strain gauge sensors in the replica of the complete denture, as determined from the palatograms for this subject.

Capteurs de force : mesures

Mirchandani et al., 2020

Consonne alvéolaire /t/

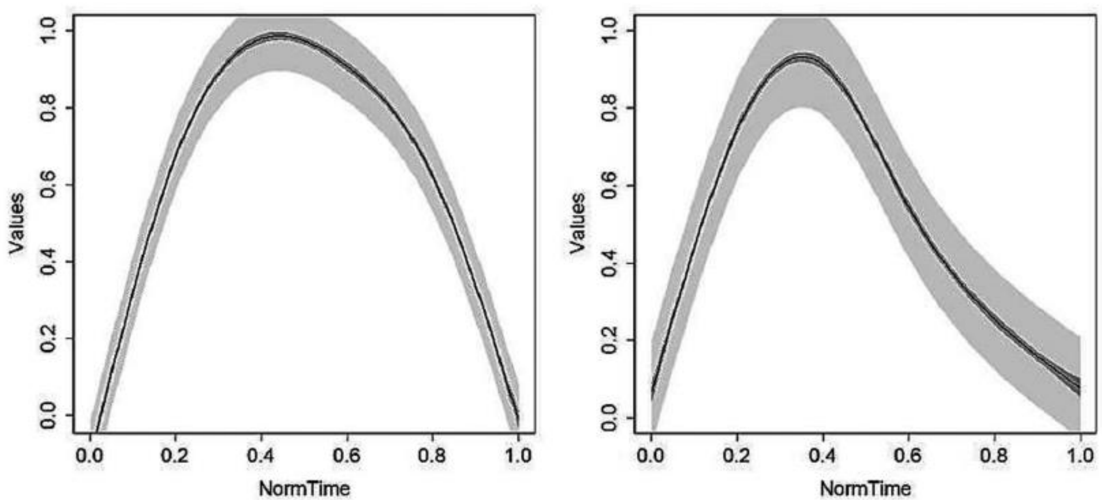

Figure 6. Pressure time patterns for /t/ in /ita/ normalized in time and in amplitude. Dark grey shaded region: 95% confidence interval; light grey shaded region: prediction interval at one standard deviation. Left panel: Sensor 5. Right panel: Sensor 6.

Capteurs de force : mesures

Mirchandani et al., 2020

Consonne vélaire /k/

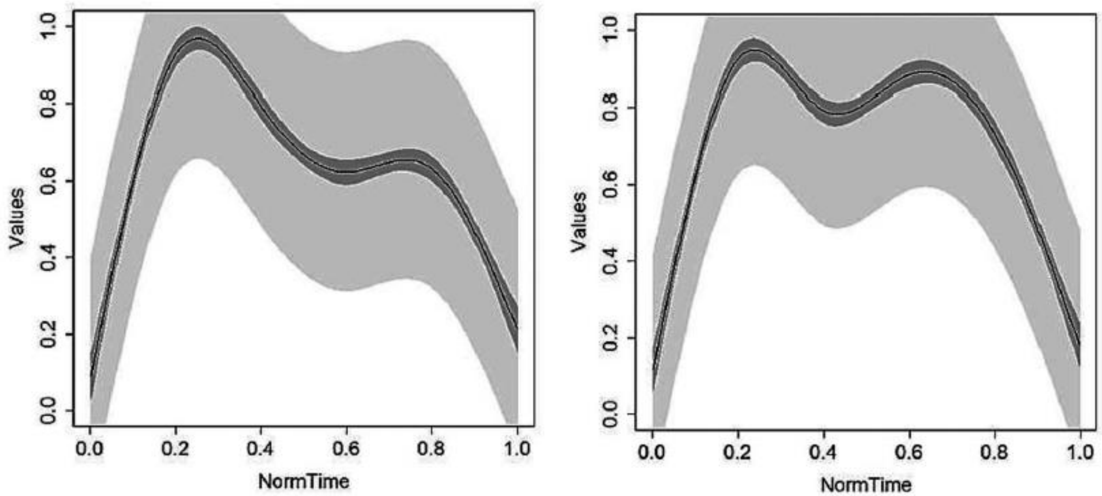

Figure 7. Pressure time patterns for /k/ in /ika/ normalized time and in amplitude. Dark grey shaded in time and in amplitude. Dark grey shaded region: 95% confidence interval; light grey shaded region: prediction interval at one standard deviation. Left panel: Sensor 1. Right panel: Sensor 2.

Mesures dynamiques
Electromyographie

Electromyographie - Principes

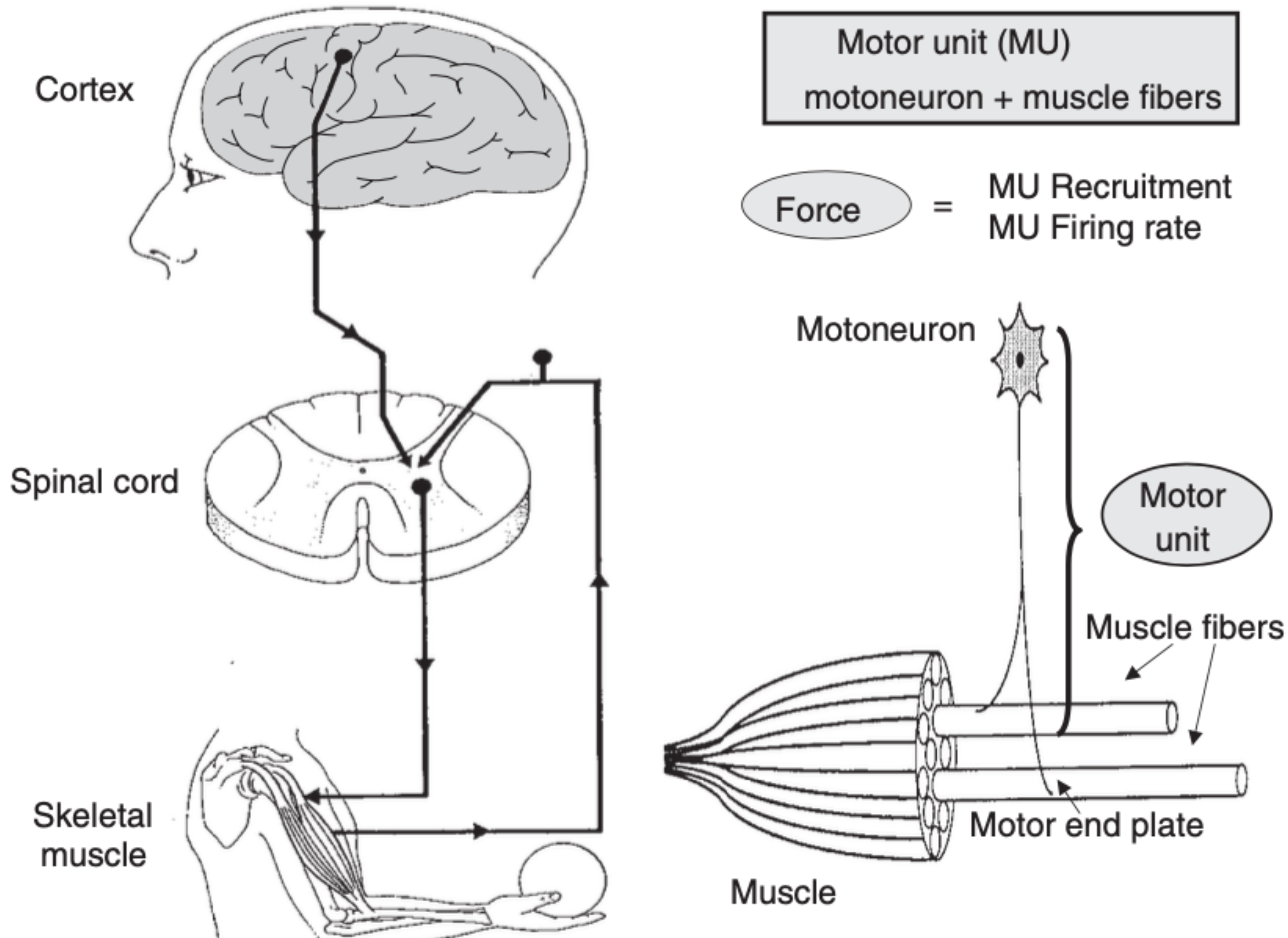

Merletti, R. & Parker, P. (2004). Wiley-Interscience

Electromyographie - Principes

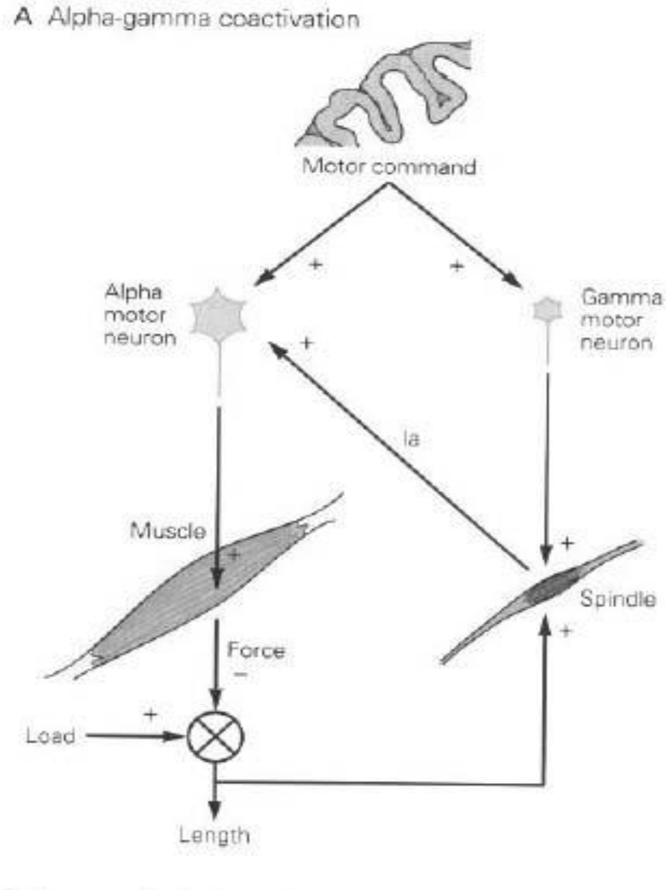

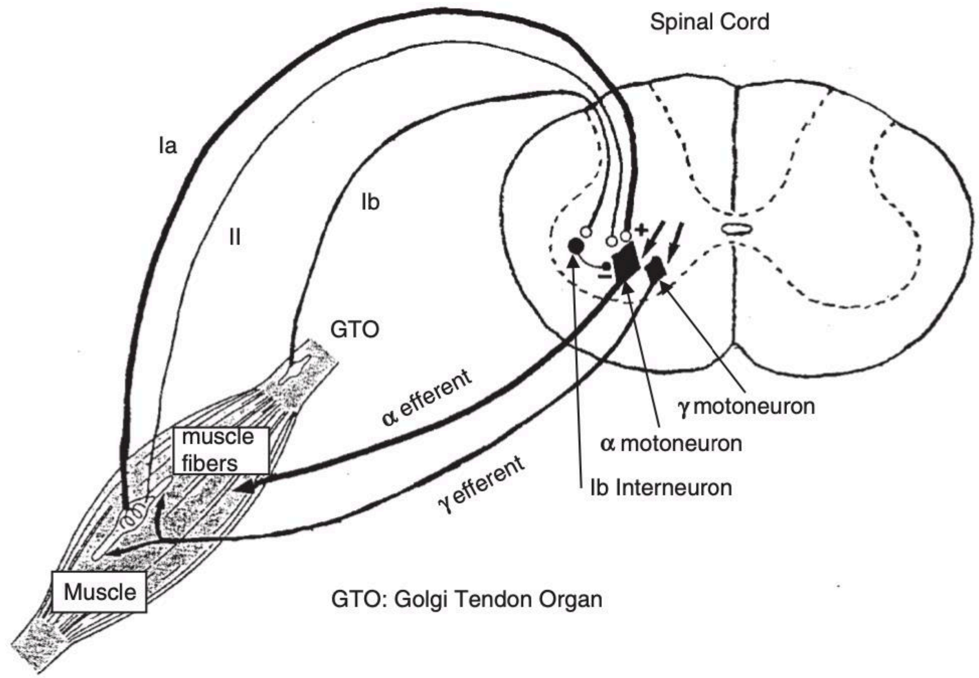

Electromyographie - Principes

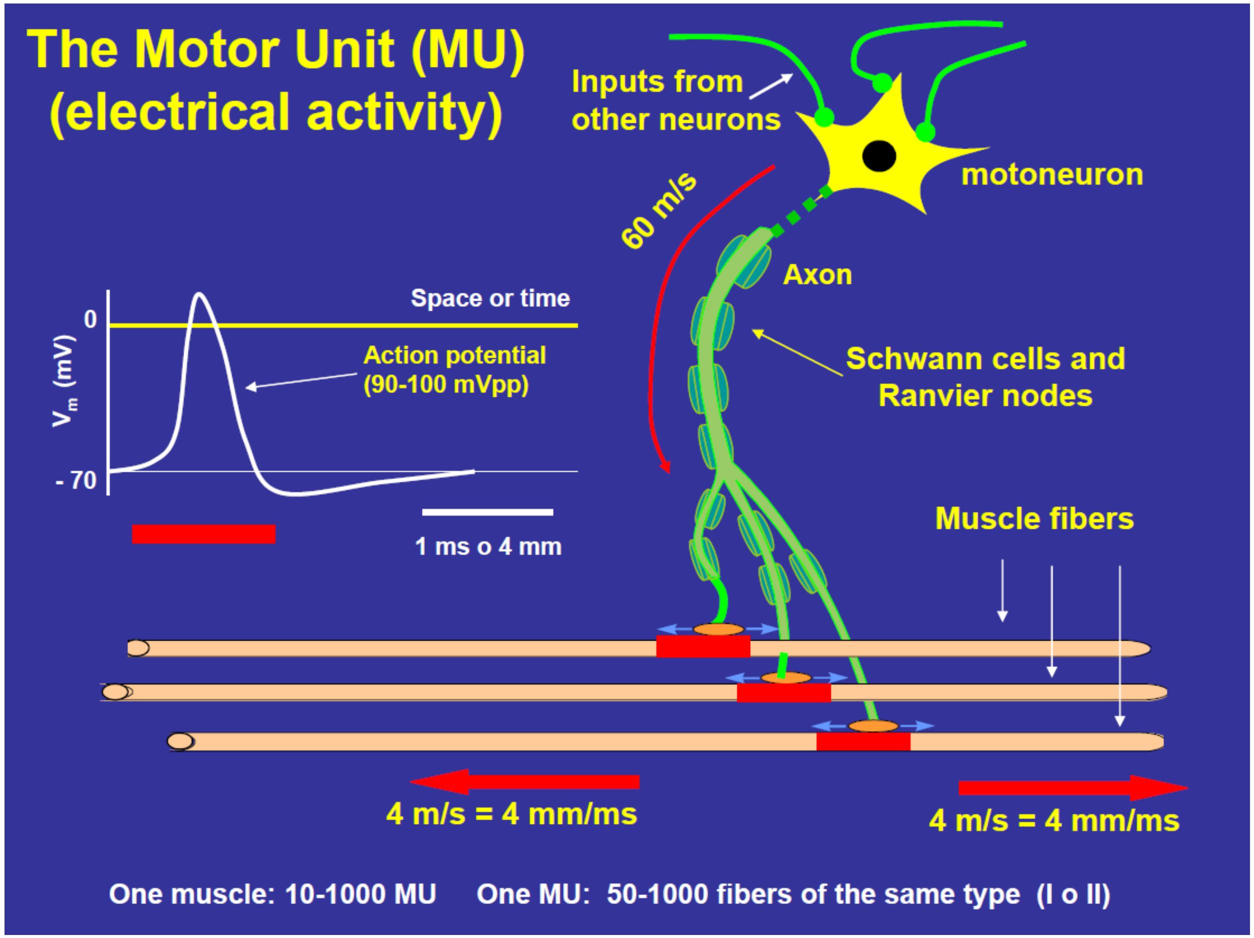

Merletti, R. (2006) - Slovenian-Italian Workshop on Quantitative Needle and High Resolution Surface EMG December 4, 2006

Electromyographie - Principes

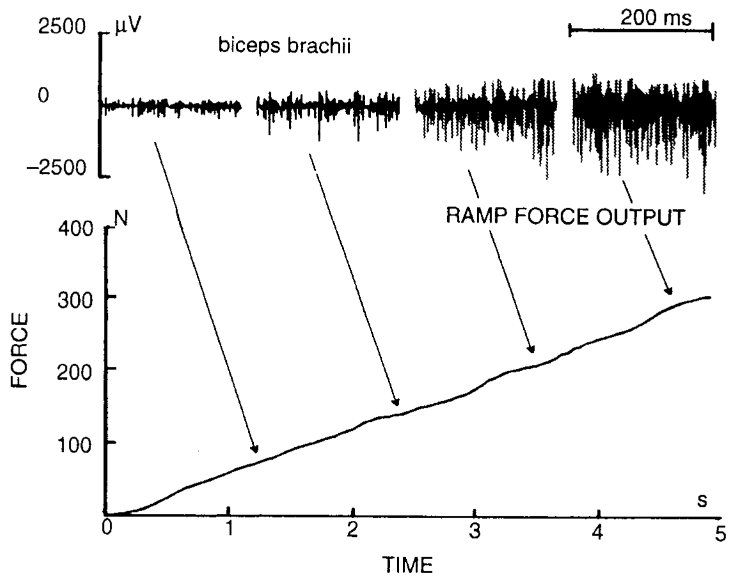

Figure 1.6. Intramuscular spike recordings obtained from the biceps brachii muscle during linearly force-varying isometric muscle contraction.

Merletti, R. & Parker, P. (2004). Wiley-Interscience

Electromyographie - Principes

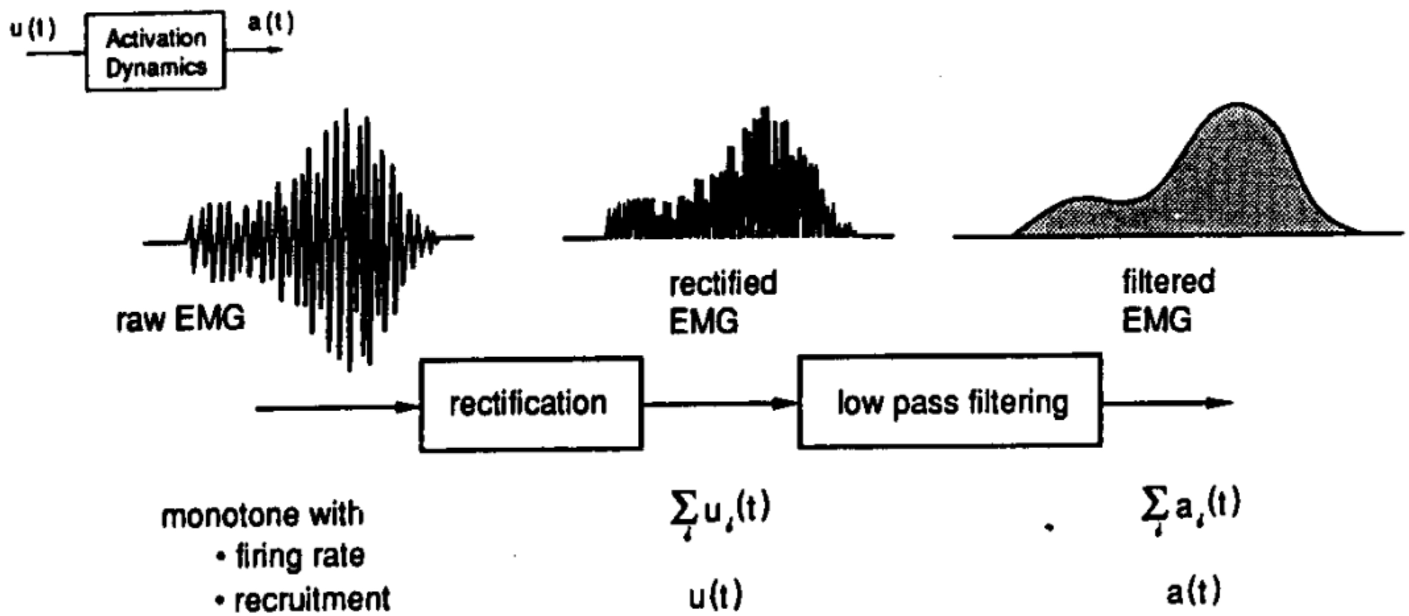

Zajac FE (1989). Crit Rev in Biomed Eng

Electromyographie - Méthode

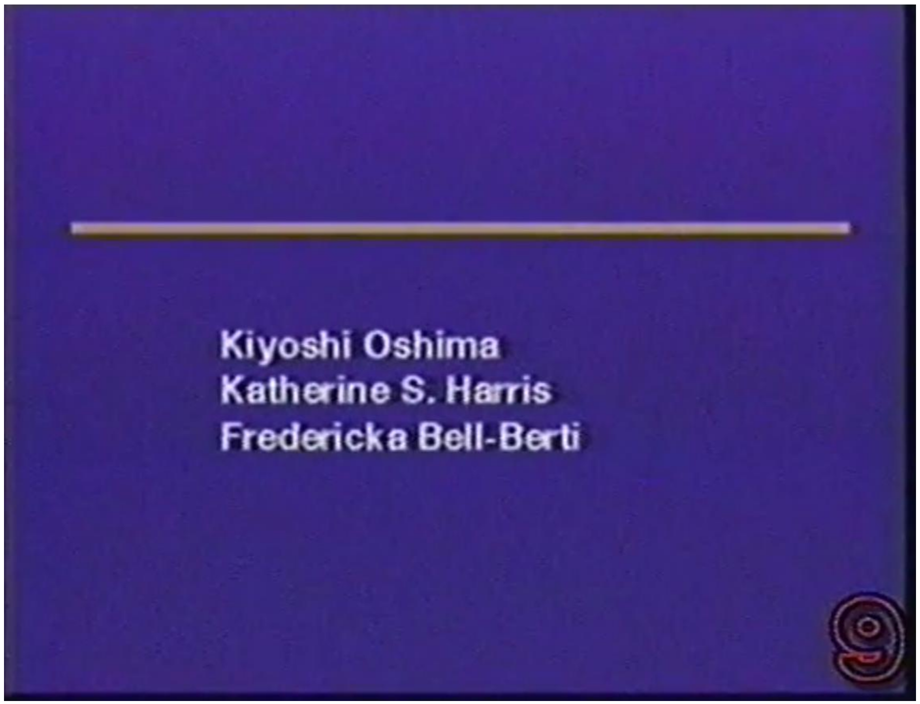

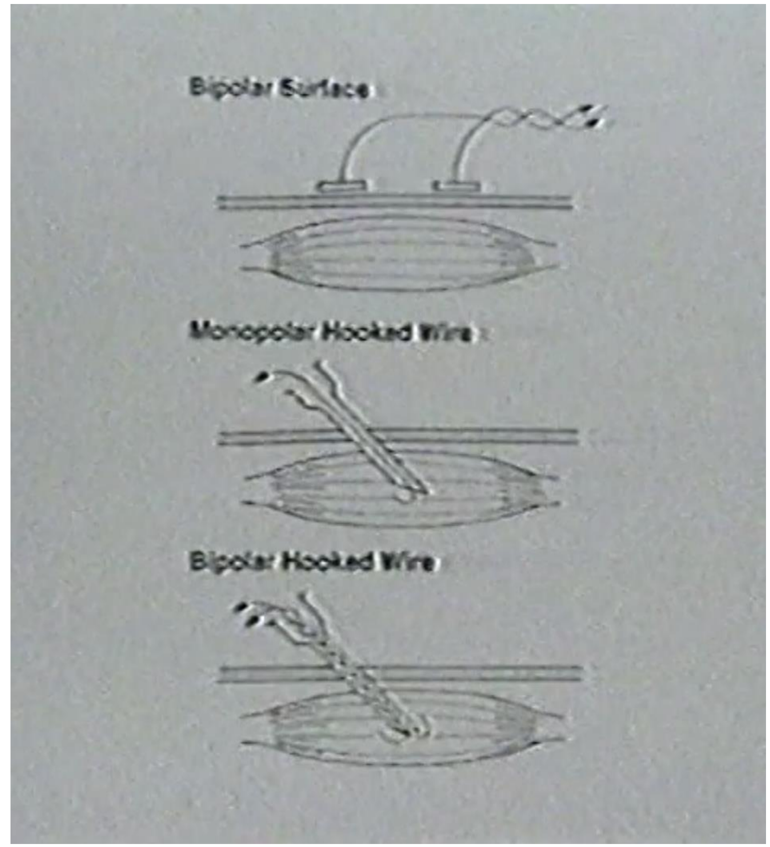

Electromyographie - Méthode

Electromyographie à l'aiguille

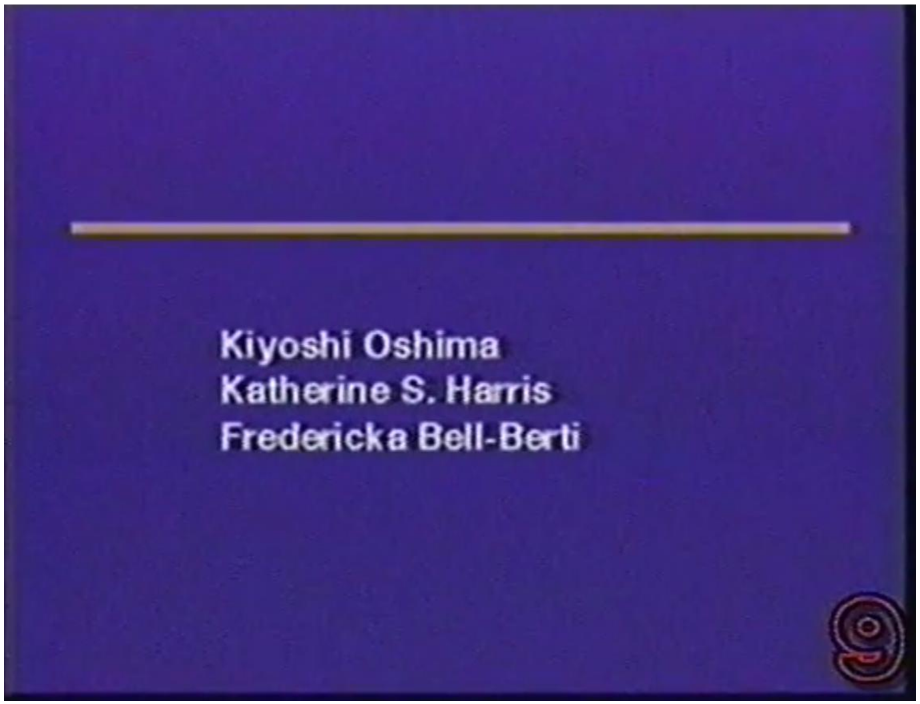

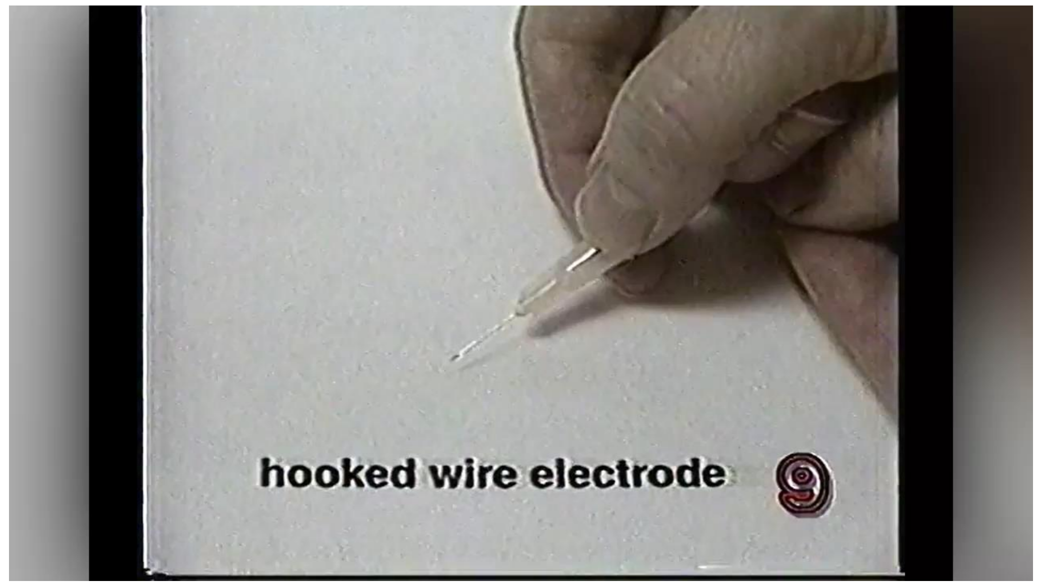

Electromyographie - Méthode

Electromyographie de surface

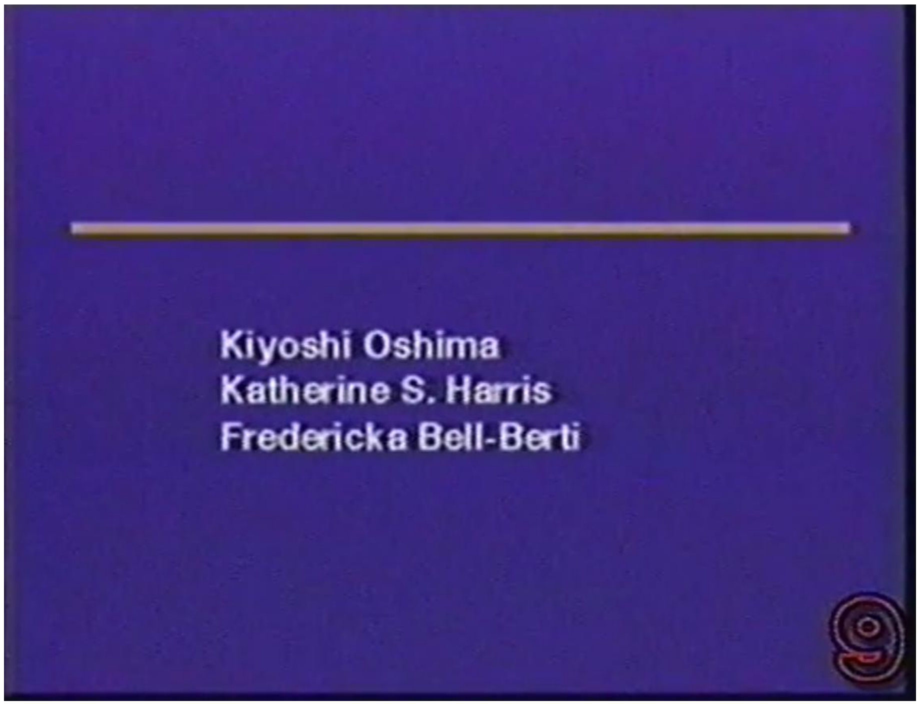

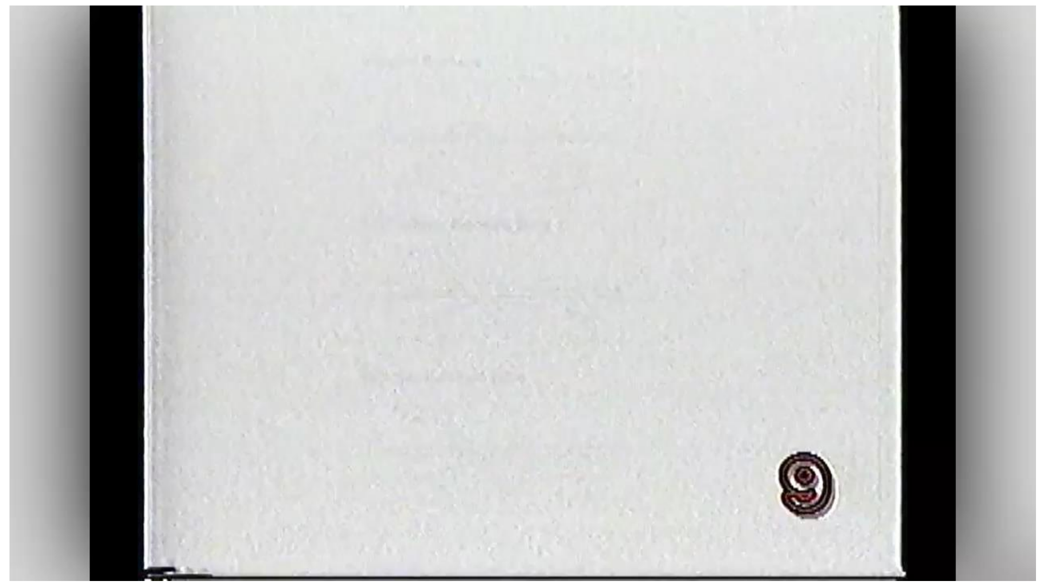

Electromyographie - Méthode

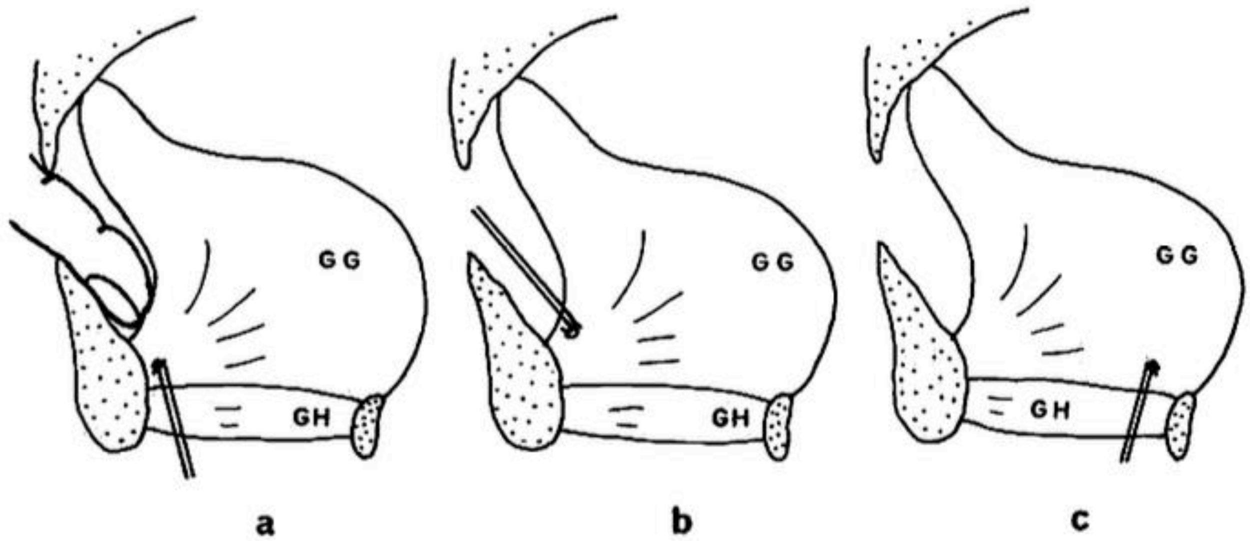

Fig. 6-a,b Insertion of the electrodes in the anterior portion of the genioglossus muscle.
Fig. 6-c Insertion of the electrodes in the posterior portion of the genioglossus muscle.

Miyawaki, et al Ann Bull RILP, 9, 91-106, 1975

Electromyographie – Nappes d'électrodes

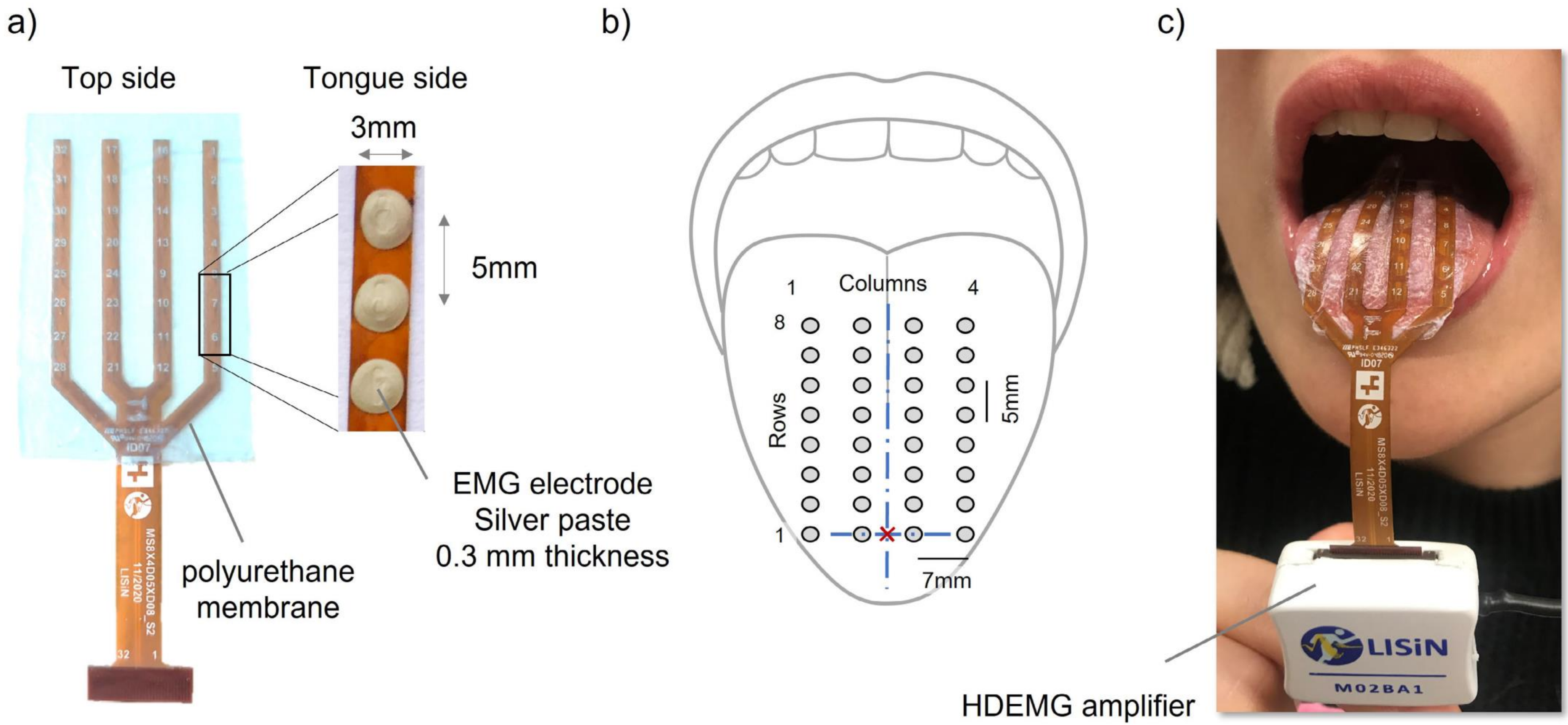

Botter et al., IEEE TRANS. ON NEURAL SYSTEMS AND REHABILITATION ENG., 2024

Electromyographie – Nappes d'électrodes

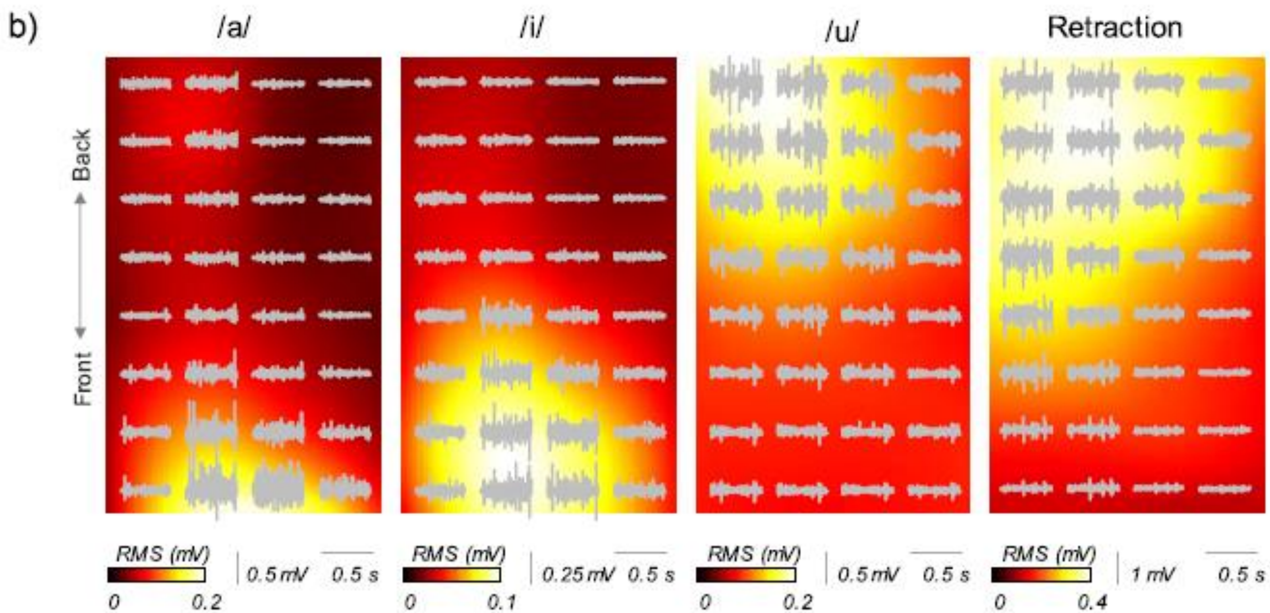

Botter et al., IEEE TRANS. ON NEURAL SYSTEMS AND REHABILITATION ENG., 2024

Exemples de paradigmes expérimentaux

Exploiter une perturbation pour connaître le rôle du réflexe proprioceptif dans le contrôle de la parole.

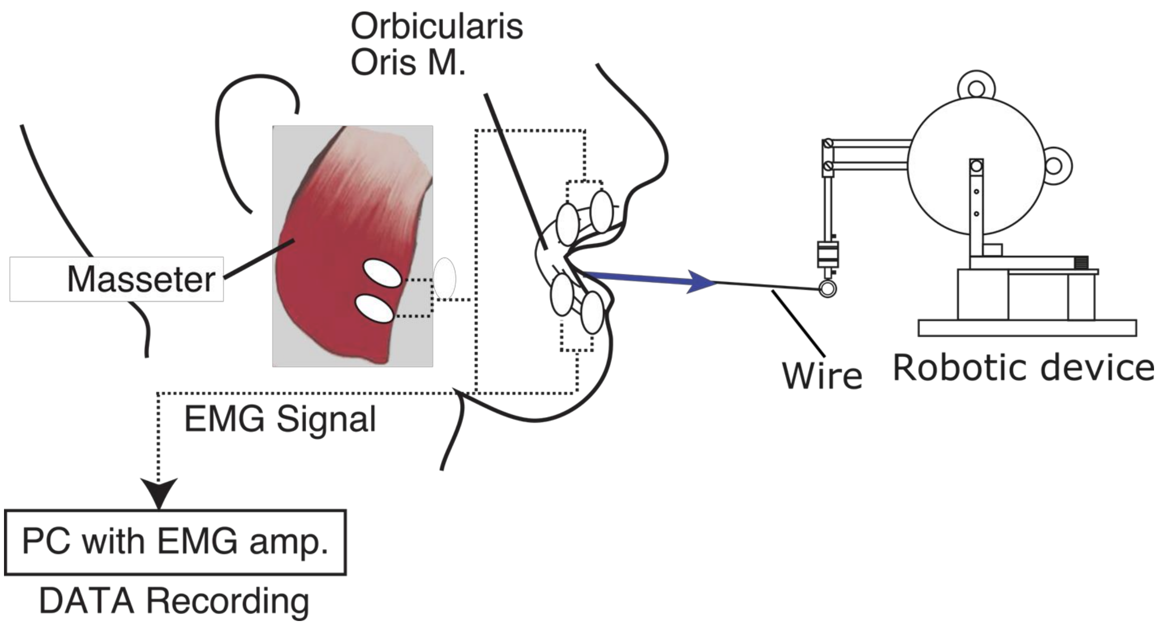

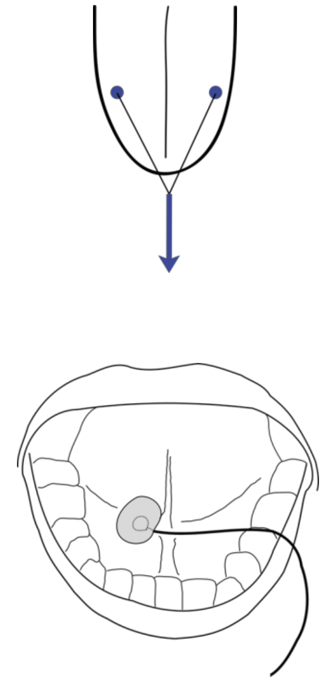

Ito, Bouguerra, Bourhis, Perrier, Scientific Reports, 2024,

Observation cinématique

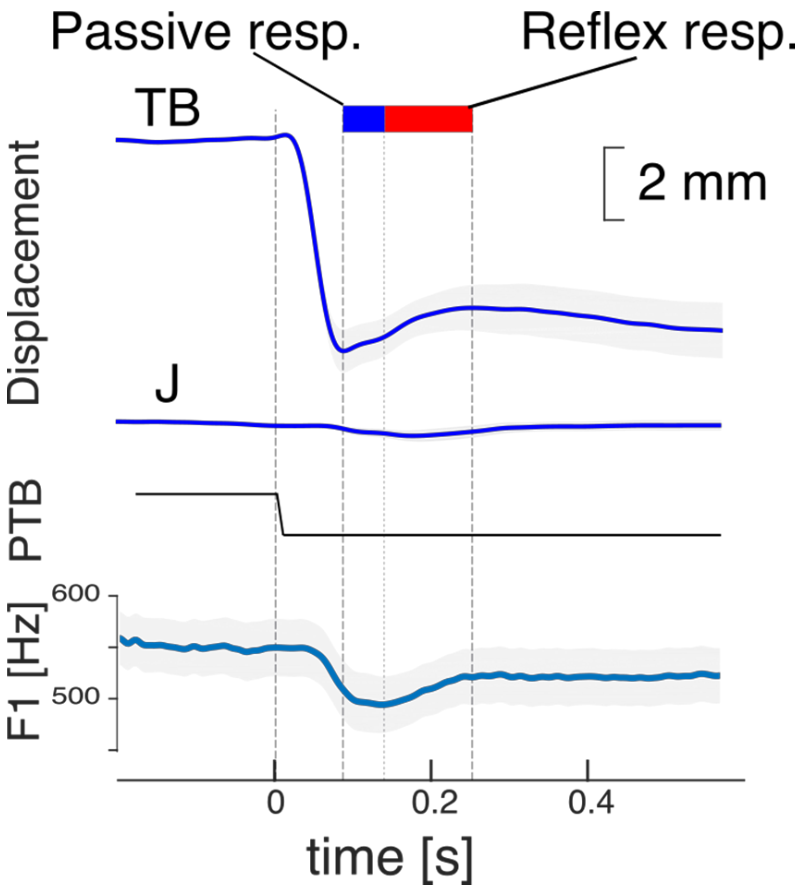

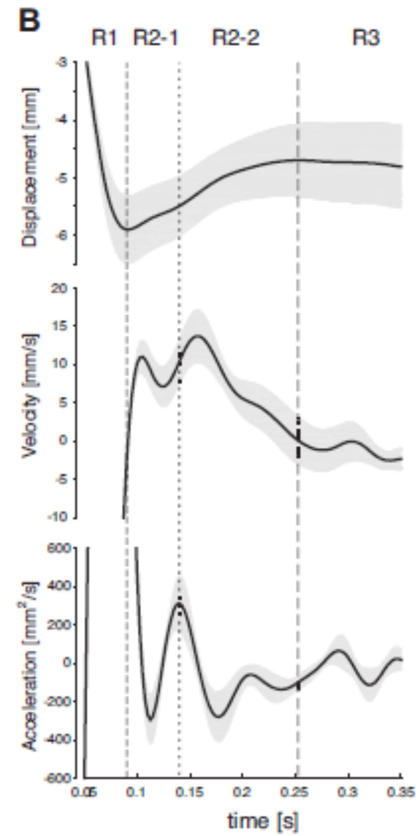

Ito, Bouguerra, Bourhis, Perrier, Scientific Reports, 2024,

Observation EMG

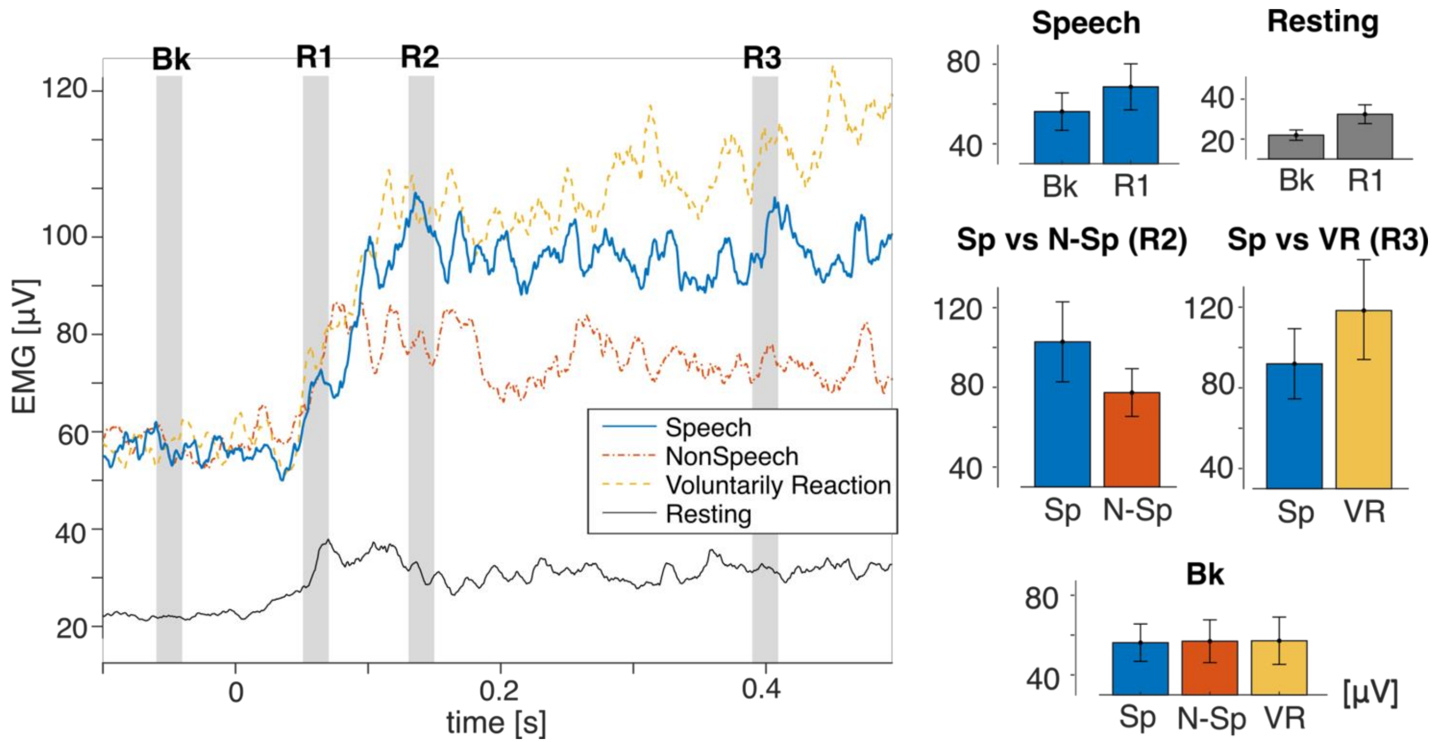

Ito, Bouguerra, Bourhis, Perrier, Scientific Reports, 2024,

Modélisation

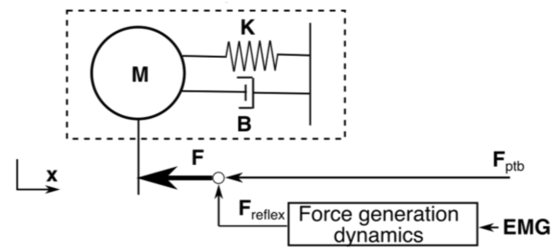

$$D(s) = \frac{G\,\omega_n^{\,2}}{s^2 + 2\zeta\omega_n s + \omega_n^{\,2}}\,e^{-\tau s}$$

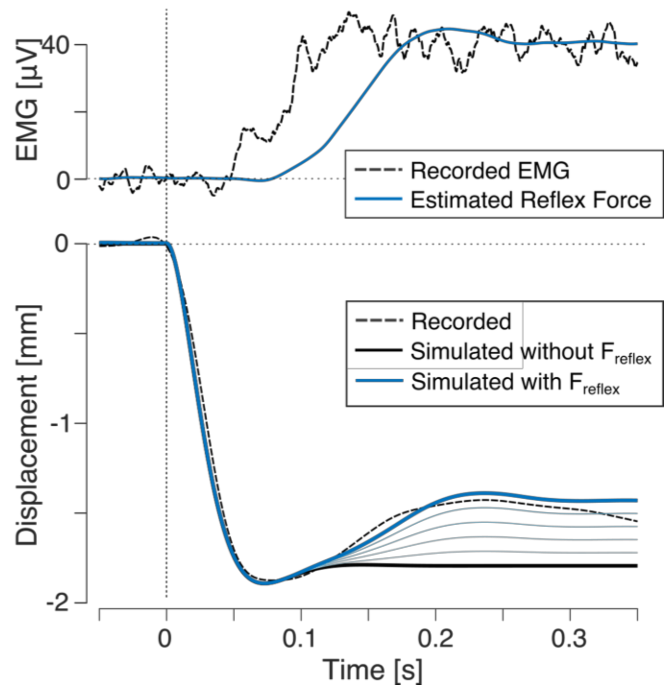

Ito, Bouguerra, Bourhis, Perrier, Scientific Reports, 2024,